USGS
science for a changing world

Prepared in cooperation with the Upper Loup Natural Resources District, the University of Nebraska Conservation and Survey Division, and the Nebraska Environmental Trust

Hydrostratigraphic Interpretation of Test-Hole and Geophysical Data, Upper Loup River Basin, Nebraska, 2008–10

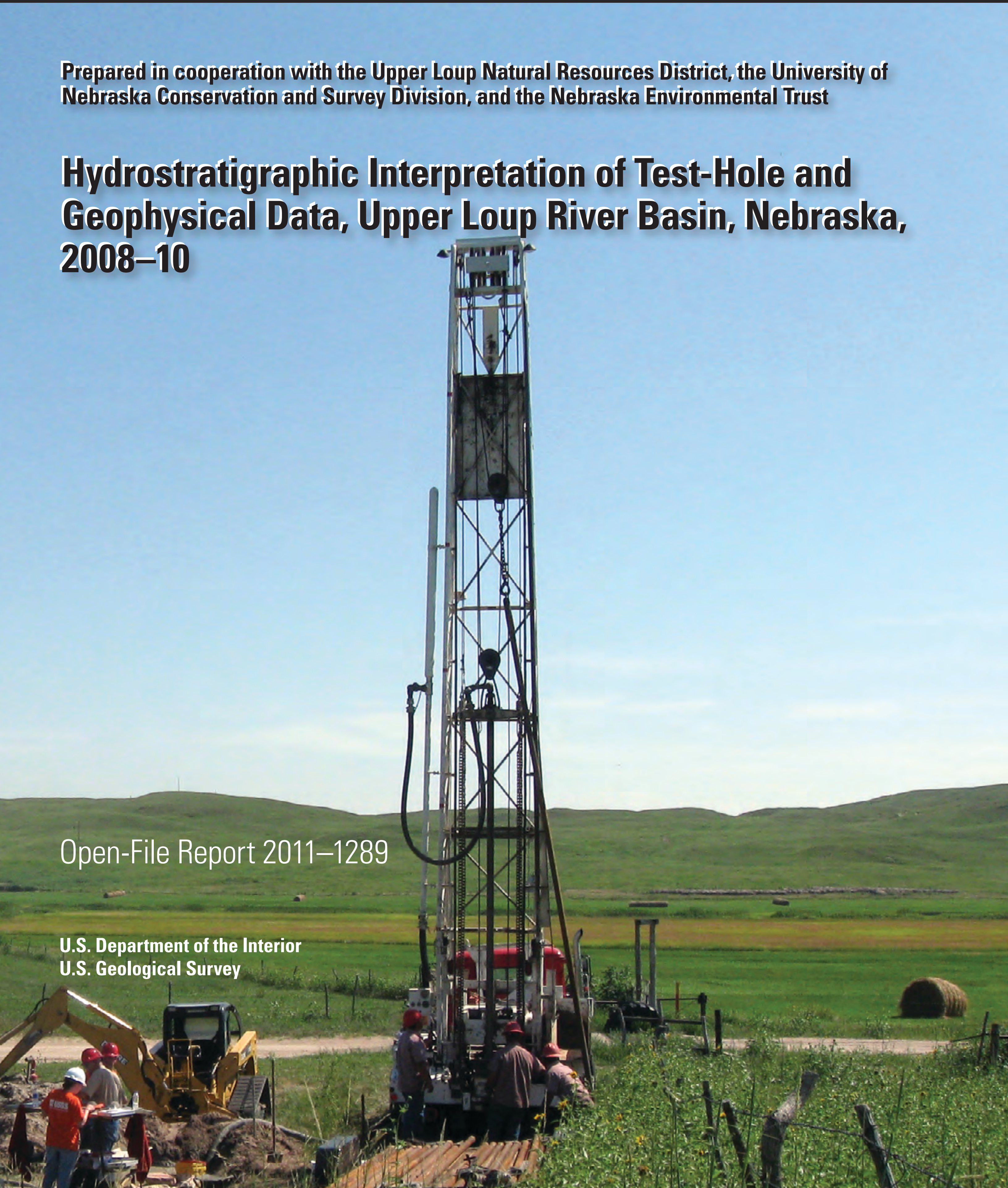

Open-File Report 2011–1289

U.S. Department of the Interior
U.S. Geological Survey

Front and back cover. Test-hole drilling south of Whitman, Nebr., Grant County, 2009.

Back cover. Grass covered eolian dunes, Thomas County, 2008 (upper photo). Strategem transmitter used in Audio Magnetotelluric survey, Thomas County, 2008 (lower photo).

Hydrostratigraphic Interpretation of Test-Hole and Geophysical Data, Upper Loup River Basin, Nebraska, 2008–10

By Christopher M. Hobza, Theodore H. Asch, and Paul A. Bedrosian

Prepared in cooperation with the Upper Loup Natural Resources District, the University of Nebraska Conservation and Survey Division, and the Nebraska Environmental Trust

Open-File Report 2011–1289

U.S. Department of the Interior
U.S. Geological Survey

U.S. Department of the Interior
KEN SALAZAR, Secretary

U.S. Geological Survey
Marcia K. McNutt, Director

U.S. Geological Survey, Reston, Virginia: 2011

Suggested citation:
Hobza, C.M., Asch, T.H., and Bedrosian, P. A., 2011, Hydrostratigraphic interpretation of test-hole and geophysical data, Upper Loup River Basin, Nebraska, 2008–10: U.S. Geological Survey Open-File Report 2011-1289, 60 p.

Contents

Figures

Tables

Conversion Factors

Inch/pound to SI

Multiply	By	To obtain
	Length	
inch (in.)	2.54	centimeter (cm)
inch (in.)	25.4	millimeter (mm)
foot (ft)	0.3048	meter (m)
mile (mi)	1.609	kilometer (km)
	Area	
acre	4,047	square meter (m^2)
acre	0.4047	hectare (ha)
acre	0.4047	square hectometer (hm^2)
acre	0.004047	square kilometer (km^2)
square foot (ft^2)	0.09290	square meter (m^2)
	Frequency	
Cycles per second	1	hertz
	Magnetic moment	
Ampere-square foot (A-ft^2)	0.09290	Ampere-square meters (A-m^2)

Hydrostratigraphic Interpretation of Test-Hole and Geophysical Data, Upper Loup River Basin, Nebraska, 2008–10

Christopher M. Hobza, Theodore H. Asch, and Paul A. Bedrosian

Abstract

Nebraska's Upper Loup Natural Resources District is currently (2011) participating in the Elkhorn-Loup Model to understand the effect of various groundwater-management scenarios on surface-water resources. During Phase 1 of the Elkhorn-Loup Model, a lack of subsurface geological information in the Upper Loup Natural Resources District, hereafter referred to as the upper Loup study area, was identified as a gap in current knowledge that needed to be addressed. To improve the understanding of the hydrogeology of the upper Loup study area, the U.S. Geological Survey, in cooperation with the Upper Loup Natural Resources District and the University of Nebraska Conservation and Survey Division, collected and described the lithology of drill cuttings from nine test holes, and concurrently collected borehole geophysical data to identify the base of the High Plains aquifer. Surface geophysical data also were collected using time-domain electromagnetic (TDEM) and audio-magnetotelluric (AMT) methods at test-hole locations and between test holes, as a quick, non-invasive means of identifying the base of the High Plains aquifer.

Test-hole drilling has indicated greater variation in the base-of-aquifer elevation in the western part of the upper Loup study area than in the eastern part reflecting a number of deep paleovalleys incised into the Brule Formation of the White River Group. TDEM measurements within the upper Loup study area were shown to be effective as virtual boreholes in mapping out the base of the aquifer. TDEM estimates of the base of aquifer were in good accordance with existing test-hole data and were able to improve the interpreted elevation and topology of the base of the aquifer. In 2010, AMT data were collected along a profile, approximately 12 miles (19 kilometers) in length, along Whitman Road, in Grant and Cherry Counties. The AMT results along Whitman Road indicated substantial variability in the elevation of the base of the High Plains aquifer and in the distribution of highly permeable zones within the aquifer.

Introduction

Newly adopted legislation in Nebraska requires a sustainable balance between long-term water supplies and uses of surface- and groundwater (Ostdiek, 2009) and requires Natural Resources Districts (NRDs) to understand the effect of groundwater use on surface-water systems when developing a groundwater management plan. The recent (2000–06) drought has increased concerns about the long-term sustainability of surface- and groundwater resources as well as concerns about the effect of groundwater use for irrigation on streamflow in Nebraska (Peterson and others, 2008).

The Upper Loup Natural Resources District (ULNRD) is located in the west-central part of the Sand Hills and overlies the nationally important High Plains aquifer (fig. 1). The Loup River and its tributaries, with their headwaters in the ULNRD, contribute substantially to supplying base flow to more intensively irrigated areas downstream. Although groundwater use for irrigation is fairly limited in the ULNRD compared to other areas of Nebraska, the streams within the ULNRD are sensitive to consumptive groundwater use because of interaction between groundwater and surface water (Peterson and others, 2008). The complexity of this hydrologic system and the interaction between the available surface-water and groundwater resources is not yet fully understood.

The ULNRD currently is participating in studies developing the Elkhorn-Loup Model (ELM) (Peterson and others, 2008; Stanton and others, 2010) to understand the impact of various groundwater management scenarios on surface-water resources. The ELM development is a coordinated effort involving 10 NRDs, the Nebraska Department of Natural Resources, the University of Nebraska, Conservation and Survey Division (CSD), and the U.S. Geological Survey (USGS). The ELM studies began in 2006 and are being completed in three separate phases. During Phase 1 of the ELM studies, a lack of subsurface geological information in the ULNRD was identified as a gap in present knowledge that needed to be addressed. Test holes drilled to the base of aquifer in the ULNRD were as much as 25 miles apart.

Given the variable character of the hydrostratigraphic units that compose the High Plains aquifer, substantial

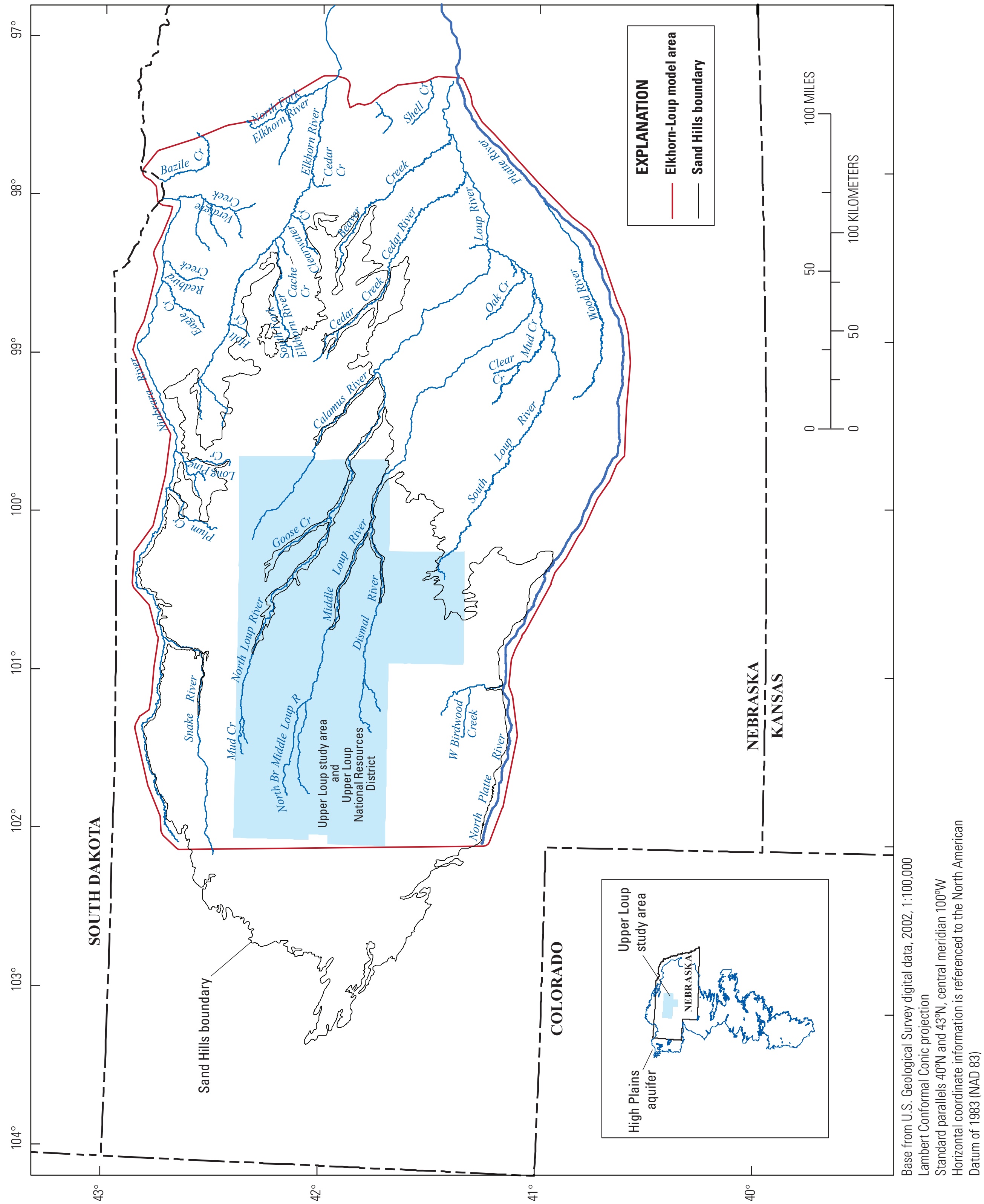

Figure 1. Location of the upper Loup study area within the Elkhorn-Loup groundwater model area.

uncertainty in aquifer thickness and characteristics can exist between test holes. In 2008, the USGS, in cooperation with the ULNRD and University of Nebraska Conservation and Survey Division, began a hydrogeologic study of the ULNRD to describe the lithology and thickness of the High Plains aquifer and the topology of the bedrock surface at the base of the aquifer. Knowledge of these characteristics is important for assessing water supplies and understanding groundwater flow systems.

Purpose and Scope

The purpose of this report is to provide a hydrostratigraphic interpretation of test-hole and surface geophysical data collected in the ULNRD. This report documents the methods of data collection and analysis, presents test-hole and surface geophysical survey results and interpretations, and examines the utility of these techniques in improving the hydrostratigraphy. The geologic and geophysical data collected from the additional test holes and surface geophysical data are intended to refine interpretations in the base-of-aquifer elevation map being used for the Phase 3 ELM groundwater model.

Of nine test holes drilled to the base of the High Plains aquifer (fig. 2; table 1), six were drilled since McGuire and Peterson (2008) previously interpreted the base of the aquifer beneath the ELM area. Surface geophysical data also were collected using time-domain electromagnetic (TDEM) and audio-magnetotelluric (AMT) methods at selected locations to supplement test holes for identifying the base of the High Plains aquifer. Included in this report are the generalized lithologic and borehole geophysical logs from all nine test holes and surface geophysical data collected.

Study Area Description

The ULNRD is the study area for this report, hereafter referred to as the upper Loup study area, which is located in the west-central Sand Hills at the headwaters of the North, Middle, and South Loup Rivers and almost the entire Dismal River drainage basin (fig. 1). The Sand Hills region of Nebraska is the largest dune field in the Western Hemisphere currently stabilized by vegetation (Bleed, 1989). Of the 4.13 million acres composing the upper Loup study area, approximately 91.5 percent is rangeland, 4.7 percent is open water and wetlands, 1.4 percent is barren, 1.1 percent is irrigated cropland, with riparian forest and woodland, dry-land crops, and unclassified land uses all constituting less than 1 percent each (Center for Advanced Land Management Information Technology, 2007).

The climate in the upper Loup study area is characterized by cold winters and warm summers typical of continental mid-latitude locations (Mast and Turk, 1999). Mean monthly temperatures ranged from 22.3 degrees Fahrenheit (ºF) in January to 74.7ºF in July during 1931–89 (National Oceanic and Atmospheric Administration, 2010). The mean annual precipitation was 20.9 inches (in.) at the Halsey 2W weather station, near Halsey, Nebr. (fig. 2) from 1931–90 (National Oceanic and Atmospheric Administration, 2010) with the greatest precipitation occurring during the spring and summer months. Potential evaporation, similar to that of precipitation, increases during the growing season, peaking in July, and often exceeds precipitation (Chen and others, 2003).

The surface of the upper Loup study area is mantled with deposits of Quaternary age: eolian dunes and alluvium in modern stream valleys (Swinehart and Diffendal, 1989). The eolian dunes presently are stabilized with grasses, but during the past 15,000 years severe droughts triggered their remobilization because of vegetative cover loss (Loope and Swinehart, 2000). Numerous lakes and wetlands formed when migrating sand dunes blocked stream systems (Loope and others, 1995; Mason and others, 1997). Such lakes and wetlands are hydrologically connected to the High Plains aquifer (Winter, 1986) and can persist even during times of prolonged drought (Loope and Swinehart, 2000).

Unique physical characteristics of the Sand Hills have allowed a net gain to the groundwater system with time and resulted in storage of a substantial amount of water beneath the upper Loup study area. Chen and others (2003) noted that the permeability of the soils in the Dismal River and Middle Loup River areas (fig. 2) combined with thick unsaturated zones beneath dunes increases the amount of precipitation reaching the water table and reduces groundwater loss to evapotranspiration. Additionally, snowmelt can contribute substantial amounts of recharge because evapotranspiration rates typically are very small at that time of year.

One aspect unique to streams in the study area compared to other streams in Nebraska is the steadiness of streamflow, which is the result of highly permeable soils and large amounts of groundwater in storage. Runoff-induced high-flow events are rare within the upper Loup study area because of the ability of permeable soils to capture precipitation. This results in streamflow that is dominated by groundwater discharge or base flow. Bentall (1989) estimated that the Middle Loup River and the Dismal River above Dunning, Nebr. (fig. 2) have groundwater contributions exceeding 95 percent of total streamflow. Szilagyi and others (2003) have reported similar findings for areas in the west-central Sand Hills. Streamflow of the Middle Loup and Dismal Rivers remains steady even during periods of drought and responds more slowly to changes in climatic conditions than do other streams in the Sand Hills east of the upper Loup study area. This was attributed to greater aquifer thicknesses, increased groundwater storage, and steeper hydraulic gradients near the Middle Loup and Dismal Rivers (Chen and others, 2003).

Geologic Setting

The upper Loup study area overlies the thickest parts of the High Plains aquifer system, where saturated thicknesses can exceed 1,000 feet (300 m) (McGuire and Fischer, 1999).

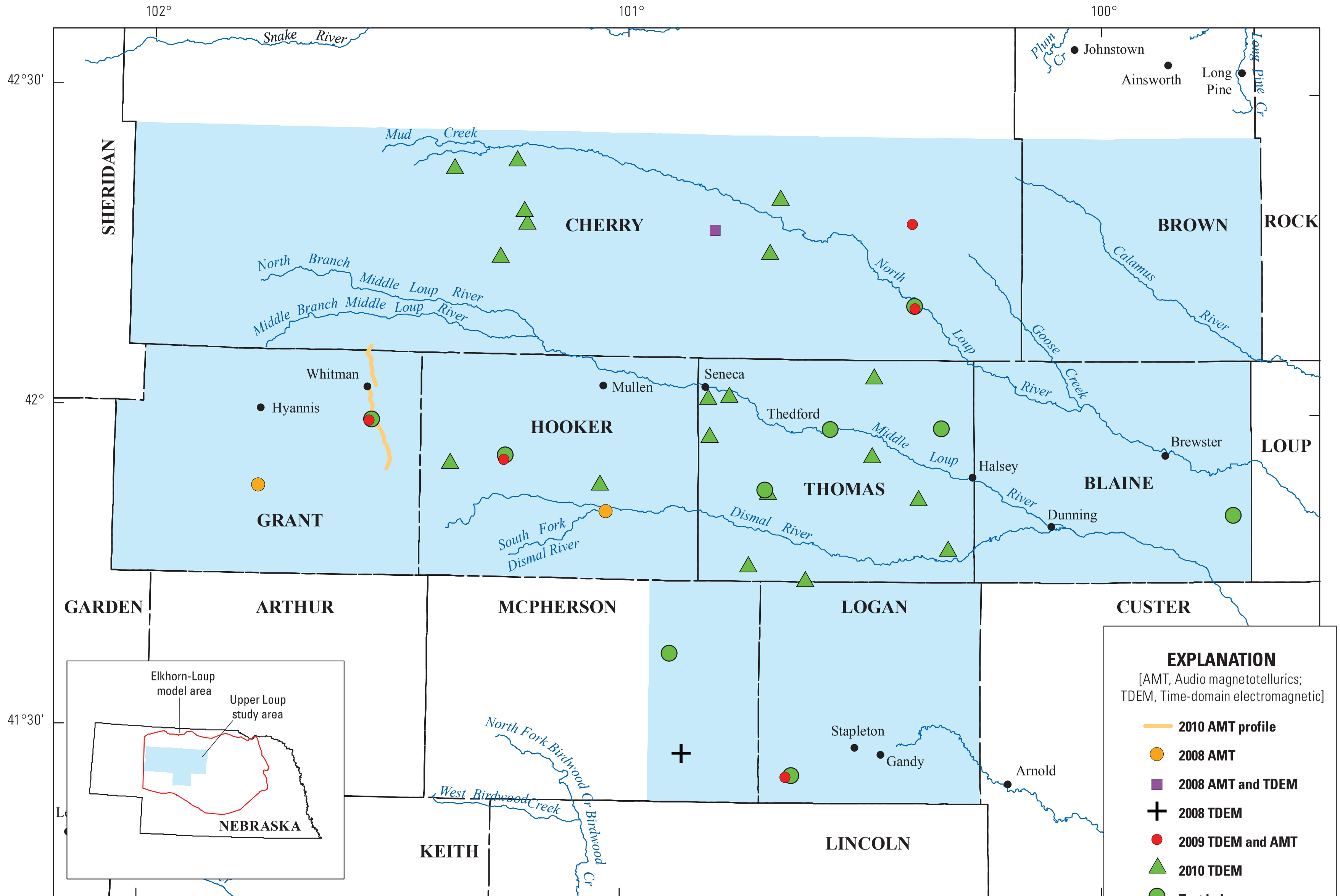

Base from U.S. Geological Survey digital data, 2002, 1:100,000
Lambert Conformal Conic projection
Standard parallels 40°N and 43°N, central meridian 100°W
Horizontal coordinate information is referenced to the North American Datum of 1983 (NAD 83)

Figure 2. Location of drilled test holes and time-domain electromagnetic (TDEM) and audio-magnetotelluric (AMT) soundings, upper Loup study area, 2008 to 2010.

Table 1. Field name, site number, location, and elevation of test holes.

[Legal descriptions: T., township; R., range; S., section; ABCD, codes for the quarter section, quarter-quarter section, quarter-quarter-quarter section, and quarter-quarter-quarter-quarter sections A, B, C, and D, respectively, where A is northeast, B is northwest, C is southwest, and D is southeast quarter of the next larger unit; Predicted minus drilled, indicates the predicted base-of-aquifer elevation from Scientific Investigations Map 2008–3042 minus the drilled base-of-aquifer elevation at test hole; -- indicates test hole was included in Scientific Investigations Map 2008–3042 and a difference not calculated]

Field name	County	Site number[1]	Legal description	Latitude[2]	Longitude[2]	Elevation[3] (feet)	Date drilled	Depth to base of aquifer (feet)	Predicted minus drilled (feet)
1-UL-08	Logan	412611100384403	T.17N R.29W S.22ABBB	41.43639	-100.64556	3,038	8/22/2008	800	--
2-UL-08	McPherson	413735100540503	T.19N R.31W S.9CCCC	41.62639	-100.90139	3,260	8/25/2008	795	--
3-UL-08	Thomas	415840100340803	T.23N R.28W S.9DBBB	41.97778	-100.5685	2,855	8/28/2008	690	--
1-UL-09	Grant	415909101314803	T.23N R.36W S.7ABAC	41.98583	-101.53000	3,600	8/4/2009	1,040	300
2-UL-09	Hooker	415554101145403	T.23N R.34W S.27CCCD	41.93167	-101.24833	3,370	8/7/2009	920	135
3-UL-09	Cherry	421016100233303	T.25N R.26W S.6BADD	42.17111	-100.39250	2,749	8/12/2009	600	5
1-UL-10	Thomas	415301100421703	T.22N R.29W S.17BBAA	41.88333	-100.70444	3,060	7/27/2010	800	-15
2-UL-10	Thomas	415848100200803	T.23N R.26W S.9ACCB	41.98000	-100.33556	2,850	7/30/2010	695	-157
3-UL-10	Blaine	415043099433103	T.22N R.21W S.26CCBB	41.84528	-99.72528	2,540	8/4/2010	605	-40

[1]Site identification number assigned by U.S. Geological Survey.

[2]Decimal degrees; North American Datum of 1983 (NAD 83).

[3]Land-surface elevation above National Geodetic Vertical Datum of 1929 (NGVD 29); elevations surveyed to nearest foot.

Here the High Plains aquifer is considered to include all hydrologically connected units of Tertiary and Quaternary age. According to Gutentag and others (1984), these rocks are the upper units of the Oligocene-age Brule Formation of the White River Group (herein referred to as the Brule Formation), the Miocene-age Arikaree Group, the Miocene-age Ogallala Formation, and Quaternary-age alluvial and eolian deposits. The Brule Formation forms the base of the High Plains aquifer in the upper Loup study area. All previously mentioned units are shown in the hydrostratigraphic column presented in figure 3.

The geologic history relevant to this present study begins roughly 70 million years ago. During Cretaceous time, the Sand Hills region was covered by a shallow inland sea, and marine sediments, including the thick Pierre Shale, were deposited. Following regression of the Cretaceous sea, uplift resulted in formation of the Chadron and Cambridge Arches striking northwest to southeast across the upper Loup study area (Swinehart and others, 1985). Subsequent fluvial erosion removed as much as 1,800 ft (550 m) of the Cretaceous section and created a structural low over the previously uplifted region.

Overlying the Pierre Shale is the Brule Formation (fig. 3), which underlies the entire study area. The Brule Formation is a massive siltstone composed of primarily eolian silt, with some alluvial deposits. Deposits of volcanic ash derived from eruptions in the western United States compose two-thirds of its volume. The Brule Formation is relatively impermeable when unfractured (Cannia and others, 2006).

Overlying the Brule Formation is the Arikaree Group, which is largely limited to the western part of the study area or may exist in paleovalleys in the eastern part of the study area (Swinehart and Diffendal, 1989). The Arikaree Group is a massive, very-fine to fine-grained sandstone with localized beds of volcanic ash, silty sand, and sandy clay (Darton, 1903; Condra and Reed, 1943). The Arikaree Group is considered part of the High Plains aquifer system; however, it does not yield large quantities of water to wells (Gutentag and others, 1984). Within the upper Loup study area, the Arikaree Group typically is not used as a water source.

The Ogallala Formation (referred to herein as the Ogallala) is the principal geologic unit in the High Plains aquifer system and can reach a thickness of 800 ft (240 m) beneath the upper Loup study area (Diffendal, 1991). The Ogallala is composed of a poorly sorted mixture of sand, silt, clay, and gravel (Condra and Reed, 1943). The Ogallala generally is unconsolidated or weakly consolidated, but contains layers of sandstone cemented by calcium carbonate. When covered by younger deposits, the Ogallala has not been subdivided into formations recognized in other areas because of the difficulty correlating these units in the subsurface. The Ogallala was deposited by aggrading streams that filled paleovalleys eroded into older rocks (Swinehart and others, 1985). Beneath the upper Loup study area, the Ogallala typically is composed of fine to medium-grained sand and sandstone (Swinehart and Diffendal, 1989). Although the lithology of this unit can be fairly uniform, the base of the Ogallala is a complex surface formed

<table>
<tr><th>PERIOD</th><th>EPOCH</th><th colspan="2">STRATIGRAPHIC UNIT</th><th>LITHOLOGY</th><th>HYDROSTRATIGRAPHY</th></tr>
<tr><td rowspan="2">Quaternary</td><td>Holocene</td><td colspan="2">Alluvium and eolian deposits</td><td rowspan="2">Gravel, sand, silt, and clay</td><td rowspan="5">High Plains aquifer</td></tr>
<tr><td>Pleistocene</td><td colspan="2">Long Pine Formation and undifferentiated alluvial and eolian deposits</td></tr>
<tr><td rowspan="5">Tertiary</td><td>Pliocene</td><td colspan="2">Broadwater Formation</td><td>Gravel and sand</td></tr>
<tr><td rowspan="2">Miocene</td><td colspan="2">Ogallala Formation</td><td>Gravel, sand, silt, and clay</td></tr>
<tr><td colspan="2">Arikaree Group</td><td>Very fine to fine-grained sandstone</td></tr>
<tr><td rowspan="2">Oligocene</td><td rowspan="2">Brule Formation</td><td>Upper</td><td>Siltstone and sandstone</td><td rowspan="3">Confining unit(s)</td></tr>
<tr><td>Lower</td><td>Siltstone and claystone</td></tr>
<tr><td>Cretaceous</td><td>Late</td><td colspan="2">Pierre Shale</td><td>Shale</td></tr>
</table>

Modified from Swinehart and Diffendal, 1989, and Gutentag and others, 1984

Figure 3. Stratigraphic, lithologic, and hydrostratigraphic column of the High Plains aquifer and confining units of the upper Loup study area.

by multiple episodes of erosion. The location of Ogallala-filled paleovalleys has been proposed by previous researchers (Swinehart and Diffendal, 1989; Swinehart and others, 1985), but may represent only a fraction of the drainage systems that existed during Miocene time. Much of the deposition was restricted to valleys along drainage systems originating from mountains in Wyoming and Colorado (Swinehart and others, 1985), but deposition may have occurred on broad, low-relief plains as well (Swinehart and Diffendal, 1989).

An unconformity of at least 1.5 million years separates the Ogallala from the Pliocene Broadwater and the Pleistocene Long Pine formations (Swinehart and Diffendal, 1989). These sediments, from sources in central Wyoming and northern Colorado (fig. 1) (Stanley and Wayne, 1972) are unevenly deposited and preserved but contain coarse sand and gravel separated by finer-grained deposits covering the Ogallala in much of the upper Loup study area. Pliocene and Pleistocene fluvial deposits average 50 ft (15 m) in thickness, but can be as thick as 300 ft (91 m) (Swinehart and Diffendal, 1989), and are in hydrologic connection with the underlying Ogallala. The Broadwater and Long Pine Formations, parts of the High Plains aquifer, are used as a water source where sufficient saturated thicknesses are present.

Much of the Quaternary deposits of gravel, sand, silt, and clay resulted from stream and eolian erosion and deposition that heavily reworked the Tertiary units (Swinehart and Diffendal, 1989; Weeks and Gutentag, 1988). Quaternary-age eolian deposits mantle the entire upper Loup study area except for the Middle and North Loup River valleys and southern Logan County (Swinehart, 1989). Most eolian deposits are mainly above the regional water table and typically are not used as a water source (Peterson and others, 2008). Quaternary-age alluvial sand and gravel are found in modern stream valleys of the Loup River system and are often used as a water source.

Methods

Site and Method Selection

This section of the report details the rationale for the selection of test-hole and geophysical data-collection locations. Site selection for test-hole drilling and surface geophysical data collection was determined by several factors, but sites primarily were chosen to fill existing spatial gaps left in the test-hole database (University of Nebraska-Lincoln, Conservation and Survey Division, 2011). Test-hole drilling and subsequent monitoring-well installation locations were chosen in coordination with the ULNRD to locate nested monitoring wells for long-term water-level and water-quality information as part of the long-term monitoring plans (Anna Baum, oral commun., 2008). Surface geophysical data were collected to provide a quick, non-invasive method to fill spatial gaps in the existing test-hole coverage. For data collected in 2008 and 2009, surface geophysical sounding locations were selected close to previously drilled or planned test holes to verify that these geophysical techniques could identify the base of the aquifer reliably. Test-hole drilling and geophysical sounding locations also depended on site accessibility and landowner permission.

Geophysical methods were selected based on physical characteristics of the hydrostratigraphic units of the upper Loup study area and the anticipated depth to the base of the aquifer. Examination of previously collected CSD borehole geophysical logs indicated a sharp contrast in electrical resistivity between the Brule Formation and the overlying units of the High Plains aquifer system. After consideration of the anticipated depth to the base of the aquifer (top of the Brule Formation), two surface geophysical methods were chosen: time-domain electromagnetic (TDEM) and audio-magnetotelluric (AMT) methods. These surface geophysical methods detect variations in the electrical properties of earth materials — in particular, electrical resistivity, or its inverse, electrical conductivity. A lower electrical resistivity corresponds to higher porosity or smaller grain size, or both, because of the higher surface area associated with fine particles that promote the transmission of electrical current (Biella and others, 1983; Kwader, 1985). Higher electrical resistivity is associated with coarse-grained deposits such as alluvial sand and gravel or sandstone. As such, electrical resistivity can be correlated with geologic units on the surface and at depth using lithologic logs to provide a picture of subsurface geology. The principles of operation and field application of each technique are explained in detail in the Surface-Geophysical Data Collection section of this report. More information regarding the electrical properties of rocks can be found in Keller (1987, 1989), Palacky (1987), Hearst and Nelson (1985), Hallenburg (1998), and Hearst and others (2000).

The depth of investigation was a consideration in the selection of the surface geophysical method. The depth of investigation for the TDEM method is variable, but is roughly 2 to 3 times the size of loop length. The AMT method is able to resolve subsurface features from tens of feet to nearly 2,500 ft (tens of meters to 760 m) in depth. For this reason, use of the AMT technique was particularly important in areas where the base of aquifer was deepest. Another advantage of the AMT technique is the ability to examine the lateral variability of the subsurface with depth. In contrast, the TDEM method provides a one-dimensional view of the subsurface, which can be viewed as a virtual borehole. Further discussion of the TDEM and AMT methods and their application is presented in the Surface-Geophysical Data Collection section of this report.

Test-Hole Drilling and Borehole Geophysics

Presented in the Test-Hole Lithologic and Borehole Geophysical Logs section and Supplemental Data section of this report are the generalized lithologic descriptions and borehole geophysical logs for nine test holes drilled to the base of the High Plains aquifer (top of Brule Formation). Original copies of the lithologic logs of each test hole are filed at the U.S. Geological Survey in Lincoln, Nebr. All borehole geophysical logs are archived in accordance with USGS protocol (U.S. Geological Survey, 2009). At the present time (2011), final stratigraphic interpretations have not been completed. Consequently, the stratigraphic units composing the High Plains aquifer are undifferentiated, and only the base of the aquifer at each test hole has been reported.

Test-Hole Drilling Method and Procedure

Test-hole drilling with mud-rotary drilling equipment has been an integral part of groundwater and geologic studies in Nebraska for many years (Goeke, 2000). Mud-rotary test-hole drilling and sampling required the use of drilling fluid suitable for geologic conditions. As the drill stem was advanced, typically in 5-ft (1.5-m) increments, the time required to advance each increment was recorded along with the drilling action. Drill cuttings were circulated to the surface, collected, examined immediately, and lithologically described. Described samples were bagged, labeled, and provided to the CSD for further examination under a petrographic microscope before the final assignment of stratigraphic intervals and their publication in county test-hole log books. Although the precise contacts of certain hydrostratigraphic units have not been determined, logged lithologic characteristics can provide information on the hydrostratigraphic units sampled. In many test-hole logs published by CSD (Goeke, 2000; Wigley, 2000; University of Nebraska-Lincoln, Conservation and Survey Division, 2011), the Ogallala is indicated by presence of siliceous plant roots (rootlets). In most areas of western and north-central Nebraska, late-Tertiary rocks contain numerous fossil seeds of grasses and forage herbs. These provide the best means to identify Tertiary units from the upper part of the Arikaree Group to the top of the Ogallala (Condra and Reed, 1943).

Data from the three test holes drilled in 2008 were included in the Scientific Investigations Map (SIM) 2008-3042 for the ELM area (McGuire and Peterson, 2008). Additional test holes drilled in 2009 and 2010 have allowed further improvements in the interpretations of the base of aquifer and will be used to refine the base-of-aquifer configuration used for the Phase 3 ELM. Locations of all test holes are shown in figure 2, and test-hole locations and dates drilled are listed in table 1.

Borehole Geophysical Data Collection

Borehole geophysical data were collected at each test-hole location using a Century 8144 Multi-Parameter electrical-log tool (Century Geophysical Corp., 2011a). The Century 8144 tool measures long-normal [64 in. (1.6 m)] and short-normal [16 in. (0.41 m)] electrical resistivity, natural gamma radiation, spontaneous potential, and fluid resistivity. The types of geophysical logs collected are described briefly in the following paragraphs. Further information regarding borehole geophysics can be found in Keys (1990).

Normal-resistivity logs measure the electrical resistivity of sediment, rocks, and water surrounding the borehole. Electrical resistivity measurements consisted of long-normal [64 in. (1.6 m)] and short-normal [16 in. (0.41 m)], each having different volumes of investigation. Short-normal logs have a smaller volume of investigation and, therefore, are affected more by the resistivity of the drilling fluid and the invaded zone that develops on the borehole wall. Correspondingly, long-normal logs have a larger volume of investigation and are less affected by drilling fluid. Intervals where these two logs diverge indicate areas of permeability where drilling fluid has invaded the formation (Anderson and others, 2009).

Natural gamma logs measure natural gamma radiation being emitted by the formation surrounding the borehole (Keys, 1990). Clay tends to accumulate radioisotopes through adsorption and ion-exchange processes. Most clays, particularly illites, have high gamma activity because of the presence of potassium in their crystal structure. As such, zones of high gamma activity typically are interpreted as being clay rich. Volcanic ash, organic shale and feldspathic or arkosic sandstones also can give higher gamma responses (Anderson and others, 2009).

Spontaneous-potential logs (often referred to as self-potential or SP) measure differences in the electrical potentials that develop in a borehole at lithologic or water-quality interfaces (Anderson and others, 2009). Differences in electrical potential often are caused by differences between the salinity of the borehole fluid and that of the formation fluid (Keys, 1990). When the borehole fluid is fresher than the formation fluid, electric current flow is such that SP will deflect in a negative direction; conversely, when the formation fluid is fresher than the borehole fluid then electric current flow is such that SP will deflect in a positive direction (Stanton and others, 2007).

Electrical conductivity (inverse of resistivity) also was recorded with an electromagnetic-induction tool, which measures the conductivity of formations and water surrounding the borehole. The electromagnetic induction log was collected using a Century 9512 slim-hole induction tool (Century Geophysical Corp., 2011b). The tool measured formation conductivity within an area 10 to 50 in. (0.25 m to 1.3 m) from an open borehole. The tool is not affected by nearby borehole fluid or where drilling fluid has invaded the formation. The induction tool was calibrated according to specified guidelines (Century Geophysical Corp., 2011b). The induction tool was lowered into the borehole and the temperature of the tool was allowed to equilibrate with the surrounding formation. Before data collection, the induction tool was quickly raised to land surface and calibrated “in air” for a zero conductivity measurement and using a 690 millimhos per meter (mmho/m) conductivity ring.

All test holes were logged with the Century 8143 Multi-Parameter E-Log tool with the exception of test hole 1-UL-08. A wiring problem in the draw works prevented data collection, and only the generalized lithologic log is provided. Intermittent problems were encountered with the Century 8144 multi-parameter tool: negative long-normal resistivity values were recorded at some test holes. As a result, the long-normal resistivity was not included for the 1-UL-09, 2-UL-10, and 3-UL-10 borehole logs. All logged test holes were logged to a depth below the base of the aquifer with the Century 8143 multi-parameter tool, with the exception of test hole 3-UL-10. An irregularity in the test hole at 3-UL-10 prevented the multi-parameter tool from being lowered below the base of the aquifer. As a result, resistivity and natural gamma data were collected using a Century 9512 electromagnetic induction tool below the base of aquifer at that site.

Surface-Geophysical Data Collection

Time-Domain Electromagnetic

Time-Domain Electromagnetic (TDEM) Method

TDEM is an inductive electromagnetic technique that provides a measure of near-surface resistivity by passing a current through a wire loop which, as explained by Ampere’s law, generates a primary magnetic field. The primary current is rapidly turned off, thereby causing a time-varying change in magnetic flux, which induces voltages, and hence eddy currents, in conductive bodies, according to Faraday’s law. In TDEM, a secondary magnetic field is produced by the decay of these subsurface eddy currents, and typically is measured as a voltage with time after primary current turnoff at one or more surface receivers. An apparent resistivity is calculated from the measured voltage at the receiver coil and the time elapsed after turnoff.

The apparent resistivity is solely a mathematical transform; however, it serves two important purposes. First, subtle differences in the measured receiver voltage caused by changes in subsurface resistivity are accentuated by the power-law dependence of apparent resistivity on elapsed time and voltage. Second, the TDEM response of a homogenous, isotropic earth is such that the apparent resistivity is time dependent, but asymptotic to the true half-space resistivity at late times after turnoff. For more complicated, heterogeneous earth structure, the variation of apparent resistivity with time can be viewed as a proxy for the variation of true-earth resistivity with depth. The actual electrical resistivity distribution in the earth is computed from the measured apparent resistivity through the process of inversion. Additional details on the TDEM sounding method can be found in Christiansen and others (2011), Fitterman and Labson (2005), Danielsen and others (2003), and Nabighian and Macnae (1991).

Time-Domain Electromagnetic (TDEM) Data Collection

A total of 26 TDEM soundings were collected within the upper Loup study area between 2008 and 2010 (fig. 2). In

2008, two soundings were acquired in close proximity to previously drilled CSD test holes. An additional five soundings were collected in 2009, three of which were followed up by new test holes. The 2010 data-collection plan was expanded to 19 soundings specifically targeting locations where little information existed. The location and site name for each sounding collected are presented in table 2.

TDEM data were collected using two systems: a Zonge NanoTEM/ZeroTEM system was used in 2008, and a Geonics ProTEM system was used in 2009–10. All data were collected using a 328-ft by 328-ft (100-m by 100-m) square transmitter loop. The depth of investigation scales with the transmitter moment (number of wire turns times transmitter current times transmitter loop area), with a rule of thumb placing the depth of investigation at 2–3 times the length of a side of the square transmitter loop; therefore, depth investigated for this study corresponds to 656 to 984 ft (200 to 300 m). At all locations, data were collected in a central-loop configuration where the receiver loop was placed at the center of the transmitter loop. From 2009 onward, additional data were collected outside of the transmitter loop at a distance of 328 ft (100 m) from the transmitter loop edge. Out-of-loop data were used as a qualitative check on the assumption of one-dimensionality (layer-cake earth structure) required for subsequent modeling and inversion. Out-of-loop data is recorded as the time derivative of the secondary magnetic field or dB/dt, where B is the magnetic induction. The out-of-loop data also were modeled and inverted jointly with the central-loop data to better constrain the final resistivity models.

Calibration of a TDEM system is essential to an accurate recovery of near-surface resistivity structure (Christiansen and others, 2011). Calibration, in this context, refers to a particular combination of data logger, transmitter, and receiver, and involves the characterization of system filters, the knowledge

Table 2. Upper Loup time-domain electromagnetic (TDEM) site coordinates, elevation, county, and acquisition year.

[Northing and easting in Nebraska State Plane coordinates]

Site	Latitude[1]	Longitude[1]	Northing (feet)	Easting (feet)	County	Elevation[2] (feet)	Year
SH7	42.28773	-100.81356	895092	1420332	Cherry	3,039	2008
SH8	41.47070	-100.87394	597630	1400990	McPherson	3,192	2008
CN1	41.98464	-101.53369	787331	1223579	Grant	3,587	2009
CN2	41.92688	-101.25098	765054	1300107	Hooker	3,399	2009
CN3	41.43396	-100.65705	583723	1460306	Logan	3,044	2009
CN4	42.16822	-100.39113	850754	1534411	Cherry	2,760	2009
CN5	42.29998	-100.39816	898768	1532725	Cherry	2,823	2009
UL1	42.39735	-101.23127	936364	1307910	Cherry	3,297	2010
UL2	42.38449	-101.36321	932215	1272207	Cherry	3,379	2010
UL3	42.31846	-101.21419	907558	1312117	Cherry	3,385	2010
UL4	42.24699	-101.26374	881714	1298341	Cherry	3,416	2010
UL5	42.29881	-101.20844	900378	1313573	Cherry	3,372	2010
UL6	41.96938	-100.82020	779132	1417436	Thomas	3,103	2010
UL7	42.03190	-100.78048	801807	1428438	Thomas	3,078	2010
UL8	42.02801	-100.82353	800498	1416734	Thomas	3,081	2010
UL9	41.87274	-100.38286	743101	1536176	Thomas	2,807	2010
UL10	41.93864	-100.48038	767239	1509756	Thomas	2,874	2010
UL11	41.79325	-100.32051	714074	1553043	Thomas	2,763	2010
UL12	42.06173	-100.47670	812077	1511005	Thomas	2,937	2010
UL13	42.34067	-100.67524	914059	1457901	Cherry	2,929	2010
UL14	42.25532	-100.69699	883009	1451772	Cherry	2,966	2010
UL15	41.76738	-100.73760	705348	1439262	Thomas	3,105	2010
UL16	41.74462	-100.61729	696799	1472014	Thomas	2,994	2010
UL17	41.92342	-101.36381	764260	1269396	Hooker	3,475	2010
UL18	41.89260	-101.04908	751838	1354877	Hooker	3,258	2010
UL19	41.88077	-100.69763	746561	1450496	Thomas	3,039	2010

[1]Decimal degrees; North American Datum of 1983 (NAD 83).

[2]Land-surface elevation above National Geodetic Vertical Datum of 1929 (NGVD 29); elevations surveyed to nearest foot.

of system geometry, measurement of the transmitted waveform, an assessment of system bias, and correction for timing and normalization errors. The ProTEM and Zonge systems used in this study were calibrated in 2009 at an established test site at Lyngby, Denmark (Geological Institute, 2002a and 2002b).

In 2009–10, data were collected at a range of base frequencies (285, 75, 30, 7.5, and 3 hertz [Hz]) using a combination of high- and low-frequency receivers together with low- and high-current transmitters. Average current was 2.5 and 8.0 amperes (A) for the low- and high-current transmitters, giving rise to an average transmitter moment of 270,000 ampere-square feet (A-ft^2) (25,000 A-m^2) and 915,000 A-ft^2 (85,000 A-m^2), respectively. All data were collected with air coil receivers with moments of 340 A-ft^2 (31.4 A-m^2) and 2,150 A-ft^2 (200 A-m^2) for high- and low-frequency coils, respectively. At each base frequency, individual voltage decay curves, corresponding to a single current pulse, were averaged over a time interval between 4 and 15 seconds. A minimum of 20 such readings were made to permit robust error calculation. Background noise measurements also were made with each receiver at each station by acquiring data with the transmitter turned off. Such noise measurements are used during processing to determine the time at which actual data fall below the measured noise envelope.

Data acquired with the Zonge system utilized low- and high-power transmitters, coupled with a single-turn 16.4-ft by 16.4-ft (5-m by 5-m) loop receiver and a TEM/3 induction coil receiver, respectively. Data were recorded at base frequencies of 32 and 2 Hz, with average currents of 7 and 26 A, respectively, giving rise to transmitter moments ranging from 322,000 A-ft^2 (30,000 A-m^2) to 2,800,000 A-ft^2 (260,000 A-m^2). At each base frequency, as many as 1,024 transients were averaged to form a single data record. A minimum of 20 data records were collected to permit robust error calculation. Noise measurements also were made with each receiver at each station by acquiring data with the transmitter turned off.

Time-Domain Electromagnetic (TDEM) Data Analysis

Data analysis for all soundings consisted of data format conversion, statistical analysis and averaging, forward modeling, data inversion, and model assessment. Data were processed and inverted using the SiTEM data processing and Single-Site Electromagnetics Data Inversion (SEMDI) software packages (Auken and Nebel, 2001). The SEMDI inversion permitted full waveform specification, the modeling of system filters, and the incorporation of data errors. Furthermore, SEMDI reported error bounds on inverted parameters (layer thicknesses and resistivities). Data were inverted for two end-member model classes – minimum-layer models and 20-layer, smooth or Occam-style, inverse models (Constable and others, 1987). The former class of models seeks to fit the measured data with as few distinct layers as possible, whereas the latter seeks to fit the data with a large number of thin layers of fixed thickness under the constraint that the resistivity varies slowly between adjacent layers. Minimum-layer models are more appropriate in settings where abrupt changes in resistivity are expected, whereas smooth inverse models are more realistic when gradual changes are expected. Independent knowledge from geologic mapping, borehole lithology, and geophysical borehole logs typically are used to assess which of the above model classes may be more appropriate in interpreting subsurface structure.

The modeling and inversion of TDEM data are commonly one-dimensional (1D) analyses. This assumption is reasonable given the nature of the regional geology (laterally expansive sedimentary deposits), the compact footprint of the TDEM method, and the limited depth of investigation (as much as 1,000 ft [305 m]). Furthermore, lithologic and stratigraphic logs from surrounding test holes indicate lateral correlation across the study area. Finally, with the exception of the 2008 soundings, where out-of-loop data were not recorded, joint inversion of the in- and out-of-loop data are consistent with a 1D subsurface resistivity structure.

Some geophysical models, including TDEM models, exhibit a degree of non-uniqueness. As such, available ground-truth from test-hole logs was needed to model TDEM data and constrain interpretations. The non-uniqueness stems from inherent resolution limitations, and incomplete and inexact data. Thus, for any measured data set, typically a range of models can be determined that adequately fit the data. For most electrical methods, equivalence exists between models with equal conductance (depth-integrated conductivity). Thus, for example, a model with a 10 ohm-m, 164-ft (50-m) thick layer produces nearly identical measured data as a 33-ft (10-m) thick layer with a resistivity of 2 ohm-m. Additionally, the TDEM method has difficulty resolving resistive layers because of the low current densities induced within them as compared to conductive layers.

Audio Magnetotelluric (AMT)

The Magnetotelluric Method

The magnetotelluric (MT) method is a passive surface geophysical technique that uses the Earth’s natural electromagnetic fields to investigate the electrical resistivity structure of the subsurface. It does so by measuring time variations in the Earth’s natural electric and magnetic fields. Worldwide lightning activity at frequencies of about 10,000 to 1 Hz and geomagnetic micropulsations at frequencies of 1 to 0.001 Hz provide the main source of signals used by the MT method. The natural electromagnetic waves propagate vertically in the Earth because of the large contrast in the resistivity between the air and the Earth, which causes a vertical refraction of the electromagnetic wave at the Earth’s surface (Vozoff, 1972). The MT method is well-suited for studying complicated geological environments because the electric and magnetic fields are sensitive to vertical and horizontal variations in electrical resistivity.

"Skin depth" is considered to be the depth of investigation at a particular frequency, given an apparent resistivity of the medium. Skin depth calculations were used during survey design to determine what frequencies would be sampled and, thus, how long the magnetotelluric fields would be sampled. At least 20–30 cycles of the data were measured at the lowest frequencies. The definition of skin depth, δ, in meters, is described in equation 1 as,

$$\delta = \sqrt{\frac{2}{\omega\mu\sigma}} \approx 503\sqrt{\frac{\rho}{f}} \tag{1}$$

where ω is the angular frequency, which is equal to $2\pi f$, in hertz
μ is the magnetic permeability of the material through which the electromagnetic wave is passing through, in henries per meter
σ is the electrical conductivity, in siemens per meter
ρ is the apparent resistivity, in ohm-meters
f is the frequency, in hertz.

Skin depth is defined as the depth at which the primary magnetic field has fallen off (decreased) by approximately 1/ e, where e is a constant equal to 2.718281828.

The natural variations of the Earth's magnetic and electric field were recorded in two orthogonal, horizontal directions at each MT station as a function of time. The recorded time-series signals were used to derive apparent resistivity and phase after first converting them to complex cross spectra by using fast Fourier transform techniques and least-squares, cross-spectral analysis (Bendat and Piersol, 1971). For a two-dimensional (2D) Earth, the MT fields can be decoupled into transverse electric (TE) and transverse magnetic (TM) modes with "transverse" indicating that the field direction is either parallel or perpendicular to the geologic strike (fig. 4). For this study 2D geology was assumed with the survey transect oriented perpendicular to the geologic strike of interest, the MT data for the TE mode are for the electric field parallel to geologic strike (or perpendicular to the survey transect, Ex on figure 4) and the data for the TM mode are for the electric field across strike (parallel to the survey transect, Ey on figure 4). 2D modeling was done to fit both modes simultaneously.

The magnetotelluric response of a resistive body, such as an alluvial paleochannel incised into siltstone bedrock, is such that the TE mode is relatively insensitive to narrow resistors along the strike of the resistive paleochannel, and the TM mode is sensitive to narrow resistors oriented along the strike of the resistive paleochannel. On the other hand, the magnetotelluric response to the geologic strike of a narrow, electrically conductive prism, such as mineralized dikes and veins or water flow along faults and joints, is such that the TE mode is more sensitive to narrow conductors oriented along strike, and the TM mode is relatively insensitive to narrow conductors along strike. These factors illustrate the importance of considering that the estimated geologic strike must be accounted for

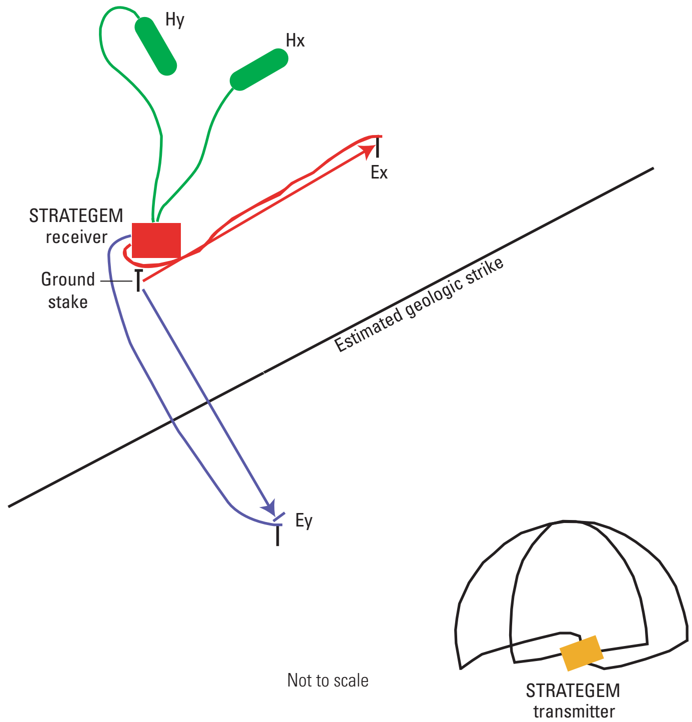

Figure 4. System layout for audio-magnetotelluric survey using STRATAGEM EH-4 system. Hx and Hy represent magnetic field receivers, and Ex and Ey represent the orthogonal ends of the dipoles used to measure the Earth's electric field. STRATAGEM transmitter usually was placed from 425 to 740 feet away from receiver station, depending on local near-surface geology. Azimuths and dipole lengths varied by site and are provided in tables 3 and 4.

when designing magnetotelluric surveys. An introduction to the MT method and references for a more advanced understanding are in Dobrin and Savit (1988), and Vozoff (1991).

The high-frequency range of magnetotellurics (ranging from approximately 10 Hz to as much as 100 kilohertz [kHz]) is usually called the audio-magnetotelluric (AMT) frequency range. With AMT methods, variations in ground electrical resistivity can be investigated from tens of feet to nearly 2,500 ft (tens of meters to 760 m) in depth. Traditionally, the use of the AMT technique was limited by a natural paucity of MT signals from around 1 to 5 kHz. However, the natural MT fields in this band were augmented by providing additional signal power with a small battery-powered transmitter (a controlled source) that reduces the potential loss of resolution at greater depths of investigation. The AMT technique is used to image shallow stratigraphy, subsurface channels, alluvium-bedrock contacts, and many kinds of bedrock structures including those associated with fracture zones.

Audio-Magnetotelluric (AMT) Data Collection

In the summer of 2008, 2009, and 2010, a total of 117 AMT soundings were acquired in the upper Loup study area (fig. 2). To take advantage of the 2D modeling capabilities

Table 3. Summary by site of audio-magnetotelluric (AMT) stations, geometry, location, and elevation for AMT data collected in 2008 and 2009.

[AMT, audio magnetotellurics; dipole length is 82 feet; azimuth given in degrees from North; northing and easting in Nebraska State Plane coordinates]

Year	County	AMT Station	Azimuth of Ex Dipole (fig. 4)	Azimuth of Ey Dipole (fig. 4)	Latitude[1]	Longitude[1]	Easting (feet)	Northing (feet)	Elevation[2] (feet)
Site 5-SH-87-AMT									
2008	Cherry	18	0	90	42.28383344	100.8143334	1420109.5	893674.5	3,060
		17			42.28474989	100.8142223	1420142.7	894008.1	3,056
		16			42.28572233	100.8141112	1420176.1	894362.1	3,054
		19			42.28666664	100.8138611	1420247.0	894705.5	3,050
		20			42.2876111	100.8139444	1420227.7	895049.8	3,041
Site 8-SH-89-AMT									
2008	Grant	25	0	90	41.88355554	101.7596113	1161435.2	751684.8	3,802
		26			41.8842779	101.7596666	1161425.5	751948.2	3,788
		24			41.88511122	101.758889	1161643.3	752247.4	3,780
		23			41.88588888	101.7583054	1161807.9	752527.4	3,764
		22			41.88669435	101.7578056	1161949.9	752818.0	3,738
Site 28-SH-87-AMT									
2008	Hooker	31	0	90	41.84341663	101.0312222	1359521.9	733863.6	3,259
		30			41.84455556	101.0316946	1359398.2	734280.0	3,255
		29			41.84544448	101.0319724	1359326.4	734604.7	3,246
		28			41.84633329	101.0321389	1359284.9	734929.0	3,241
		27			41.84722224	101.0321667	1359281.2	735252.9	3,219
Site Grant-AMT									
2009	Grant	1	0	90	41.9844302	101.5328736	1223799.7	787251.9	3,587
		2			41.98483688	101.5328053	1223820.9	787399.7	3,590
		4			41.98528899	101.5327266	1223845.2	787564.0	3,595
Site Hooker-AMT									
2009	Hooker	5	0	90	41.92631125	101.2500157	1300365.1	764844.3	3,399
		6			41.92676198	101.2499953	1300373.0	765008.4	3,398
		7			41.92676198	101.2499953	1300373.0	765008.4	3,398
Site Logan-AMT									
2009	Logan	8	0	90	41.43348388	100.6572313	1460255.7	583548.1	3,046
		9			41.43396096	100.6572434	1460253.7	583721.9	3,047
		10			41.43438465	100.6572306	1460258.4	583876.2	3,044
Site Cherry South-AMT									
2009	Cherry	11	270	0	42.16733104	100.3906835	1534529.4	850430.7	2,768
		13			42.16738668	100.3912779	1534368.4	850451.7	2,772
		14			42.16744259	100.3918722	1534207.4	850472.8	2,776
Site Cherry North-AMT									
2009	Cherry	15	0	90	42.29886574	100.397966	1532776.2	898361.6	2,768
		16			42.29931619	100.3979518	1532780.8	898525.7	2,772
		17			42.29977499	100.3979861	1532772.3	898692.9	2,776

[1]Decimal degrees; North American Datum of 1983 (NAD 83).

[2]Surveyed land-surface elevation above National Geodetic Vertical Datum of 1929 (NGVD 29).

Table 4. Location and elevation for all audio-magnetotelluric (AMT) stations where AMT data were acquired in 2010 along Whitman Road profile, Cherry and Grant Counties, Nebr.

[AMT, audio magnetotellurics; dipole length is 50 feet; azimuth is given in degrees from North; azimuth of Ey dipole is 90 degrees; northing and easting in Nebraska State Plane coordinates]

AMT Station	Latitude[1]	Longitude[1]	Easting (feet)	Northing (feet)	Elevation[2] (feet)
North segment					
61	42.04364	101.5237959	1226646.8	808773.7	3,657
62	42.04588	101.5243195	1226519.0	809592.1	3,660
63	42.04804	101.5251784	1226299.7	810383.2	3,605
64	42.05	101.5266461	1225913.9	811106.7	3,621
65	42.05187	101.5279643	1225568.0	811791.3	3,618
66	42.05393	101.5288684	1225335.9	812549.4	3,597
67	42.05629	101.5289858	1225319.2	813408.5	3,597
68	42.05859	101.5289924	1225332.2	814244.9	3,644
69	42.06091	101.5291208	1225312.3	815090.9	3,681
70	42.06311	101.5296919	1225171.5	815896.0	3,663
71	42.06542	101.5299648	1225112.3	816738.1	3,615
72	42.06776	101.5301544	1225075.9	817590.4	3,641
73	42.07004	101.5305474	1224984.0	818425.6	3,643
74	42.07218	101.5311279	1224840.2	819204.5	3,617
75	42.07428	101.5310785	1224867.2	819972.2	3,599
76	42.07643	101.5303421	1225080.9	820752.0	3,635
77	42.07874	101.5297324	1225261.2	821587.2	3,665
78	42.08081	101.530794	1224986.5	822348.1	3,632
79	42.0817	101.5335133	1224254.4	822687.0	3,621
80	42.08336	101.5360455	1223578.0	823302.1	3,619
81	42.08533	101.5376231	1223162.7	824028.5	3,621
82	42.0875	101.5396442	1222628.4	824829.0	3,618
83	42.0898	101.5400743	1222526.6	825667.3	3,617
84	42.09189	101.5390941	1222806.1	826425.0	3,644
85	42.0937	101.5372917	1223306.8	827073.8	3,636
86	42.09535	101.535375	1223837.5	827667.1	3,598
87	42.09739	101.5339205	1224245.3	828403.4	3,598
South segment					
1	41.98585	101.5298516	1224630.1	787753.7	3,597
2	41.98494	101.5273654	1225299.9	787410.7	3,595
3	41.98335	101.5249368	1225949.7	786821.5	3,587
4	41.98173	101.5226156	1226570.1	786218.9	3,575
5	41.97991	101.5208419	1227040.5	785548.8	3,578
6	41.97891	101.5179179	1227828.8	785171.2	3,588
7	41.97686	101.5159541	1228349.4	784413.2	3,636
8	41.97524	101.5137424	1228940.2	783813.5	3,644
9	41.97371	101.51262	1229235.5	783249.6	3,639
10	41.9715	101.5116766	1229477.9	782442.4	3,594
11	41.96932	101.5113008	1229566.1	781643.2	3,574

Table 4. Location and elevation for all audio-magnetotelluric (AMT) stations where AMT data were acquired in 2010 along Whitman Road profile, Cherry and Grant Counties, Nebr.—Continued

[AMT, audio magnetotellurics; dipole length is 50 feet; azimuth is given in degrees from North; azimuth of Ey dipole is 90 degrees; northing and easting in Nebraska State Plane coordinates]

AMT Station	Latitude[1]	Longitude[1]	Easting (feet)	Northing (feet)	Elevation[2] (feet)
12	41.9674	101.5097291	1229981.1	780936.5	3,579
13	41.96554	101.5081837	1230389.4	780252.6	3,580
14	41.9636	101.5064909	1230837.3	779539.6	3,580
15	41.96082	101.5047651	1231288.8	778518.5	3,579
16	41.95883	101.503541	1231609.0	777787.6	3,576
17	41.95668	101.5031186	1231710.2	777001.7	3,579
18	41.95444	101.5028381	1231772.3	776185.8	3,580
19	41.95225	101.5020287	1231978.5	775384.7	3,580
20	41.94993	101.5016359	1232070.6	774536.4	3,579
21	41.94811	101.4996466	1232600.0	773863.8	3,599
22	41.94617	101.4982199	1232975.7	773150.0	3,629
23	41.94397	101.4973738	1233191.9	772345.8	3,639
24	41.9425	101.4950969	1233801.8	771798.7	3,633
25	41.9402	101.4941388	1234047.9	770958.8	3,621
26	41.93817	101.4929981	1234345.3	770211.3	3,605
27	41.93645	101.4916405	1234703.7	769579.2	3,600
28	41.9345	101.4911303	1234830.2	768865.8	3,614
29	41.93234	101.4911791	1234803.4	768081.6	3,616
30	41.93025	101.492147	1234527.0	767324.1	3,586
31	41.92814	101.4912687	1234752.6	766549.5	3,579
32	41.92628	101.4895321	1235213.3	765866.2	3,576
33	41.92405	101.4886854	1235429.6	765048.8	3,577
34	41.92155	101.4898063	1235109.0	764143.1	3,595
35	41.91959	101.4918042	1234553.2	763438.0	3,624
36	41.91741	101.4923704	1234385.5	762648.9	3,656
37	41.91528	101.4931074	1234171.6	761875.7	3,612
38	41.91321	101.4946908	1233727.8	761129.3	3,578
39	41.98457	101.5276408	1225222.7	787278.6	3,589
40	41.98598	101.5302556	1224521.2	787804.9	3,599
41	41.9885	101.5305121	1224467.7	788722.5	3,650
42	41.991	101.5300194	1224617.7	789629.5	3,674
43	41.99318	101.5296355	1224736.1	790424.5	3,614
44	41.99517	101.5282896	1225114.6	791140.7	3,596
45	41.99724	101.5274903	1225345.1	791891.2	3,601
46	42.00016	101.5275212	1225355.5	792953.9	3,683
47	42.00199	101.5278838	1225268.8	793625.2	3,695
48	42.004	101.5280719	1225230.6	794356.1	3,619
49	42.00711	101.5279292	1225289.4	795488.2	3,592
50	42.00931	101.5284151	1225171.6	796293.6	3,626
51	42.0113	101.5303537	1224657.8	797028.7	3,687

Table 4. Location and elevation for all audio-magnetotelluric (AMT) stations where AMT data were acquired in 2010 along Whitman Road profile, Cherry and Grant Counties, Nebr.—Continued

[AMT, audio magnetotellurics; dipole length is 50 feet; azimuth is given in degrees from North; azimuth of Ey dipole is 90 degrees; northing and easting in Nebraska State Plane coordinates]

AMT Station	Latitude[1]	Longitude[1]	Easting (feet)	Northing (feet)	Elevation[2] (feet)
52	42.01294	101.5324714	1224093.1	797635.3	3,693
53	42.01503	101.5341726	1223644.5	798404.0	3,663
54	42.01719	101.5338841	1223736.8	799188.9	3,611
55	42.0194	101.5328128	1224042.1	799989.5	3,613
56	42.02179	101.5324965	1224143.4	800856.5	3,658
57	42.02396	101.532595	1224130.7	801650.0	3,638
58	42.02608	101.5337783	1223823.0	802426.9	3,599
59	42.02813	101.5344033	1223666.5	803176.1	3,603
60	42.02988	101.5362004	1223189.8	803823.1	3,600

[1]Decimal degrees; North American Datum of 1983 (NAD 83).

[2]Surveyed land-surface elevation above National Geodetic Vertical Datum of 1929 (NGVD 29).

afforded by the magnetotelluric technique, short AMT profiles using three to five stations were recorded at or near each location (tables 3 and 4; fig. 2). AMT data in 2008 were nominally acquired every 328 ft (100 m), approximately 164 ft (50 m) in 2009, and 656 ft (200 m) in 2010 using the arrangement shown in figure 4. The exact survey locations and short-profile orientation were selected based on either (a) being in the vicinity of the borehole sites that were being studied in 2008 or, (b) in 2009, were directed away from cultural electromagnetic interference features, such as electrically powered center-pivot irrigation systems, fences, pipelines, communication lines, railways, and other manmade conductors. Buried power lines along roads resulted in some stations having to be relocated. A summary of site location and AMT system geometry for each AMT station where data were collected in 2008 and 2009 is provided in table 3. The geologic strike was unknown at specific survey locations, but was postulated from paleodrainage patterns from Swinehart and Diffendal (1989) and other sources. In 2010, the Whitman Road profile in Cherry and Grant Counties (fig. 2) was designed to be perpendicular to the assumed general strike of the subsurface paleochannel features under investigation. The AMT stations, system geometry, location, and surface elevation for each AMT station along the Whitman Road profiles are listed in table 4.

All AMT surveys in the upper Loup study area used a Geometrics EH-4 STRATAGEM system (Geometrics, 2007). A schematic of the EH-4 STRATAGEM system as used in this study is shown in figure 4. The STRATAGEM transmitter complements the natural signal in the range of 1 to 72 kHz. The STRATAGEM does not measure the vertical component of the magnetic field. Electric field components, Ex and Ey, were measured using long multi-strand, single-wire dipoles having lengths of either 50 ft (15 m) or 82 ft (25 m), and magnetic fields were measured using EMI BF-6 high-frequency magnetic induction coils (Geometrics, 2007).

Audio-Magnetotelluric (AMT) Data Analysis

Electric and magnetic field time-series data were acquired and field processed by fast Fourier transforms into spectral crosspowers (Jiracek, 2011) in real time by the STRATAGEM acquisition software. This allowed for immediate quality control of the acquired data in the field. During post processing the recorded AMT time-series data were transformed to the frequency domain and processed to determine a 2D apparent resistivity and phase tensor (Jiracek, 2011) at each station. Time-series data sets were selected based on optimal signal-to-noise characteristics before the crosspower calculations. Noisy data in the time series, spectral, and resistivity data were culled at this stage. Crosspower and MT impedance data files were created with the STRATAGEM data-acquisition program (IMAGEM) and used as input to the 2D inversion-modeling program. Because the STRATAGEM is a single-station system, data acquisition cannot be acquired simultaneously at more than one location.

During the 2D analysis and interpretation process, each station was rotated to a fixed angle defined by the perpendicular direction to the nominal profile orientation. Rotation of the impedance tensor (Jiracek, 2011) into this coordinate system thus allows for decoupling into the quasi-TE and quasi-TM modes. The true TM and TE modes are uniquely determined by the geologic strike, which in most cases is unknown at the survey location.

After data collection and field processing, 2D forward and inverse modeling of the AMT data was performed.

Wannamaker (1983) determined that although some MT responses are fundamentally three-dimensional (3D) in nature, for elongated structures 2D modeling could be used to construct reasonable estimates of the resistivity cross sections along each profile. Wannamaker and others (1984) demonstrated that approximating a 3D structure beneath a centrally located profile with 2D modeling is best achieved when fitting the TM curve, even at the expense of a poor fit of the TE curve. However, because TM data are relatively insensitive to the vertical extent of a subsurface conductive body (Eberhart-Phillips and others, 1995), the depths to the base of the bodies in the model were not well constrained. Hence, mixed-mode analysis (modeling the TM and TE mode together) was used to help clarify the modeling results. Mixed-mode analysis commonly is referred to as TMTE mode and is an average of all data in orthogonal directions.

Two-dimensional inverse-resistivity models were constructed for each of the short profiles acquired at each AMT station. Not all soundings were included in each inversion if an unusual amount of cultural noise (for example, center-pivot irrigation systems) was observed.

First, 2D inversions of the AMT data were conducted using the computer program, RLM2DI (Mackie and others, 1997; Rodi and Mackie, 2001) within GEOTOOLS (Geotools, 1998), a shell program specifically designed to process and facilitate interpretation of MT and AMT data. RLM2DI uses a finite-difference network analog to the Maxwell’s equations governing magnetotellurics (Jiracek, 2011) to calculate the forward solution. A nonlinear conjugate gradient optimization approach (Rodi and Mackie, 2001) is applied directly to the minimization of the objective function for the inverse problem.

Inversion was followed by the application of the 2D forward-modeling program, PW2D, developed by Wannamaker and others (1987). The results of the RLM2DI two-dimensional inversion were used as the initial input model for the forward modeling (PW2D) where a sensitivity analysis was performed on the conductive structures derived from the inversion results. PW2D is a finite-element algorithm that simulates transverse electric and magnetic fields across each finite element (Wannamaker and others, 1987). The number of iterations of forward modeling (PW2D) depended on how complex the profile inversion results were from RLM2DI.

Hydrostratigraphic Interpretation Of Test-Hole And Surface-Geophysical Data

Test-Hole Lithologic and Borehole Geophysical Logs

Generalized lithologic descriptions and selected borehole geophysical logs for all test holes are presented in figures 5 through 13. An example test hole with generalized lithologic description and borehole geophysical logs is shown in figure 5. Logs from all other test holes (figs. 6–13) can be found in the Supplemental Data section of this report. Borehole geophysical logs include data for long- and short-normal resistivity, natural gamma activity, and spontaneous potential. Examination of the resistivity data collected from the borehole logs in comparison with the lithologic test-hole data has enabled the following interpretations of geophysical data.

The base of aquifer is indicated by the top of the siltstone unit of the Brule Formation in the generalized lithologic log. The long- and short-normal resistivity logs indicate the base of the principal aquifer by sharp contrasts in resistivity between the Brule Formation and the overlying units. Examining the long- and short-normal resistivity, the sediments overlying the Brule Formation range from less than 50 to greater than 250 ohm-m. Resistivity for the Ogallala (units containing rootlets) ranged between 50 to 200 ohm-m (and more typically between 75 to 150 ohm-m), with higher resistivity values indicating the presence of coarser deposits or a greater degree of cementation of the sandstone units. Coarse sand and gravel deposits typically had resistivity ranges for 150 ohm-m to more than 250 ohm-m. In contrast, the resistivity of the Brule Formation typically was less than 25 ohm-m and, in most cases, less than 15 ohm-m.

Other logs provide further support for the base-of-aquifer interpretation. Natural gamma logs indicate an increase in activity near the base of the aquifer because of increased volcanic ash content of the Brule Formation. Spontaneous-potential logs can indicate the degree to which the drilling fluid invaded the formation, and the relative impermeability of the Brule Formation typically results in a positive deflection indicating that minimal drilling fluid invaded this interval.

Differences in the elevation of the base of the principal aquifer for test holes drilled after the completion of SIM 2008-3042 (McGuire and Peterson, 2008) are presented in table 1. The range of differences between the elevations of the drilled base of aquifer and the predicted base of aquifer was from -157 to 300 ft (-48 to 91 m). In test holes 1-UL-09 and 2-UL-09, within the western part of the upper Loup study area, the test-hole base-of-aquifer elevation was more than 100 ft lower than that predicted by McGuire and Peterson (2008). This may indicate that the test holes were drilled into paleovalleys eroded into the Brule Formation. Furthermore, both of

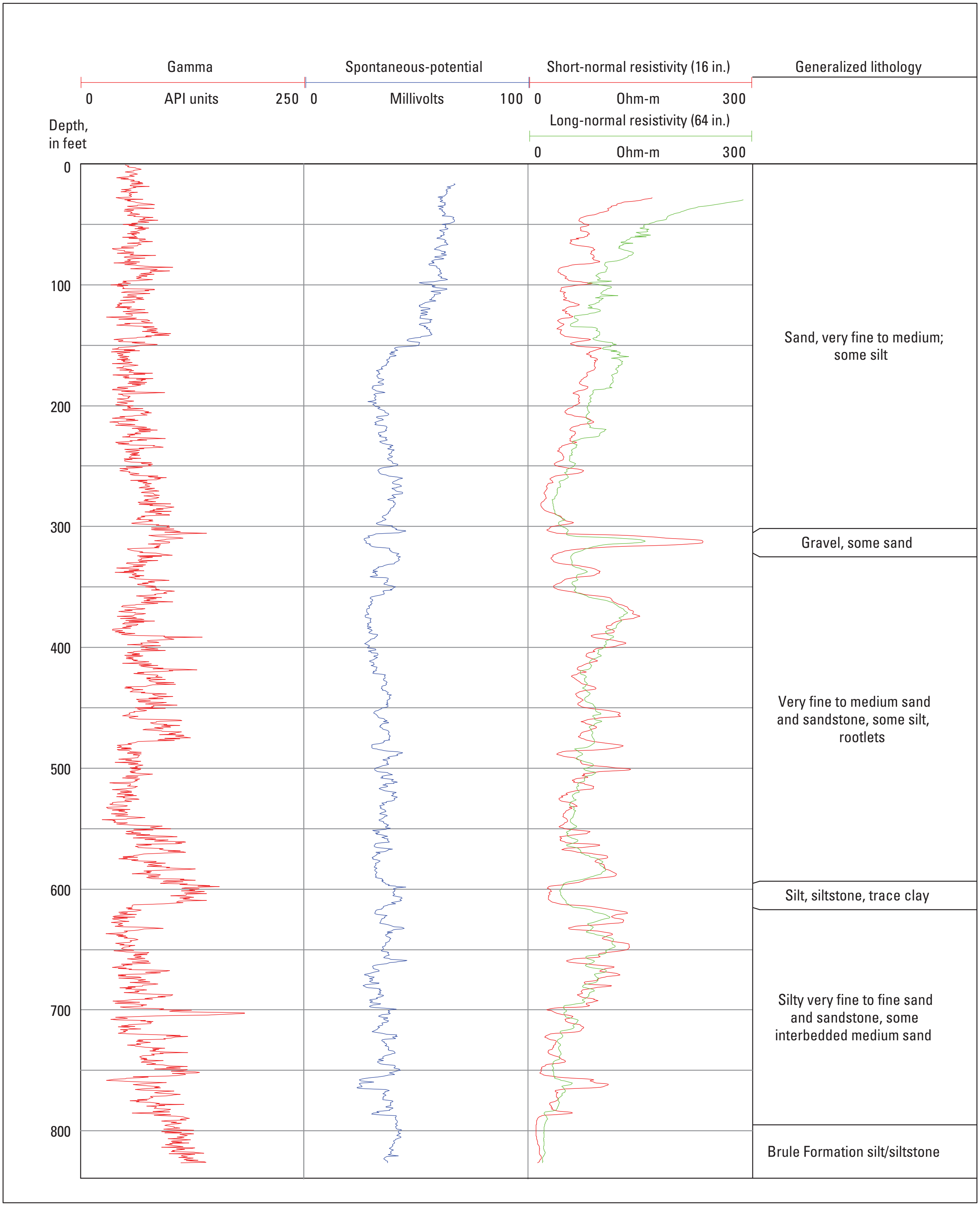

Figure 5. Composite of generalized lithologic description and geophysical logs for test hole 2-UL-08, McPherson County, Nebr. Short-normal resistivity, in ohm-meters; long-normal resistivity, in ohm-meters; natural gamma activity, in American Petroleum Institute units; spontaneous potential, in millivolts.

these test holes lie in close proximity to the proposed location of paleovalleys in Grant and Hooker Counties (table 1; fig. 2) (Swinehart and Diffendal, 1989).

Researchers have indicated that Pliocene-age or younger gravel covers much of the upper Loup study area (Swinehart and Diffendal, 1989). Gravel overlying intervals of sandstone containing rootlets was encountered in every test hole with the exception of 1-UL-09 (fig. 8) and 3-UL-09 (fig. 10). Although the age was not determined for this study, the authors infer by superposition that these sand and gravel units are of Miocene age or younger. At the location of test hole 1-UL-09, Miocene or younger sand and gravel were absent and only finer-grained deposits overlie sand and sandstone containing siliceous rootlets. At test hole 3-UL-09, rootlets were encountered 10 ft below land surface, which is indicative of the Ogallala Formation of Miocene age. It can be inferred that if Miocene or younger gravel had existed at in this location, it would have been eroded and reworked by the modern North Loup River (fig. 2; table 1). Where present, thicknesses of sand and gravel deposits were less than 50 ft with the exception of test hole 3-UL-10 (fig. 13). Here, sand and gravel deposits were nearly 75 ft (23 m) thick.

TDEM Survey Results

TDEM Models

Figures 14 through 27 present the measured data from the 26 TDEM stations together with best-fit inverse models. An example sounding is shown in figure 14. All other soundings (figs. 15–27) are located in the Supplemental Data section of this report. At each station, the left panel shows the forward responses whereas the right panel shows the best-fit minimum-layer (red) and smooth (blue) inverse model. The right panel, additionally, shows the forward responses of the two inverse models. For all soundings, the central-loop data are plotted as apparent resistivity. Out-of-loop data for the secondary magnetic field, which were collected for all soundings collected

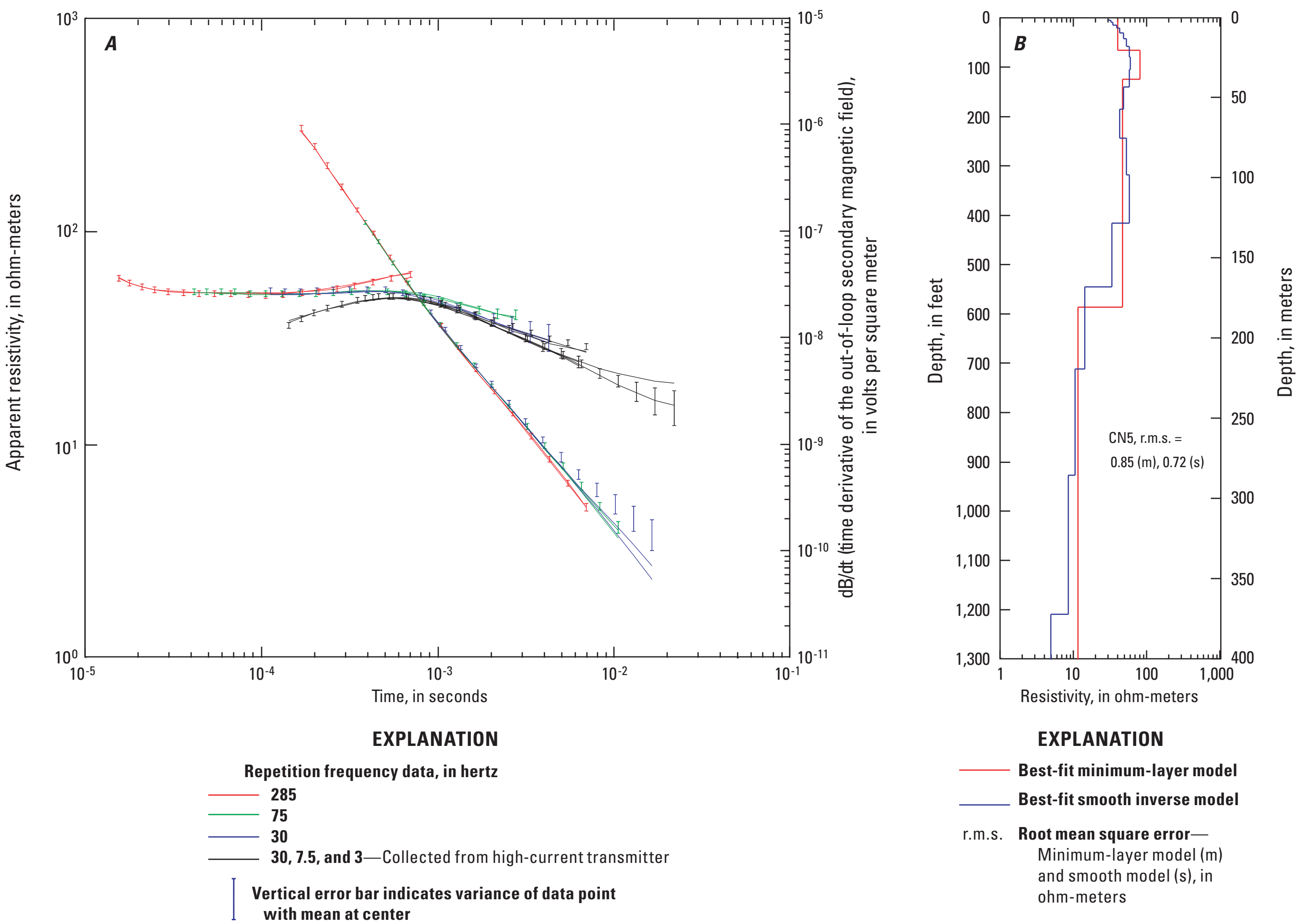

Figure 14. Relations between *A*, central-loop resistivity, out-of-loop vertical magnetic field (time-derivative, right axis), and time; *B*, depth below land surface and subsurface resistivity modeled from TDEM sounding for site CN5 (table 2).

in 2009 and 2010, are plotted as the time derivative (dB/dt) in volts per square meter. In most cases the model response falls within the measured data errors; exceptions are for the out-of-loop vertical magnetic field data, which over conductive ground suffers a sign change at early times. This sign change is associated with passage of time for the peak current density outward from the transmitter loop, and is extremely sensitive to the position of the receiver relative to the transmitter loop.

In general, data quality was high, reflecting the low density of human population, and subsequent low level of cultural noise (power lines, pipelines, well pumps, electric fences) within the survey area. A small number of soundings suffered from cultural noise, identified as oscillatory behavior in the vertical component of the secondary magnetic field (dB/dt) decay curves. At these locations data quality was compromised at late times; however, removal of the late-time data resulted in interpretable sounding data, albeit with a reduced depth of investigation.

Time-Domain Electromagnetic (TDEM) Model Uncertainty

The TDEM data were processed and inverted using the SiTEM data processing and SEMDI software packages (Auken and Nebel, 2001). For a detailed discussion on TDEM noise and inversion calculation of the root-mean-square (r.m.s.) errors in the SiTEM program refer to Effersø and others (1999). The TDEM models in almost all cases reproduce the measured data to within estimated measurement (r.m.s. error is less than 1 ohm-meter). The r.m.s. error for all soundings collected for this report are indicated in figures 14 through 27. In general, the r.m.s. error is slightly larger for the minimum-layer models, than for the smooth models, reflecting the greater difficulty in fitting the data with a small number of model parameters. Average errors were, however, similar for the smooth and minimum-layer models, suggesting that the minimum-layer parameterization can adequately represent the subsurface resistivity structure, and by inference, the hydrostratigraphy. This is consistent with the previously known geologic history, with a number of (sharp) unconformities associated with erosion and changes from marine to alluvial to eolian deposition.

Time-Domain Electromagnetic (TDEM) Model Interpretation

The data generally supported a 3–5 layer model for resistivity stratigraphy, and beyond 300–400 ft (91–120 m) depth exhibited decreasing resistivity with increasing depth. Within the upper Loup study area, some spatial trends were observed in the deep resistivity structure, with greater-than-average resistivities observed along a northwest to southeast trend axis through parts of southwest Cherry, Grant, Hooker, Thomas, and McPherson Counties (fig. 28). Although the Brule Formation is expected beneath this entire area, the TDEM data, at later times, reflect a volume average of the deeper stratigraphic section. Thus, although the depth to the conductive interface reflects the top of the Brule Formation, the apparent resistivity itself reflects an average of the Brule Formation and underlying units (for example, Pierre Shale of Cretaceous age). The greater resistivities observed along this northwest-southeast corridor are consistent with thinning or removal of the Pierre Shale near the Chadron Arch, and suggest that the TDEM data are sensing (but not imaging) structural changes within the Cretaceous section. Some of the greatest resistivity values occurred along the eastern flank of the Chadron Arch and were more than double the average base resistivity of 11 ohm-m.

The models in figures 14 to 27 show conductors extending to 1,300 ft (400 m) deep; however, the depth of investigation is, in most cases, less than this. The TDEM models do accurately recover the top of this "basement" conductor and its conductivity; however, the greater conductance of the Brule Formation or underlying Pierre Shale precludes defining stratigraphic contacts much below the Ogallala-Brule interface. The models should, thus, be viewed as a proxy for the geologic structure for the section extending to the depth at which the conductive horizon is encountered.

Assuming that this conductive horizon represents the base of the High Plains aquifer, the base-of-aquifer elevation was examined, as inferred from the TDEM models, and compared to the base of aquifer as determined from test-hole derived mapping (McGuire and Peterson, 2008) (fig. 29). An eastward decrease in the base-of-aquifer elevation is evident in both data sets, reflecting the southeast dip of the stratigraphic column. With few exceptions, the base of aquifer inferred from the TDEM models indicates close correspondence with the test-hole-derived base of aquifer. Outliers occur in western Hooker (site UL17; inferred base-of-aquifer elevation 3,181 ft) and southern Cherry Counties (site UL4; inferred base-of-aquifer elevation 2,977 ft), where modeled soundings suggest a shallower (higher-elevation) conductor than either the test-hole data or nearby TDEM models indicate.

In general, greater variation in the base-of-aquifer elevations is observed in the west. This reflects a number of deep paleovalleys incised into the Brule Formation, some of which have been identified from test-hole data. This is evident at site CN1 in Grant County, where the TDEM model indicated a base-of-aquifer elevation nearly 400 ft (120 m) deeper than McGuire and Peterson (2008) (fig. 29; table 2). The drilled base-of-aquifer elevation from nearby test-hole 1-UL-09 was 300 ft (91 m) deeper than predicted, and thus, was in general agreement with the TDEM estimates.

The topology of the base-of-aquifer surface, in particular the configuration of paleochannels, is of primary importance in understanding groundwater flow. The depth to the base of the aquifer (fig. 30), however, provides an estimate of total aquifer thickness and is important in assessing groundwater supply. The depth to the base of the High Plains aquifer varies by more than a factor of two within the surveyed area. The thickest section falls within Grant, Hooker, and Thomas Counties, with 900 ft (270 m) or more between the land surface and the base of the aquifer.

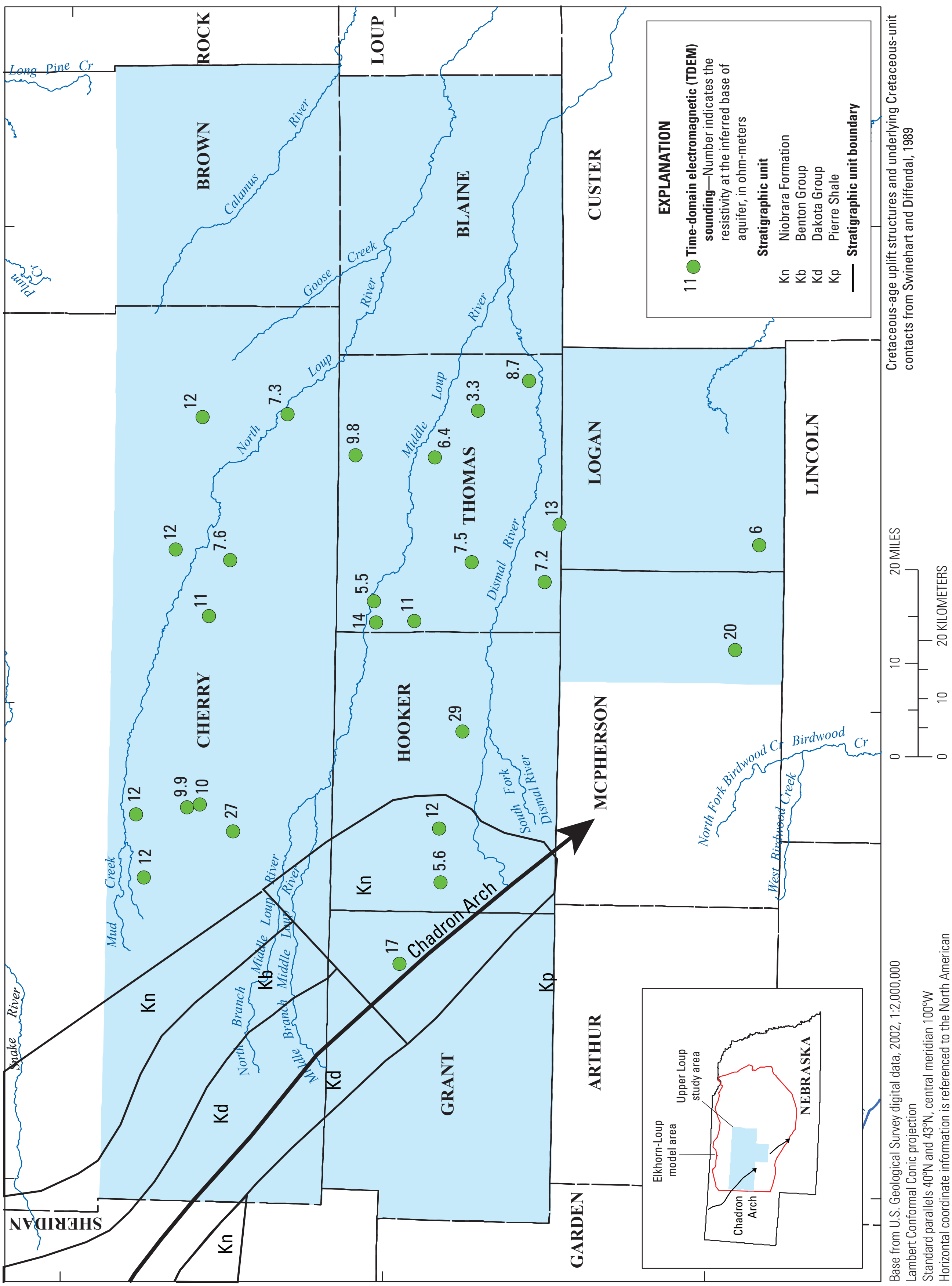

Figure 28. Resistivity at the inferred base of High Plains aquifer.

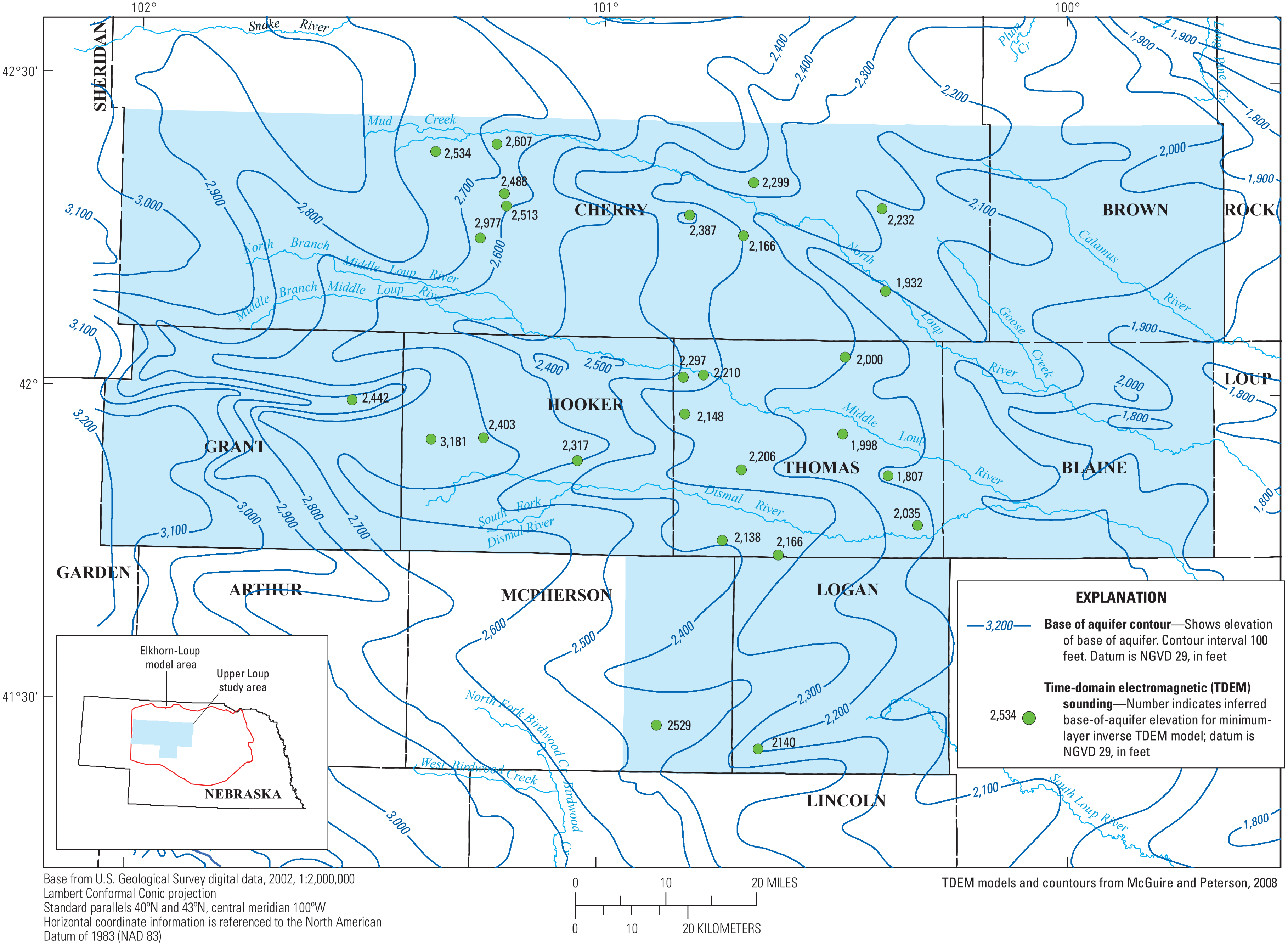

Figure 29. Inferred base-of-aquifer elevation from minimum-layer inverse time-domain electromagnetic (TDEM) models and contours derived primarily from test-hole data.

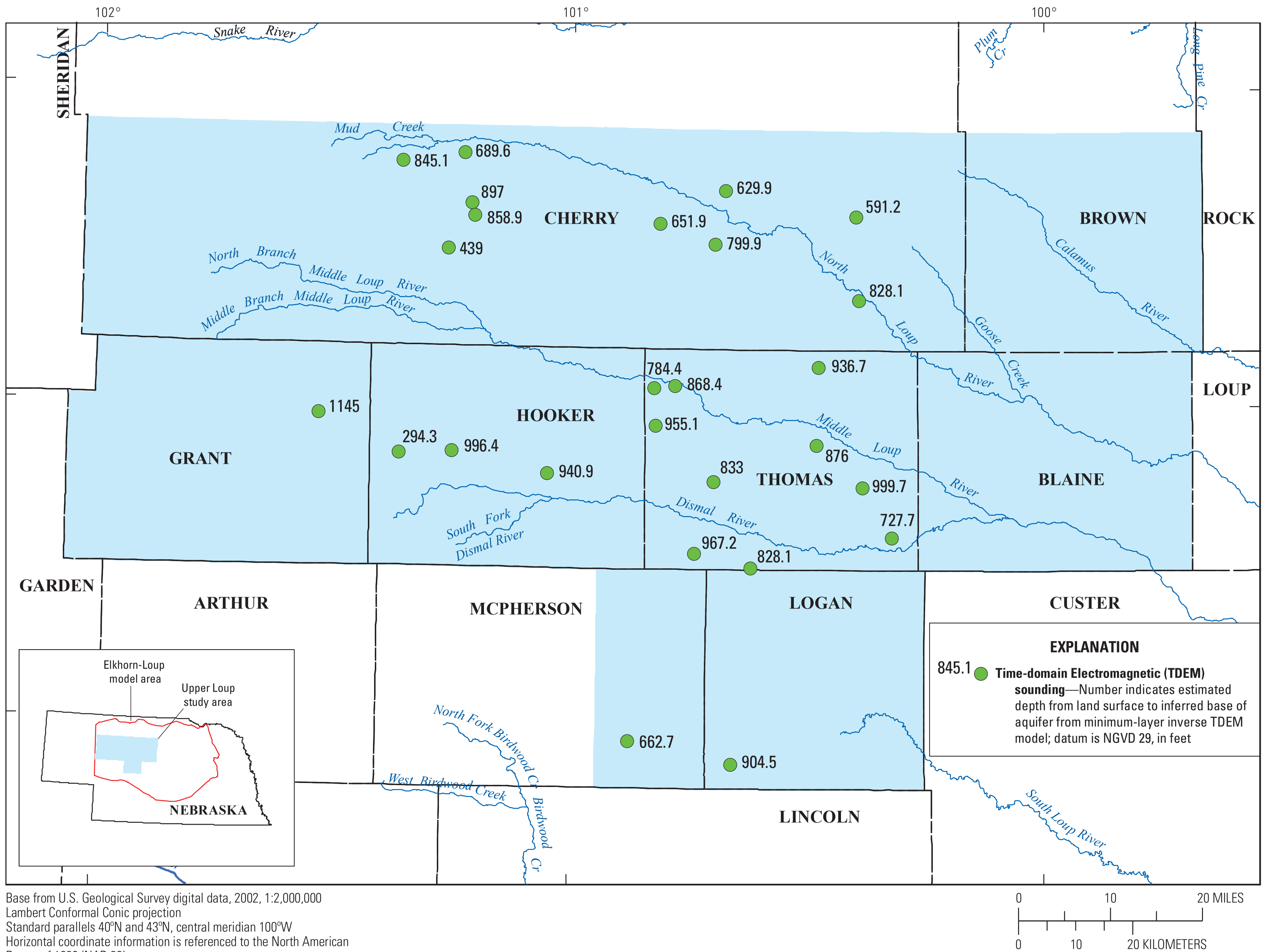

Base from U.S. Geological Survey digital data, 2002, 1:2,000,000
Lambert Conformal Conic projection
Standard parallels 40°N and 43°N, central meridian 100°W
Horizontal coordinate information is referenced to the North American Datum of 1983 (NAD 83)

Figure 30. Inferred depth from land surface to base of High Plains aquifer from minimum-layer time-domain electromagnetic (TDEM) inverse models. The thickest part of the aquifer within the study area is located in Grant, Hooker, and Thomas Counties.

Audio-Magnetotelluric (AMT) Survey Results

2008 and 2009 Two-Dimensional Inversion Modeling Results

In 2008, a series of short reconnaissance profiles were surveyed near previously drilled CSD test holes shown in figure 2 and listed in table 3. An example profile is presented in figure 31. These inversion results illustrate the variability in subsurface resistivity over short lateral distances of a few hundred feet where zones of resistive material (the warm colors in fig. 31) alternate with zones of more conductive material (cool colors) in the profile. This profile indicates that there is variability not only at the base of aquifer, but also within the High Plains aquifer itself.

To model AMT data and accurately image subsurface features with short reconnaissance profiles, the geologic strike of the contact at the base of aquifer must be known. At the time of data collection the true strike direction of subsurface structures, including the base-of-aquifer contact was unknown at the survey locations. A regional approximation of strike was used but is not adequate when collecting short reconnaissance profiles. As a result, visual depictions of the mixed-mode 2D inversion results potentially are misleading and, therefore, are not presented in this report. For the locations surveyed in 2008 and 2009, a pilot survey needs to be completed first to assess the actual strike direction of subsurface features before collecting a profile, so that it can be inverted and used for interpretation. It also was determined from the 2008 and 2009 data that short profiles are not the best way to apply this technique when only a regional estimate of subsurface features, including the base-of-aquifer strike direction, is applied.

2010 Two-Dimensional (2D) Inversion Modeling Results

In 2010, AMT data were not collected as short reconnaissance profiles; rather data were collected along an approximately 12-mi-(19-km-)long profile along Whitman Road, which runs approximately north-south in Grant and Cherry Counties (figs. 2 and 32). This location was selected for resurvey because test hole 1-UL-09 indicated the base-of-aquifer topography and the surface was poorly constrained in this area. AMT stations, listed in table 4, were spaced approximately 656 ft (200 m) apart along the road. Data were not acquired within the town limits of Whitman because of the presence of substantial electromagnetic interference. The data were divided into northern (*A to A'*) and southern (*B to B'*) segments. The northern segment consists of data acquired north of Whitman, whereas the southern segment consists of data acquired south of Whitman. The results of the 2D inversion modeling are presented in figures 33 and 35 as vertically exaggerated 2D cross sections and in figures 34 and 36 as 3D views shown from two different oblique aerial viewpoints to depict the sinuosity of the actual profile line.

The inverted 2D model for the northern segment (figs. 33 and 34) depicts, in simplest terms, a four-layer model: a resistive zone (layer 1) about 60 to 70 ft (18 to 21 m) thick over a relatively continuous conductive zone (layer 2), about 60 to 75 ft (18 to 23 m) thick, over a moderately to very resistive zone (layer 3), greater than 150 ft (45 m) in thickness, over a very thick basal conductive zone (layer 4). The upper conductive zone (layer 2) may consist of fluvial deposits of silts and clays, possibly from riverine overbank flows. Some resistive material occurs below the base-of-aquifer surface (interface between zones 3 and 4). These more resistive zones are not interpreted as coarser sediments within the Brule Formation; rather, they are the result of edge effects and inversion artifacts.

In the inverted 2D model for the southern segment (figs. 35 and 36), the upper conductive layer does not appear to be as continuous as in the northern segment. In fact, it appears that the upper conductive zone pinches out around AMT stations 4 to 5 and from there northward is discontinuous. Data north of stations 51 extending to station 59 suffer from cultural noise caused by a registered USTA (National Earthquake Information Center, 2011) seismic station (L28) collecting data nearby. As such, the deeper data near the base-of-aquifer surface below these stations are suspect and were not used for interpretation.

The generalized lithology log from test hole 1-UL-09 (fig. 8) was compared to the resistivity section at about AMT station 1 (fig. 35), which was collected 30 ft (10 m) west of the 1-UL-09 test-hole location. A visual interpretation of the resistivity model results for the data collected in 2010 (fig. 35) indicate the depth to the base of aquifer is around 1,100 feet, which agrees with the test hole 1-UL-09 (fig. 8) and base-of-aquifer elevation TDEM site CN1 (fig. 15). Examination of the borehole geophysical log also indicates the absence of layer 2, which is consistent with the AMT profile (fig. 35). At this location the modeled profile indicates moderately resistive material that extends to the base of the aquifer. Similarly modeled AMT data collected in 2009, collected approximately 1,500 ft (460 m) west of 1-UL-09 (fig. 32) displays a different subsurface resistivity distribution including some of the upper conductor described in the 4-layer interpretation. This is another example of considerable variation in subsurface hydrostratigraphy over a short distance.

The inferred elevation of the base of High Plains aquifer along the northern and southern segments using the inverted models of the 2010 AMT data is listed in table 5 and table 6, respectively. These points indicate only where base-of-aquifer elevations were picked and do not indicate individual AMT stations. The inferred elevation of the base of the aquifer from the AMT models indicates abrupt changes in the topology over short distances. This interpretation is consistent with AMT data collected in 2008–09 elsewhere in the upper Loup study area where AMT-based models indicated abrupt changes in the elevation of the base of the High Plains aquifer as compared with test-hole data.

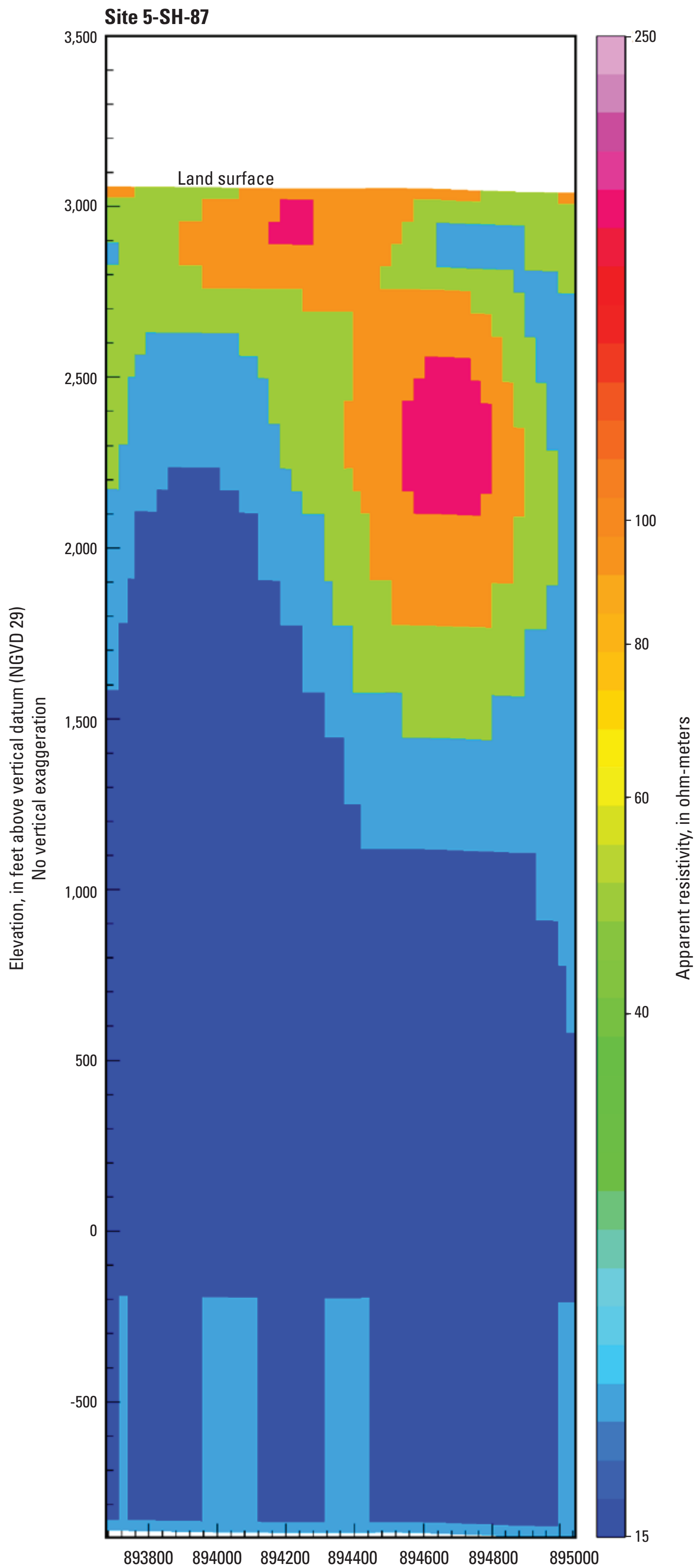

Figure 31. Mixed-mode two-dimensional (2D) inversion results for stations near test hole 5-SH-87. No vertical exaggeration.

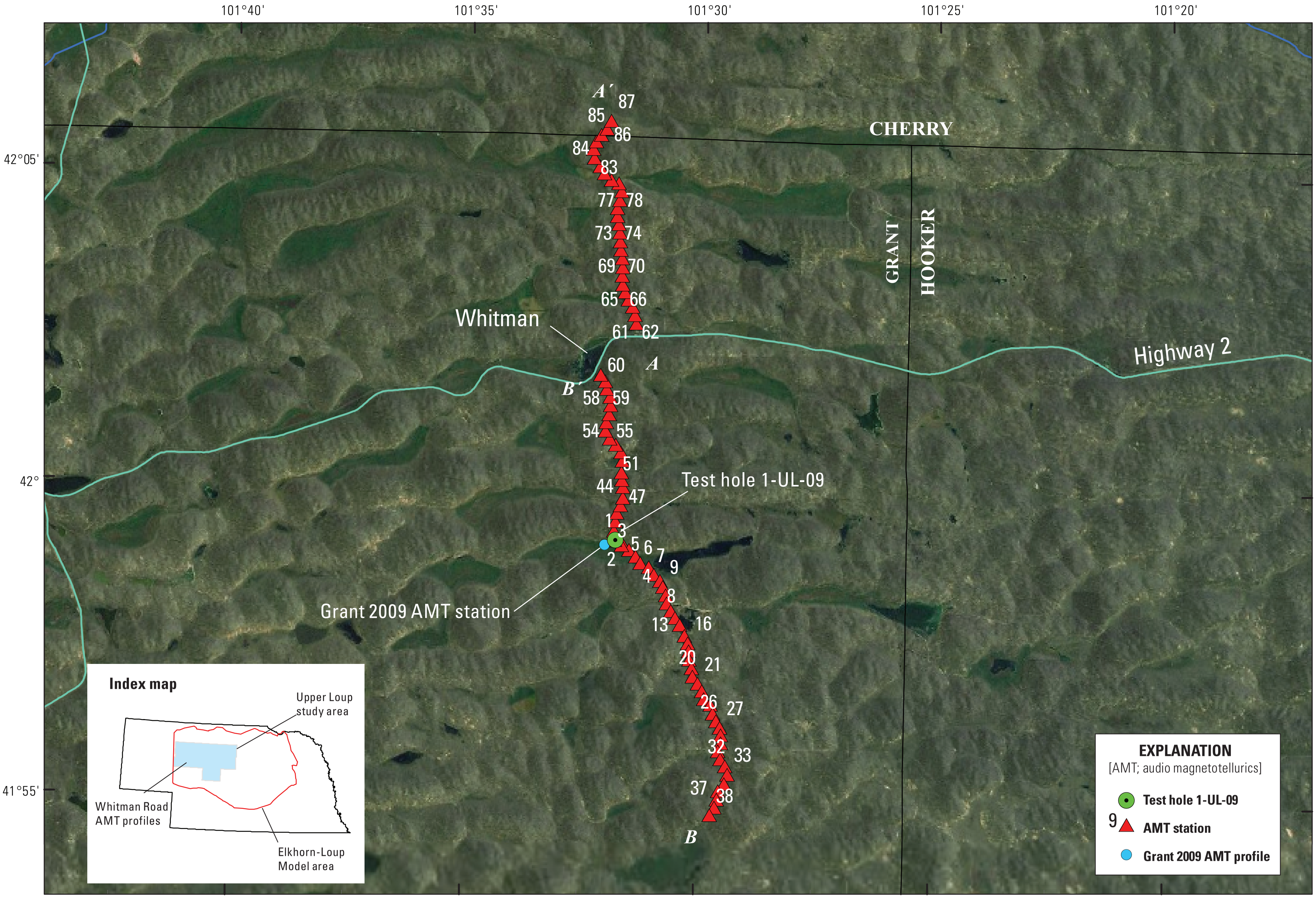

Base from U.S. Department of Agriculture, Aerial Photography Field Office
Digital orthophotography, 2007, 1:100,000
Universal Transverse Mercator projection, Zone 14
Horizontal coordinate information is referenced to the North American Datum of 1983 (NAD 83)

Figure 32. Location of audio-magnetotelluric (AMT) stations along Whitman Road, Cherry and Grant Counties, Nebr., where 2010 stations occurred. Stations north of Highway 2 compose the north segment (*A* to *A'*), and stations south of Highway 2 compose the south segment (*B* to *B'*).

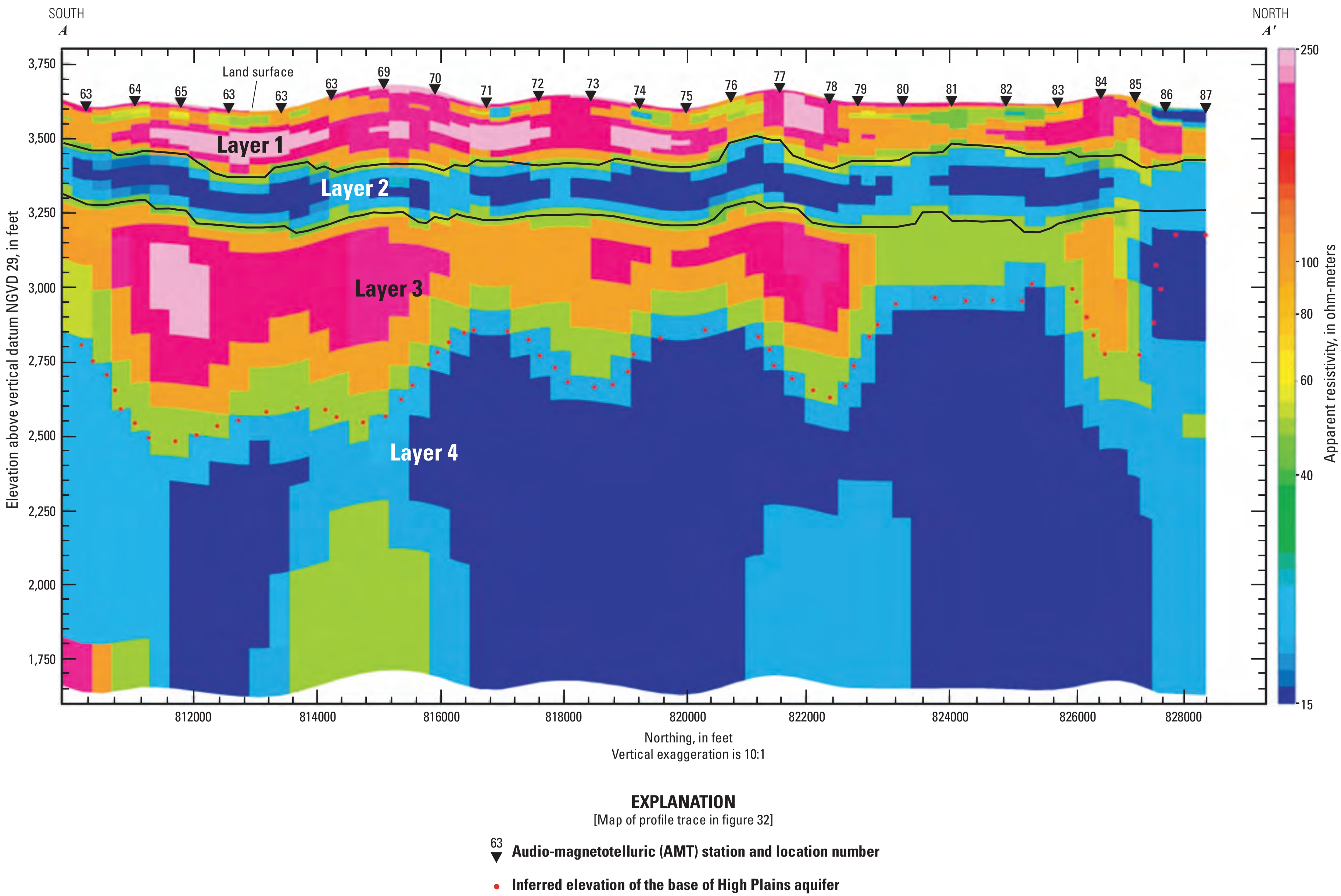

Figure 33. Mixed-mode two-dimensional (2D) inversion results from 2010 audio-magnetotelluric (AMT) stations for the north segment (*A* to *A*′) along Whitman Road, Cherry and Grant Counties, Nebr.

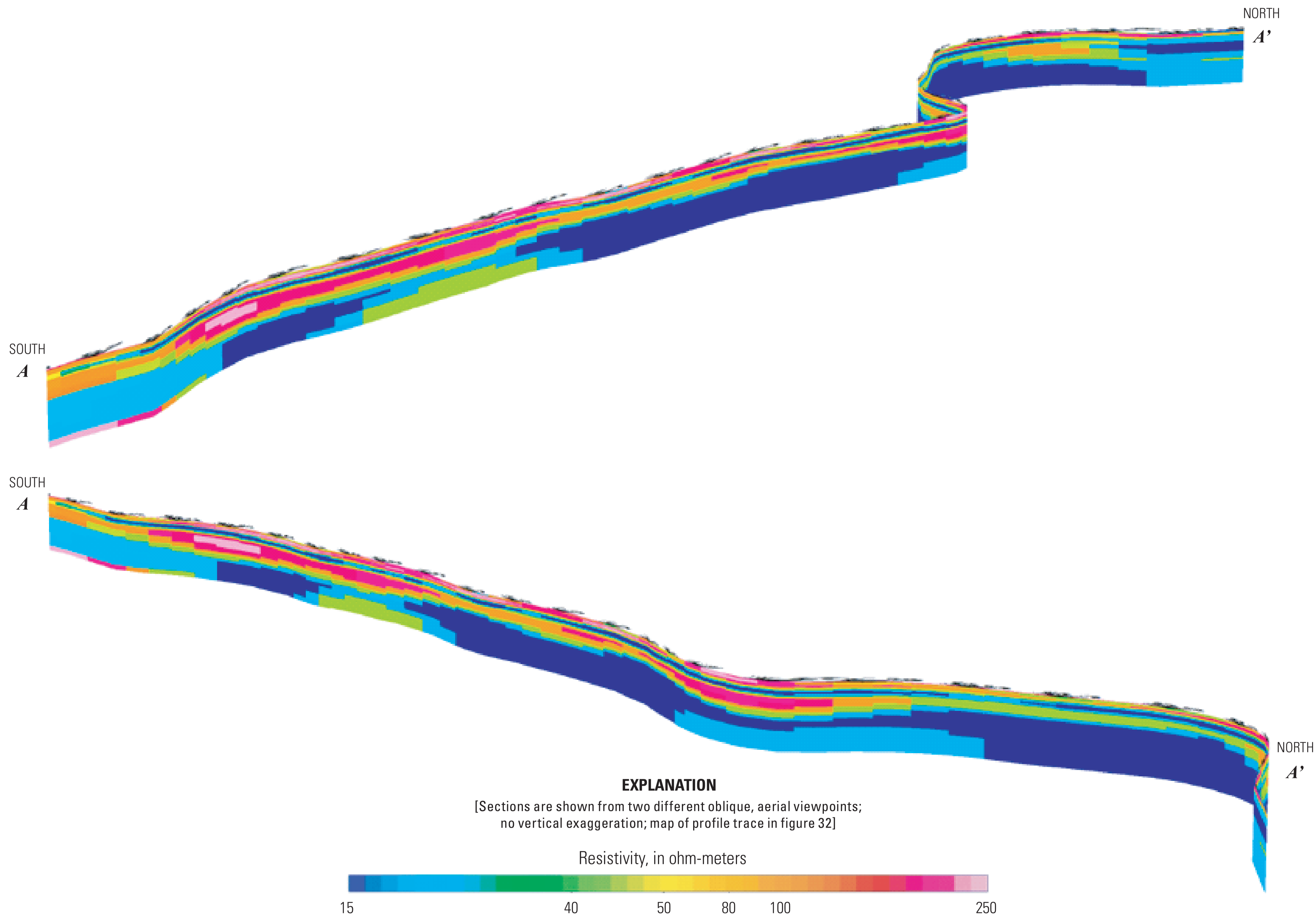

Figure 34. Mixed-mode two-dimensional (2D) inversion results from 2010 audio-magnetotelluric (AMT) stations for the north segment (*A* to *A'*) along Whitman Road, Cherry and Grant Counties, Nebr.

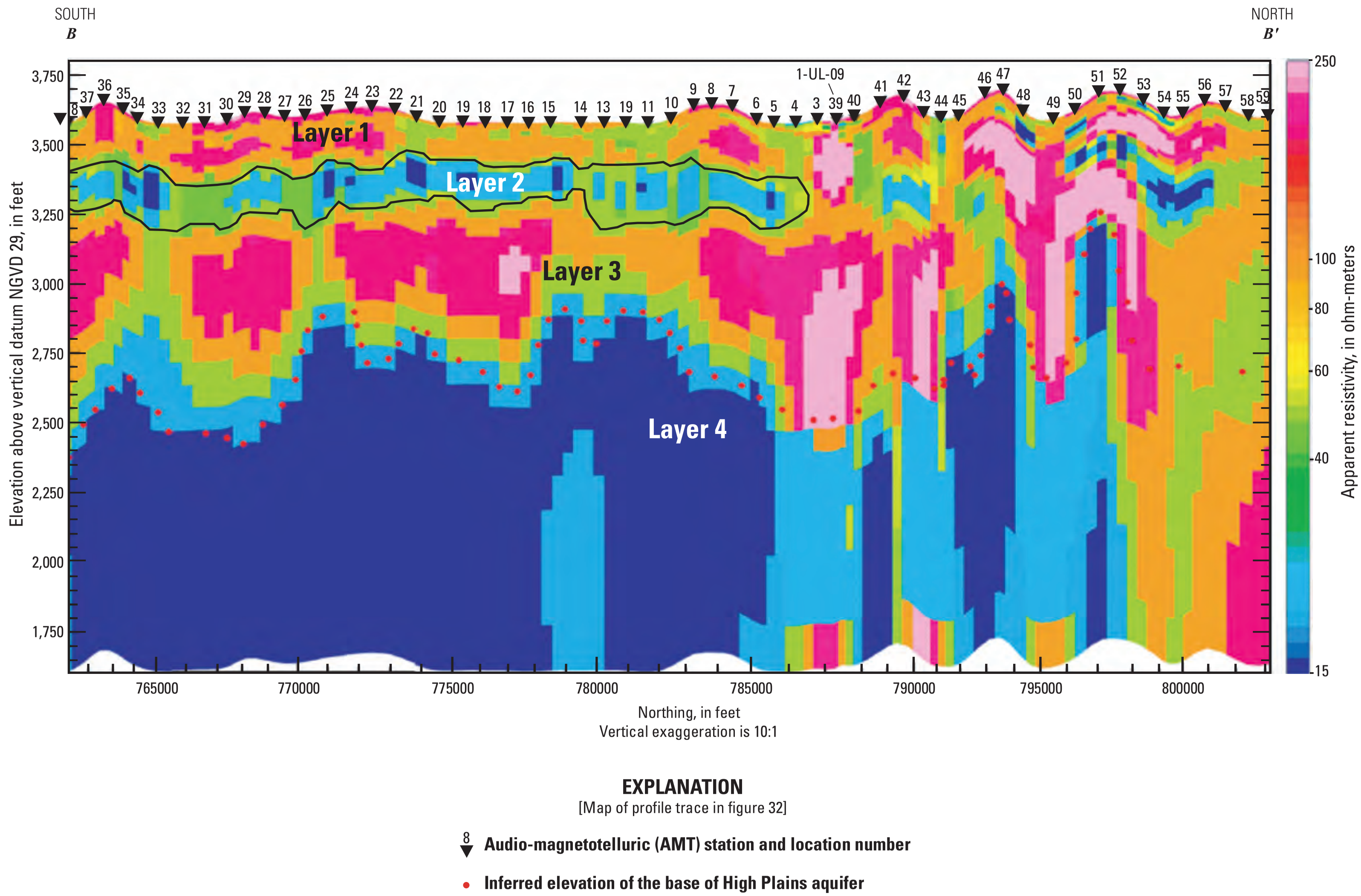

Figure 35. Mixed-mode two-dimensional (2D) inversion results from 2010 audio-magnetotelluric (AMT) stations for the south segment (*B* to *B′*) along Whitman Road, Grant County.

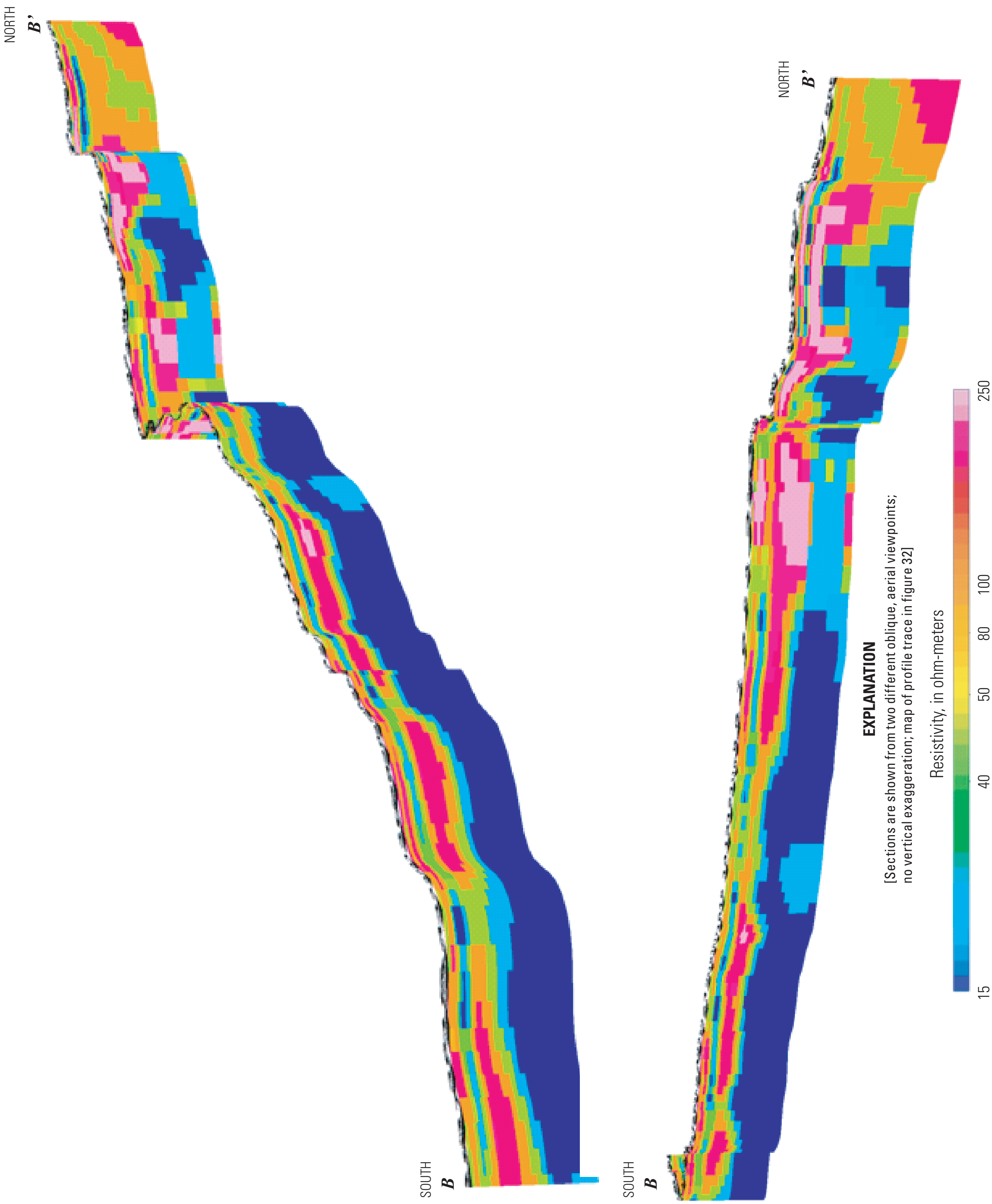

Figure 36. Mixed-mode two-dimensional (2D) inversion results from 2010 audio-magnetotelluric (AMT) soundings for the south segment (*B* to *B'*) along Whitman Road, Grant County, Nebr.

Table 5. Location and inferred elevation of base of High Plains aquifer, north segment of Whitman Road profile, Grant and Cherry Counties, Nebr., 2010.

[Northing and easting in Nebraska State Plane coordinates]

Latitude[1]	Longitude[1]	Northing (feet)	Easting (feet)	Elevation[2] (feet)
42.04536	101.5242	809404	1226552	2,279
42.04439	101.524	809048	1226608	2,884
42.04563	101.5243	809504	1226534	2,877
42.04664	101.5246	809871	1226458	2,851
42.04783	101.5251	810308	1226329	2,805
42.0483	101.5254	810479	1226253	2,751
42.04887	101.5258	810691	1226149	2,706
42.04922	101.526	810817	1226079	2,653
42.04944	101.5262	810900	1226033	2,590
42.05001	101.5266	811109	1225913	2,542
42.05058	101.5271	811319	1225799	2,493
42.05168	101.5278	811722	1225600	2,481
42.05255	101.5283	812044	1225469	2,502
42.05345	101.5287	812372	1225371	2,533
42.05437	101.5289	812708	1225319	2,551
42.05563	101.529	813167	1225312	2,581
42.05703	101.529	813676	1225325	2,595
42.05829	101.529	814137	1225331	2,588
42.0588	101.529	814322	1225334	2,563
42.06	101.529	814759	1225332	2,545
42.06099	101.5291	815122	1225305	2,565
42.06167	101.5293	815369	1225269	2,622
42.06216	101.5294	815547	1225234	2,669
42.06289	101.5296	815815	1225187	2,740
42.06326	101.5297	815949	1225165	2,780
42.06375	101.5298	816130	1225147	2,814
42.06444	101.5299	816380	1225127	2,846
42.06488	101.5299	816540	1225120	2,855
42.06638	101.53	817088	1225100	2,851
42.06732	101.5301	817431	1225084	2,823
42.06782	101.5302	817613	1225074	2,769
42.0685	101.5302	817863	1225055	2,728
42.06906	101.5303	818067	1225034	2,681
42.07023	101.5306	818493	1224969	2,663
42.07102	101.5308	818782	1224912	2,672
42.07169	101.531	819027	1224868	2,715
42.07194	101.5311	819117	1224855	2,774
42.07312	101.5312	819549	1224827	2,828
42.07521	101.5308	820307	1224945	2,855
42.07775	101.5299	821229	1225216	2,833
42.07827	101.5298	821419	1225248	2,789
42.07847	101.5297	821490	1225257	2,735

Table 5. Location and inferred elevation of base of High Plains aquifer, north segment of Whitman Road profile, Grant and Cherry Counties, Nebr., 2010.—Continued

[Northing and easting in Nebraska State Plane coordinates]

Latitude[1]	Longitude[1]	Northing (feet)	Easting (feet)	Elevation[2] (feet)
42.07928	101.5298	821787	1225243	2,692
42.08018	101.5302	822115	1225147	2,653
42.08084	101.5309	822358	1224963	2,629
42.08135	101.5322	822550	1224613	2,667
42.08159	101.5331	822643	1224359	2,735
42.0821	101.5344	822835	1224015	2,833
42.08241	101.5349	822950	1223883	2,873
42.08311	101.5358	823210	1223650	2,943
42.08469	101.5371	823791	1223301	2,964
42.08592	101.5382	824246	1223008	2,953
42.08697	101.5392	824634	1222734	2,955
42.08821	101.5399	825086	1222555	2,953
42.08863	101.5401	825242	1222525	2,987
42.08863	101.5401	825242	1222525	3,009
42.0905	101.5399	825920	1222584	2,993
42.0907	101.5398	825993	1222609	2,950
42.09118	101.5395	826167	1222678	2,898
42.09152	101.5393	826292	1222736	2,837
42.09209	101.5389	826497	1222853	2,774
42.09395	101.537	827166	1223395	2,771
42.09472	101.5361	827442	1223650	2,880
42.0951	101.5357	827576	1223756	2,993
42.09484	101.5359	827485	1223689	3,074
42.09586	101.5351	827851	1223919	3,175
42.09738	101.5339	828398	1224242	3,175

[1] Decimal degrees; North American Datum of 1983 (NAD 83).

[2] Land-surface elevation above National Geodetic Vertical Datum of 1929 (NGVD 29); elevations surveyed to nearest foot.

Table 6. Location and inferred elevation of base of High Plains aquifer, south segment of Whitman Road profile, Grant County, Nebr., 2010.

[Northing and easting in Nebraska State Plane coordinates]

Latitude[1]	Longitude[1]	Northing (feet)	Easting (feet)	Elevation[2] (feet)
41.9131	101.4948	761088	1233700	2,374
41.91508	101.4932	761802	1234135	2,492
41.9165	101.4926	762316	1234314	2,546
41.91833	101.4922	762981	1234435	2,621
41.92056	101.4909	763789	1234812	2,659
41.92205	101.4894	764324	1235222	2,605
41.92411	101.4887	765070	1235417	2,535
41.92515	101.4889	765451	1235368	2,465
41.92828	101.4913	766601	1234736	2,460
41.93027	101.4921	767329	1234541	2,444
41.93221	101.4913	768034	1234781	2,422
41.93429	101.4911	768790	1234834	2,492
41.93621	101.4916	769490	1234722	2,562
41.93741	101.4924	769932	1234516	2,654
41.93792	101.4928	770121	1234404	2,756
41.93844	101.4932	770310	1234291	2,831
41.9398	101.494	770811	1234093	2,880
41.9427	101.4954	771874	1233712	2,896
41.94293	101.4958	771958	1233624	2,847
41.94326	101.4963	772082	1233485	2,777
41.94369	101.497	772243	1233289	2,713
41.94561	101.4981	772945	1233016	2,729
41.94661	101.4984	773311	1232921	2,783
41.9479	101.4994	773788	1232653	2,837
41.94897	101.5007	774184	1232312	2,820
41.9496	101.5013	774414	1232151	2,745
41.95193	101.502	775266	1231987	2,724
41.95423	101.5028	776109	1231791	2,681
41.95588	101.5031	776709	1231721	2,627
41.95771	101.5032	777377	1231683	2,611
41.95901	101.5037	777853	1231579	2,670
41.9597	101.504	778105	1231484	2,777
41.96063	101.5046	778448	1231324	2,869
41.96211	101.5055	778993	1231087	2,907
41.96358	101.5065	779533	1230836	2,864
41.96371	101.5066	779580	1230810	2,794
41.96486	101.5076	780003	1230549	2,783
41.96575	101.5084	780332	1230344	2,864
41.96716	101.5095	780851	1230032	2,901
41.96882	101.511	781460	1229651	2,896
41.9704	101.5115	782038	1229510	2,869
41.97145	101.5117	782423	1229475	2,820

Table 6. Location and inferred elevation of base of High Plains aquifer, south segment of Whitman Road profile, Grant County, Nebr., 2010.—Continued

[Northing and easting in Nebraska State Plane coordinates]

Latitude[1]	Longitude[1]	Northing (feet)	Easting (feet)	Elevation[2] (feet)
41.97246	101.512	782793	1229396	2,767
41.9733	101.5124	783099	1229292	2,681
41.97552	101.5141	783915	1228849	2,664
41.97766	101.5166	784708	1228169	2,632
41.97907	101.5184	785231	1227702	2,589
41.98056	101.5217	785787	1226824	2,546
41.98311	101.5244	786731	1226087	2,508
41.98433	101.5275	787188	1225252	2,514
41.98621	101.5305	787887	1224463	2,541
41.98772	101.5307	788440	1224418	2,632
41.98989	101.5302	789227	1224564	2,675
41.99216	101.5299	790053	1224660	2,659
41.99449	101.5288	790898	1224977	2,621
41.99563	101.528	791307	1225183	2,632
41.99563	101.528	791307	1225183	2,654
41.99651	101.5277	791627	1225288	2,713
41.99863	101.5274	792396	1225382	2,702
41.99909	101.5274	792565	1225379	2,670
41.9997	101.5275	792788	1225369	2,740
42.00045	101.5276	793063	1225342	2,826
42.00075	101.5276	793172	1225328	2,917
42.0018	101.5278	793553	1225279	2,998
42.00224	101.5279	793717	1225261	2,966
42.00255	101.528	793827	1225250	2,869
42.00472	101.5281	794618	1225241	2,777
42.00504	101.528	794734	1225249	2,697
42.00647	101.5279	795256	1225281	2,659
42.00846	101.5281	795983	1225248	2,713
42.00945	101.5285	796343	1225138	2,799
42.00945	101.5285	796343	1225138	2,966
42.0101	101.529	796583	1225009	3,106
42.0106	101.5295	796767	1224880	3,197
42.01143	101.5305	797074	1224614	3,256
42.01248	101.5319	797463	1224251	3,176
42.01283	101.5323	797593	1224132	3,047
42.01356	101.5331	797862	1223918	2,933
42.01392	101.5335	797998	1223818	2,794
42.01562	101.5342	798618	1223637	2,691
42.01892	101.533	799814	1223986	2,702
42.0255	101.5334	802213	1223912	2,681
42.03291	101.5356	804924	1223385	2,681

[1] Decimal degrees; North American Datum of 1983 (NAD 83).

[2] Land-surface elevation above National Geodetic Vertical Datum of 1929 (NGVD 29); elevations surveyed to nearest foot.

Conclusions and Implications for Future Study

The differences between the predicted base-of-aquifer elevation and the elevation from McGuire and Peterson (2008) suggests that in areas of the upper Loup study area the base of aquifer is not well-constrained. The range of differences was from -157 to 300 feet (-48 to 91 m). Test holes 1-UL-09 and 2-UL-09, drilled in the western part of the upper Loup study area, had base-of-aquifer elevations more than 100 feet (30 m) deeper than predicted by SIM 2008-3042. This indicates that the test holes likely were drilled in paleovalleys eroded into the Brule Formation.

TDEM-based estimates of the base-of-aquifer elevation were in good accordance with those from existing test-hole data. The TDEM method was able to constrain the elevation and topology of the base of the High Plains aquifer. The TDEM method also provided information regarding the thickness of the Quaternary eolian sands, Pliocene or younger sand and gravel, and the Miocene Ogallala Group. TDEM is, thus, a valuable and cost-effective tool for mapping hydrostratigraphy throughout the High Plains aquifer and can provide additional subsurface characterization needed in regional groundwater models.

Short reconnaissance profiles were collected with the AMT method to determine the base of aquifer. To model subsurface features using this approach, the geologic strike of subsurface features, including the base-of-aquifer surface, must be known in advance. When collecting short profiles (roughly 650 to 1,300 ft; 200 to 400 m), the assumption of west-to-east alignment of drainages and paleovalleys may be invalid in the upper Loup study area; therefore, a pilot survey would need to be completed before collecting a short profile.

In 2010, AMT data were collected along an approximately 12-mile-(19-km-) long profile along Whitman Road, in Grant and Cherry Counties. The AMT results from the Whitman Road profile are in general accordance with TDEM sounding CN1 and test hole 1-UL-09. The AMT profile indicated substantial variability in the topography of the base of the High Plains aquifer and in the distribution of high permeability zones within the aquifer. This indicates that the subsurface geology in this area is poorly understood and local-scale variability of the High Plains aquifer cannot be captured with test-hole drilling alone. Parallel profiles, such as those provided by airborne TDEM methods, would be needed to adequately characterize the hydrostratigraphy in the upper Loup study area.

A combination of test-hole drilling and surface-geophysical data collection was used to improve the understanding of the hydrogeology in the upper Loup study area in support of the ELM groundwater model. The data collected for this study can be incorporated into existing data sets to improve the estimated thickness of the aquifer and the configuration of the base-of-aquifer surface.

Summary

The Elkhorn-Loup Model (ELM) and related studies were collaboratively begun to understand the impact of various groundwater management scenarios on surface-water resources. During Phase 1 of the ELM study, a lack of subsurface geological information in the Upper Loup Natural Resources District (ULNRD) area was identified as a gap in current (2011) understanding that needed to be addressed. To improve the understanding of the hydrogeology of the upper Loup study area, the U.S. Geological Survey, in cooperation with the ULNRD and the University of Nebraska Conservation and Survey Division, included lithologic description of circulated drill cuttings collected from nine test holes and borehole geophysical data to improve aquifer thickness estimates and enhance the understanding of the groundwater system. Surface geophysical data also were collected using time-domain electromagnetic (TDEM) and audio-magnetotelluric (AMT) methods at test-hole locations and between test holes as a quick, non-invasive means of identifying the base of the High Plains aquifer.

Sites primarily were chosen to fill existing spatial gaps in the University of Nebraska Conservation and Survey Division test-hole database. Geophysical methods were selected based on the physical characteristics of the hydrostratigraphic units of the study area and the anticipated depth to the base of the aquifer (top of the Brule Formation). Two surface geophysical methods were chosen: TDEM and AMT methods.

Nine test holes were drilled to below the base of the aquifer and logged with a borehole geophysical logging system. A total of 26 TDEM and 117 AMT soundings were collected within the study area between 2008 and 2010. Soundings collected in 2008 and 2009 were in close proximity to previously drilled or planned test holes. The data collection in 2010 was expanded to specifically include locations where little information previously existed.

Previous test-hole drilling has indicated greater variation in the base-of-aquifer elevation in the west, reflecting a number of deep paleovalleys incised into the Brule Formation. Two of the new test holes were located in close proximity to the previously interpreted paleovalleys in Grant and Hooker Counties.

TDEM soundings within the study area were documented to be effective as virtual boreholes in mapping the base-of-aquifer elevation beneath the study area. TDEM estimates of the base of aquifer were in good accordance with existing test-hole data and are useful in improving topology of the base of aquifer, and details of the overlying stratigraphic section. Uplift structures, such as the Chadron Arch, were identified in the modeled TDEM results as subtle changes in the deep resistivity structure.

In 2010, AMT data were collected along an approximately 12-mile-(19-km-) long profile along Whitman Road, in Grant and Cherry Counties. The AMT results indicated substantial variability in the elevation of the base of the High

Plains aquifer and in the distribution of high permeability zones within the aquifer.

A combination of test-hole drilling and surface-geophysical data collection was used to improve the understanding of the hydrogeology in the upper Loup study area in support of the ELM groundwater model. The data collected for this study can be incorporated into existing data sets to improve the estimated thickness of the aquifer and the configuration of the base-of-aquifer surface. TDEM is a valuable and cost-effective tool for mapping hydrostratigraphy throughout the High Plains aquifer. The AMT technique is a useful tool when assessing the variability within the High Plains aquifer and distribution of high permeability zones. Both techniques, when properly applied, are useful in improving the regional hydrostratigraphic framework needed in groundwater models.

References Cited

Anderson, J.A., Morin, R.H., Cannia, J.C., and Williams, J.H., 2009, Geophysical log analysis of selected test holes and wells in the High Plains aquifer, central Platte River Basin, Nebraska: U.S. Geological Survey Scientific Investigations Report 2009–5033, 16 p.

Auken, E., and Nebel, K., 2001, Getting started with SiTEM and SEMDI: University of Aarhus, Hydro Geophysics Group, Aarhus, Denmark, not paginated.

Bendat, J.S., and Piersol, A.G., 1971, Random data—Analysis and measurement procedures: New York, Wiley Interscience, 407 p.

Bentall, Ray, 1989, Streams, *in* Bleed, A.S., and Flowerday, C.A., eds., An atlas of the Sand Hills: University of Nebraska, Lincoln, Nebr., Conservation and Survey Division, Resource Atlas no. 5a, p. 93–114.

Biella, G., Lozej, A., and Tabacco, I., 1983, Experimental study of some hydrogeophysical properties of unconsolidated porous media: Ground Water, v. 21, no. 6, p. 741–751.

Bleed, A., 1989, Groundwater, *in* Bleed, A.S., and Flowerday, C.A., eds., An atlas of the Sand Hills: University of Nebraska, Lincoln, Nebr., Conservation and Survey Division, Resource Atlas no. 5a, p. 67–92.

Cannia, J.C., Woodward, Duane, and Cast, L.D., 2006, Cooperative Hydrology Study (COHYST) hydrostratigraphic units and aquifer characterization report: Lincoln, Nebraska Department of Natural Resources, 96 p., accessed December 2010, at *http://cohyst.dnr.ne.gov/document/dc012hydro_aquifer_022406.pdf.*

Center for Advanced Land Management Information Technologies, 2007, 2005 Nebraska land use map: Lincoln, University of Nebraska, CALMIT geospatial data, accessed November 2, 2010, at *http://www.calmit.unl.edu/2005landuse/statewide.shtml*.

Century Geophysical Corp., 2011a, 9144 Series E logging tool: Tulsa, Okla., accessed June 21, 2011, at *http://www.century-geo.info/dnn/EquipmentSales/LoggingTools/9144LoggingTool.aspx*.

Century Geophysical Corp., 2011b, 9512 Slim hole induction tool: Tulsa, Okla., accessed June 21, 2011, at *http://www.century-geo.info/dnn/EquipmentSales/LoggingTools/9512LoggingTool.aspx*.

Chen, X., Chen, X.H., Rowe, C., Hu, Q., and Andersen, M., 2003, Geological and climatic controls on streamflows in the Nebraska Sand Hills: Journal of the American Water Resources Association, v. 39, p. 217–228.

Christiansen, A.V., Auken, E., and Viezzoli, A., 2011, Quantification of modeling errors in airborne TDEM caused by inaccurate system description: Geophysics, v. 76, p. 43–52, doi:10.1190/1.3511354.

Condra, G.E., and Reed, E.C., 1943, The geological section of Nebraska: Nebraska Geological Survey Bulletin (Conservation and Survey Division, University of Nebraska-Lincoln), v. 14, p. 82.

Constable, S.C., Parker, R.L., and Constable, C.G., 1987, Occam's inversion—A practical algorithm for generating smooth models from electromagnetic sounding data: Geophysics, v. 52, no. 3, p. 289–300.

Danielsen, J.E., Auken, E., Jørgensen, F., Søndergaard, V., and Sørensen, K.I., 2003, The application of the transient electromagnetic method in hydrogeophysical surveys: Journal of Applied Geophysics, v. 53, no. 4, p. 181–198.

Darton, N.H., 1903, Preliminary report on the geology and water resources of Nebraska west of the one hundred and third meridian: U.S. Geological Survey Professional Paper 17, 69 p., 43 pls.

Diffendal, R.F., Jr., 1991, Geologic map showing configuration of the bedrock surface, North Platte 1º x 2º quadrangle, Nebraska: U.S. Geological Survey Miscellaneous Investigation Series Map I–2277, scale 1:250,000.

Dobrin, M.D., and Savit, C.H., 1988, Introduction to geophysical prospecting (4th ed.): New York, McGraw-Hill, 867 p.

Eberhart-Phillips, D., Stanley, W.D., Rodriguez, B.D., and Lutter, W.J., 1995, Surface seismic and electrical methods to detect fluids related to faulting: Journal of Geophysical Research, v. 100, no. B7, p. 12,919–12,936.

Effersø, F., Auken, E., and Sørensen, K.I., 1999, Inversion of band-limited TEM responses: Geophysical prospecting, v. 47, p. 551–564.

Fitterman, D.V., and Labson, V.F., 2005, Electromagnetic induction methods for environmental problems, *in* Butler, D.K., ed., Near surface geophysics: Tulsa, Okla., Society of Exploration Geophysicists, no. 13, p. 301–356.

Geological Institute, 2002a, Vejledning i kalibrering af TEM måleudstyr (in Danish): Aarhus, Denmark, Aarhus University, 12 p.

Geological Institute, 2002b, Test og sammenligning af Transient Elektromagnetiske instrumenter i Danmark (in Danish): Aarhus University, 118 p.

Geometrics, 2007, STRATAGEM 26716-01 rev. F, operation manual for sysTDEMs running IMAGEM ver. 2.19: San Jose, Calif., Geometrics, Inc., 45 p.

Geotools, 1998, Geotools MT user's guide: AOA Geophsyics Inc., Moss Landing, Calif., 450 p.

Goeke, James W., 2000, McPherson County test-hole logs: Lincoln, Nebr., University of Nebraska-Lincoln, Conservation and Survey Division, Nebraska Water Survey Test-Hole Report no. 60, 50 p.

Gutentag, E.D., Heimes, F.J., Krothe, N.C., Luckey, R.R., and Weeks, J.B., 1984, Geohydrology of the High Plains aquifer in parts of Colorado, Nebraska, New Mexico, Oklahoma, South Dakota, Texas, and Wyoming: U.S. Geological Survey Professional Paper 1400–B, 63 p.

Hallenburg, J.K., 1998, Non-hydrocarbon methods of geophysical formation evaluation: Boca Raton, Fla., Lewis Publishers, 265 p.

Hearst, J.R., and Nelson, P.H., 1985, Well logging for physical properties: New York, McGraw-Hill, 571 p.

Hearst, J.R., Nelson, P.H., and Paillet, F.L., 2000, Well logging for physical properties, 2nd ed.: New York, John Wiley, 483 p.

Jiracek, G.R., 2011, The Magnetotelluric Method, accessed August 25, 2011, at *http://www.geology.sdsu.edu/people/emeritus/jiracek/sage/documents/The%20Magnetotelluric%20Method.pdf.*

Keller, G.V., 1987, Rock and mineral properties, *in* Nabighian, M.N., ed., Electromagnetic methods in applied geophysics theory: Tulsa, Okla., Society of Exploration Geophysicists, v. 1, p. 13–51.

Keller, G.V., 1989, Electrical properties, *in* Carmichael, R.S., ed., Practical handbook of physical properties of rocks and minerals: Boca Raton, Florida, CRC Press, 359–427.

Keys, W.S., 1990, Borehole geophysics applied to groundwater investigations: U.S. Geological Survey Techniques of Water-Resources Investigations, book 2, chap. E2, p. 48–83.

Kwader, T., 1985, Estimating aquifer permeability from formation resistivity factors: Ground Water, v. 23, no. 6, p. 762–766.

Loope, D.B., and Swinehart, J.B., 2000, Thinking like a dune field— Geologic history in the Nebraska Sand Hills: Great Plains Research, v. 10, p. 5–35.

Loope, D.B., Swinehart, J.B., and Mason, J.P., 1995, Dune-dammed paleovalleys of the Nebraska Sand Hills: intrinsic versus climatic controls on the accumulation of lake and marsh sediments: Geological Society of America Bulletin, v. 107, no. 4, p. 396–406.

Mackie, R., Rieven, S., and Rodi, W., 1997, Users manual and software documentation for two-dimensional inversion of magnetotelluric data: AOA Geophysics Inc., Moss Landing, Calif., GEOTOOLS User's Guide RLM2DI Supplement, 10 p.

Mason, J.P., Swinehart, J.B., and Loope, D.B., 1997, Holocene history of lacustrine and marsh sediments in a dune-blocked drainage, southwestern Nebraska Sand Hills, U.S.A.: Journal of Paleolimnology, v. 17, p. 67–83.

Mast, M.A., and Turk, J.T., 1999, Environmental characteristics and water quality of Hydrologic Benchmark Network stations in the West-Central United States, 1963–95: U.S. Geological Survey Circular 1173–C, 105 p.

McGuire, V.L., and Peterson, S.M., 2008, Base of principal aquifer for the Elkhorn-Loup model area, north-central Nebraska: U.S. Geological Survey Scientific Investigations Map 2008–3042, 1 sheet. Also available at *http://pubs.usgs.gov/sim/3042*.

McGuire, V.L., and Fischer, B.C., 1999, Water-level changes, 1980 to 1997, and saturated thickness, 1996–97, in the High Plains aquifer: U.S. Geological Survey Fact Sheet 124–99, 4 p.

Nabighian, M.N., and Macnae, J.C., 1991, Time-domain electromagnetic prospecting methods, *in* Nabighian, M.N., ed., Electromagnetic methods in applied geophysics, v. 2: Tulsa, Okla., Society of Exploration Geophysicsists, 427–520.

National Earthquake Information Center, 2011, USGS Earthquake Hazards Program–USTA Network: U.S. Geological Survey digital data, accessed November 2, 2011, at *http://neic.usgs.gov/neis/station_book/USTA_NETWORK.html.*

National Oceanic and Atmospheric Administration, 2010, Climate data inventories: Asheville, N.C., National Climatic Data Center digital data, accessed November 1, 2010, at *http://www4.ncdc.noaa.gov/cgi-win/wwcgi.dll?wwDI~StnSrch~StnID~20013324.*

Ostdiek, Amy, 2009, The integrated management planning process: Lincoln, Nebr., Nebraska Department of Natural Resources, Water Matters, no. 1, 4 p., accessed November 3, 2010, at *http://www.dnr.state.ne.us/IWM/WaterMatters/WaterMatters_No1.pdf*.

Palacky, G.J., 1987, Resistivity characteristics of geologic targets, *in* Nabighian, M.N., ed., Electromagnetic methods in applied geophysics theory: Tulsa, Okla., Society of Exploration Geophysicists, v. 1, p. 53–129.

Peterson, S.M., Stanton, J.S., Saunders, A.T., and Bradley, J.R., 2008, Simulation of ground-water flow and effects of ground-water irrigation on base flow in the Elkhorn and Loup River Basins, Nebraska: U.S. Geological Survey Scientific Investigations Report 2008–5143, 65 p.

Rodi, William, and Mackie, R.L., 2001, Nonlinear conjugate gradients algorithm for 2–D magnetotelluric inversion: Geophysics, v. 66, no. 1, p. 174–187.

Stanley, K.O., and Wayne, W.J., 1972, Epeirogenic and climatic controls of early Pleistocene fluvial sediment dispersal in Nebraska: Geological Society of America, v. 83, p. 3,675–3,690.

Stanton, G.P., Kress, W.H., Teeple, A.P., Greenslate, M.I., and Clark, A.K., 2007, Geophysical analysis of the Salmon Peak Formation near Amistad Reservoir Dam, Val Verde County, Texas, and Coahuila, Mexico, March 2006, to aid in piezometer placement: U.S. Geological Survey Scientific Investigations Report 2007–5143, 70 p.

Stanton, J.S., Peterson, S.M., and Fienen, M.N., 2010, Simulation of groundwater flow and effects of groundwater irrigation on stream base flow in the Elkhorn and Loup River Basins, Nebraska, 1895–2055–Phase two: U.S. Geological Survey Scientific Investigations Report 2010–5149, 78 p.

Swinehart, J.B., 1989, Wind-blown Deposits, *in* Bleed, A.S., and Flowerday, C.A., eds., An atlas of the Sand Hills: University of Nebraska, Lincoln, Nebr., Conservation and Survey Division, Resource Atlas no. 5a, p. 43–56.

Swinehart, J.B., and Diffendal, R.F., 1989, Geology, *in* Bleed, A.S., and Flowerday, C.A., eds., An atlas of the Sand Hills: University of Nebraska, Lincoln, Nebr., Conservation and Survey Division, Resource Atlas no. 5a, p. 29–42.

Swinehart, J.B., Souders, V.L., DeGraw, H.M., and Diffendal, R.F., 1985, Cenozoic paleogeography of western Nebraska, *in* Flores, R.M., and Kaplan, S.S., eds., Cenozoic paleogeography of the West-Central United States: Denver, Colo., p. 209–229.

Szilagyi, Jozsef, Harvey, F.E., and Ayers, J.F., 2003, Regional estimation of base recharge to ground water using water balance and a base flow index: Ground Water, v. 41, no. 4, p. 504–513.

U.S. Geological Survey, 2009, Archiving borehole-geophysical data: Reston, Va., USGS, Office of Groundwater Technical Memorandum No. 2010.01, accessed November 16, 2010, at *http://water.usgs.gov/usgs/ogw/bgas/borehole_archiving/*.

University of Nebraska-Lincoln, Conservation and Survey Division, 2011, Test-hole database: Lincoln, Nebr., Conservation and Survey Division digital data, accessed March 22, 2011, at *http://snr.unl.edu/data/geographygis/NebraskaTestHole/NebraskaTestHole.asp*.

Vozoff, Keeva, 1972, The magnetotelluric method in the exploration of sedimentary basins: Geophysics, v. 37, p. 98–141.

Vozoff, Keeva, 1991, The magnetotelluric method, *in* Nabighian, M.N., ed., Electromagnetic methods in applied geophysics: Tulsa, Okla., Society of Exploration Geophysicists, v . 2, pt. B, p. 641–711.

Wannamaker, P.E., 1983, Resistivity structure of the northern Basin and Range: Davis, Calif., Geothermal Resources Council, Special Report no. 13, p. 345–361.

Wannamaker, P.E., Hohmann, G.W., and Ward, S.H., 1984, Magnetotelluric responses of three-dimensional bodies in layered earths: Geophysics, v. 49, no. 9, p. 1,517–1,533.

Wannamaker, P.E., Stodt, J.A., and Rijo, L., 1987, PW2D—Finite element program for solution of magnetotelluric responses of two-dimensional earth resistivity structure (User documentation): Salt Lake City, Utah, Earth Science Laboratory, University of Utah Research Institute, 40 p.

Weeks, J.B., and Gutentag, E.D., 1988, Region 17, High Plains, Chap. 20, *in*, Back, W., Rosenshein, J.S., and Seaber, P.R., eds., Hydrogeology, Geology of North America, v. O-2: Boulder, Colo., Geological Society of Amercia, p. 157–164.

Wigley, P.B., 2000, Logan County test-hole logs: Lincoln, Nebr., University of Nebraska-Lincoln, Conservation and Survey Division, Nebraska Water Survey Test-Hole Report no. 57, 17 p.

Winter, T.C., 1986, Effect of ground-water recharge on configuration of the water table beneath sand dunes and on seepage in lakes in the Sandhills of Nebraska, U.S.A: Journal of Hydrology, v. 86, p. 221–237

Supplemental Data

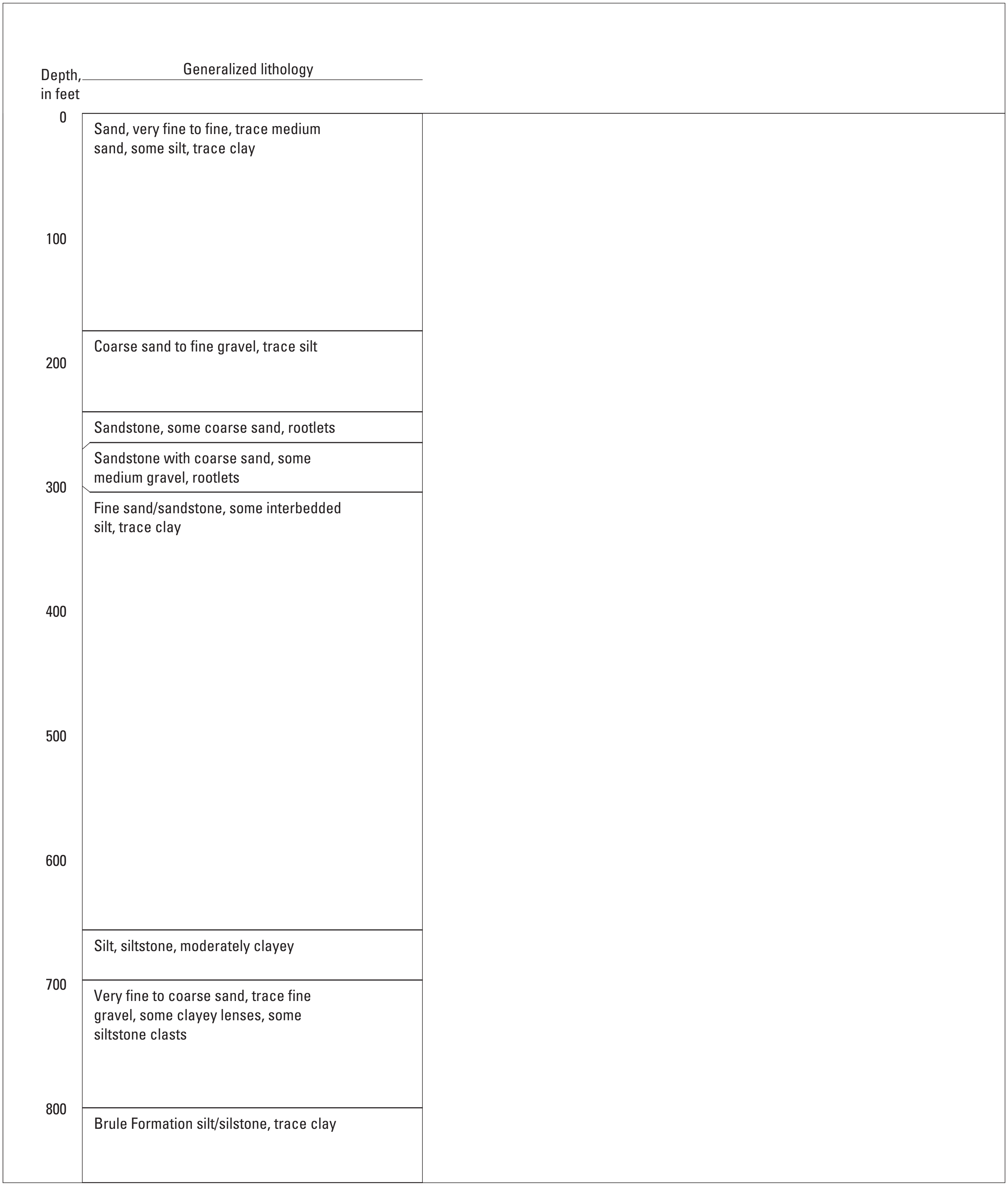

Figure 6. Generalized lithologic description of test hole1-UL-08, Logan County, Nebr.

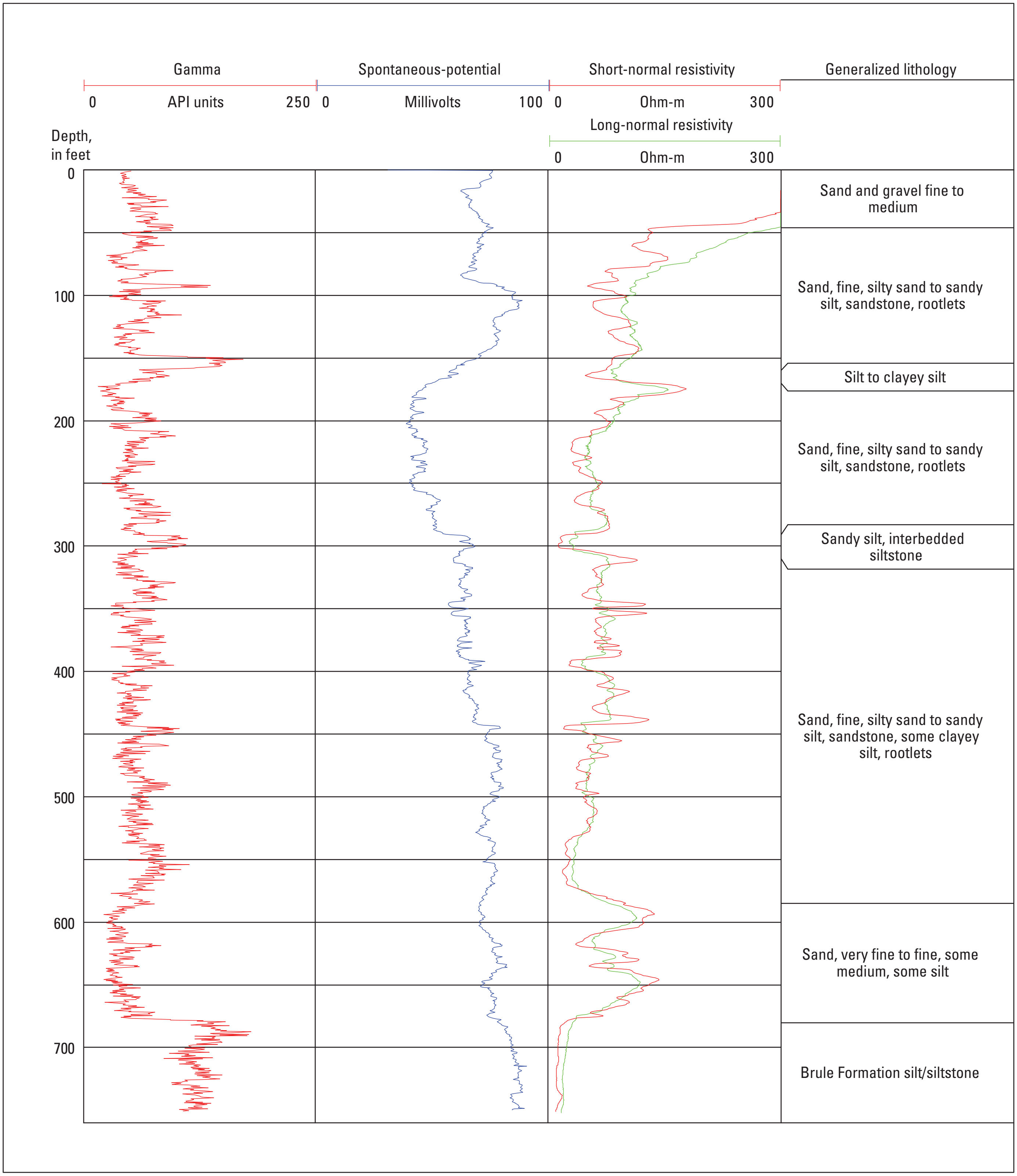

Figure 7. Composite of generalized lithologic description and geophysical logs for test hole 3-UL-08, Thomas County, Nebr. Short-normal resistivity, in ohm-meters; long-normal resistivity, in ohm-meters; natural gamma activity, in American Petroleum Institute units; spontaneous potential, in millivolts.

Figure 8. Composite of generalized lithologic description and geophysical logs for test hole 1-UL-09, Grant County, Nebr. Short-normal resistivity, in ohm-meters; long-normal resistivity, in ohm-meters; natural gamma activity, in American Petroleum Institute units; spontaneous potential, in millivolts.

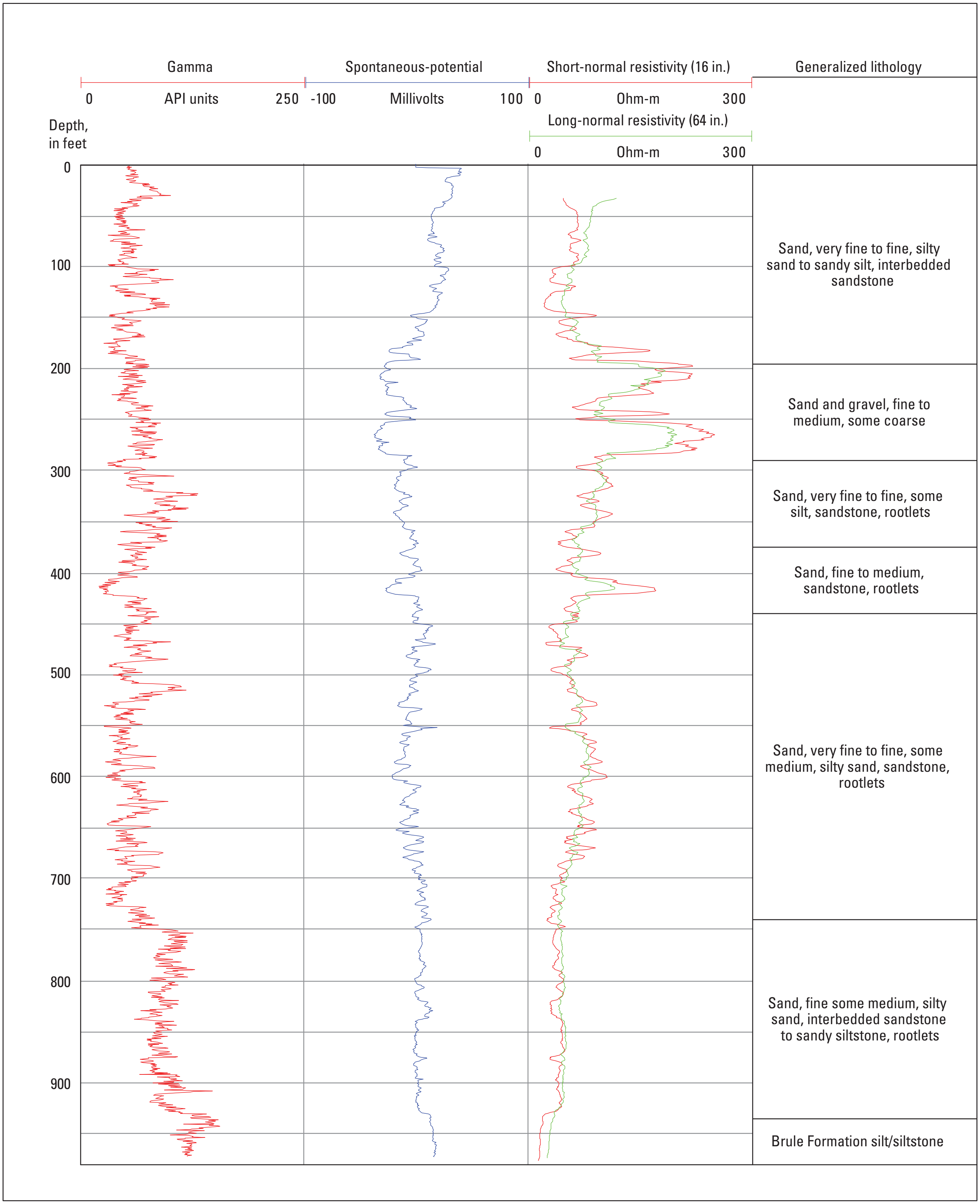

Figure 9. Composite of generalized lithologic description and geophysical logs for test hole 2-UL-09, Hooker County, Nebr. Short-normal resistivity, in ohm-meters; long-normal resistivity, in ohm-meters; natural gamma activity, in American Petroleum Institute units; spontaneous potential, in millivolts.

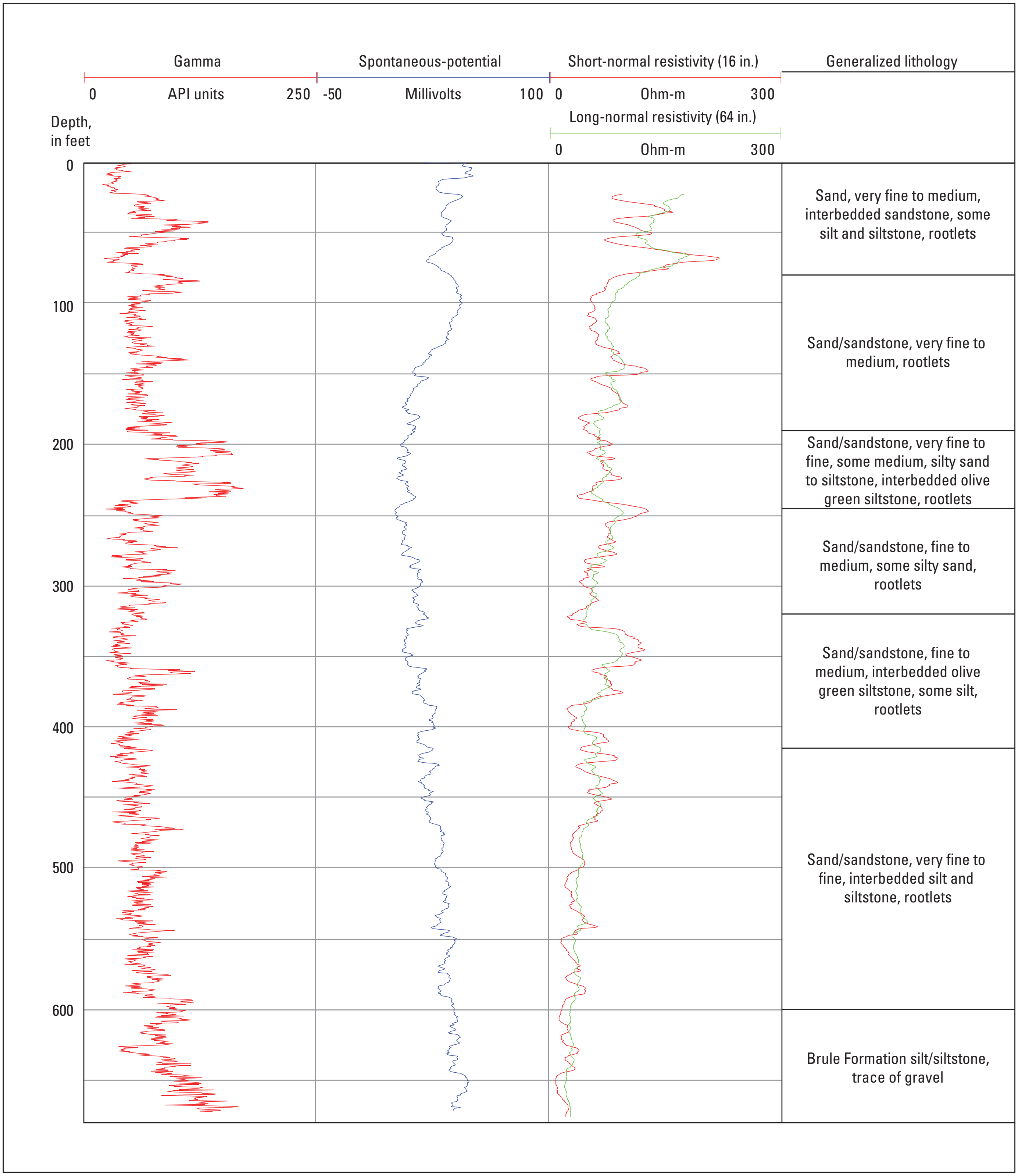

Figure 10. Composite of generalized lithologic description and geophysical logs for test hole 3-UL-09, Cherry County, Nebr. Short-normal resistivity, in ohm-meters; long-normal resistivity, in ohm-meters; natural gamma activity, in American Petroleum Institute units; spontaneous potential, in millivolts.

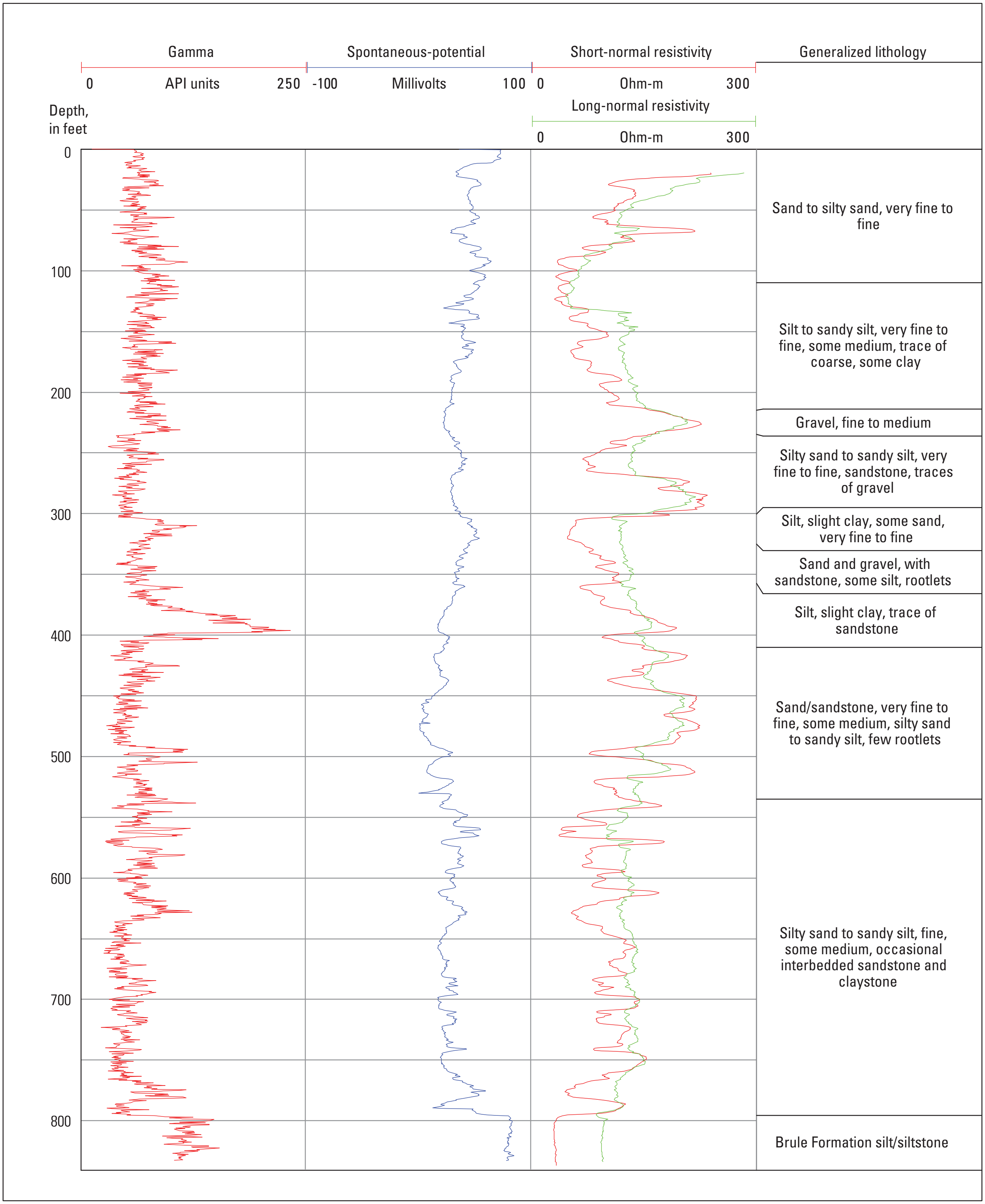

Figure 11. Composite of generalized lithologic description and geophysical logs for test hole 1-UL-10, Thomas County, Nebr. Short-normal resistivity, in ohm-meters; long-normal resistivity, in ohm-meters; natural gamma activity, in American Petroleum Institute units; spontaneous potential, in millivolts.

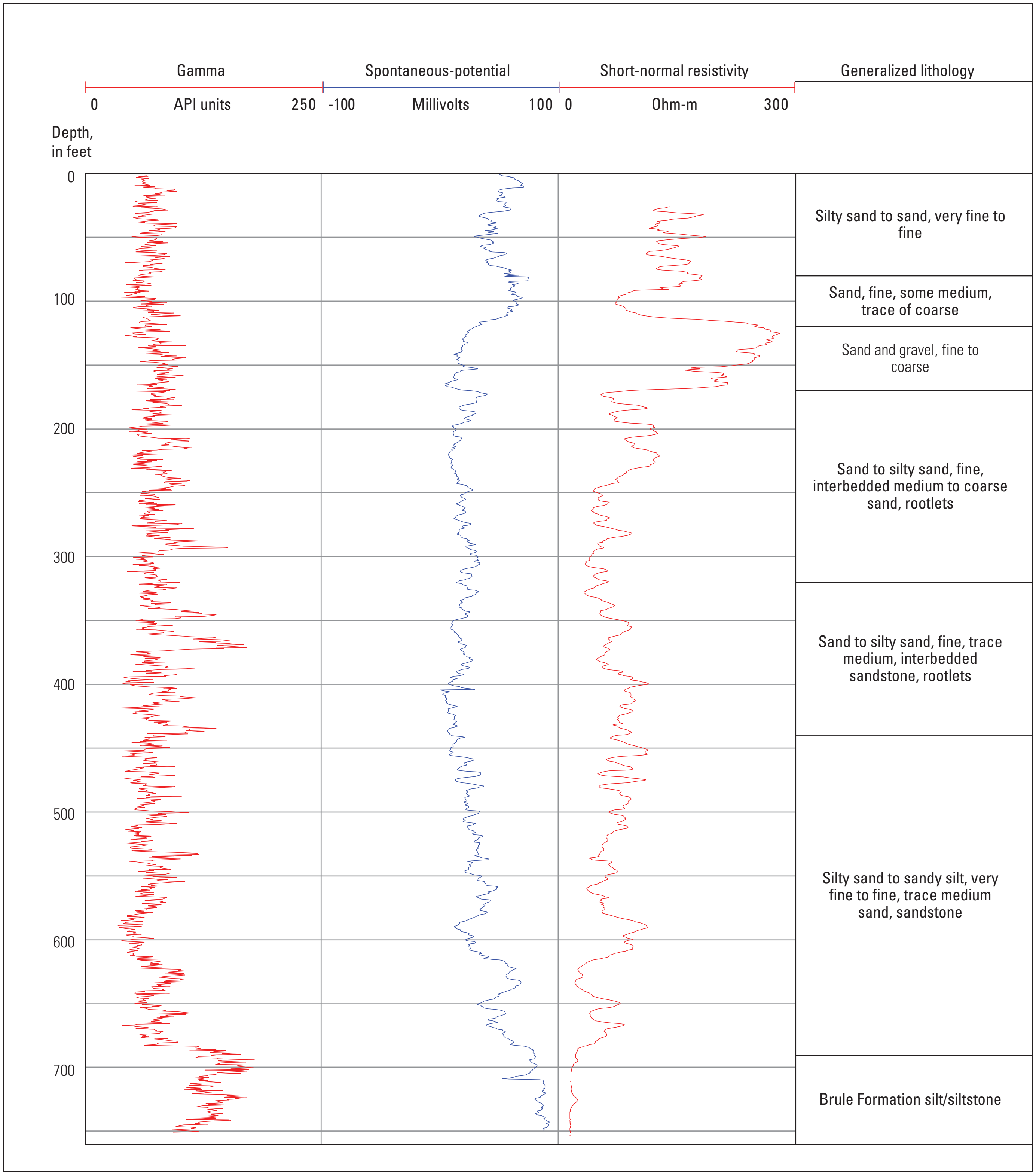

Figure 12. Composite of generalized lithologic description and geophysical logs for test hole 2-UL-10, Thomas County, Nebr. Short-normal resistivity, in ohm-meters; long-normal resistivity, in ohm-meters; natural gamma activity, in American Petroleum Institute units; spontaneous potential, in millivolts.

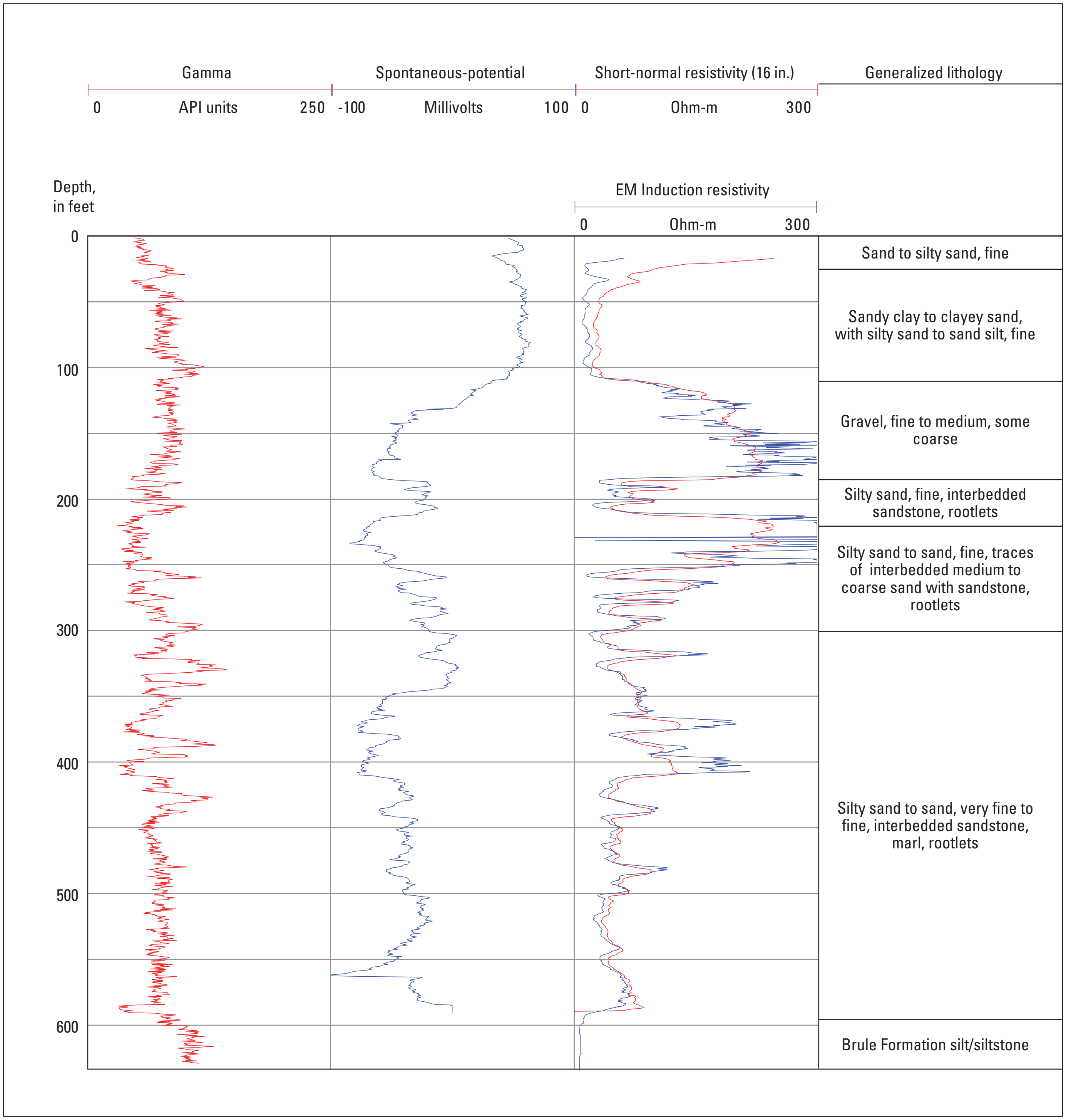

Figure 13. Composite of generalized lithologic description and geophysical logs for test hole 3-UL-10, Blaine County, Nebr. Short-normal resistivity, in ohm-meters; long-normal resistivity, in ohm-meters; electromagnetic induction resistivity, in ohm-meters; natural gamma activity, in American Petroleum Institute units; spontaneous potential, in millivolts.

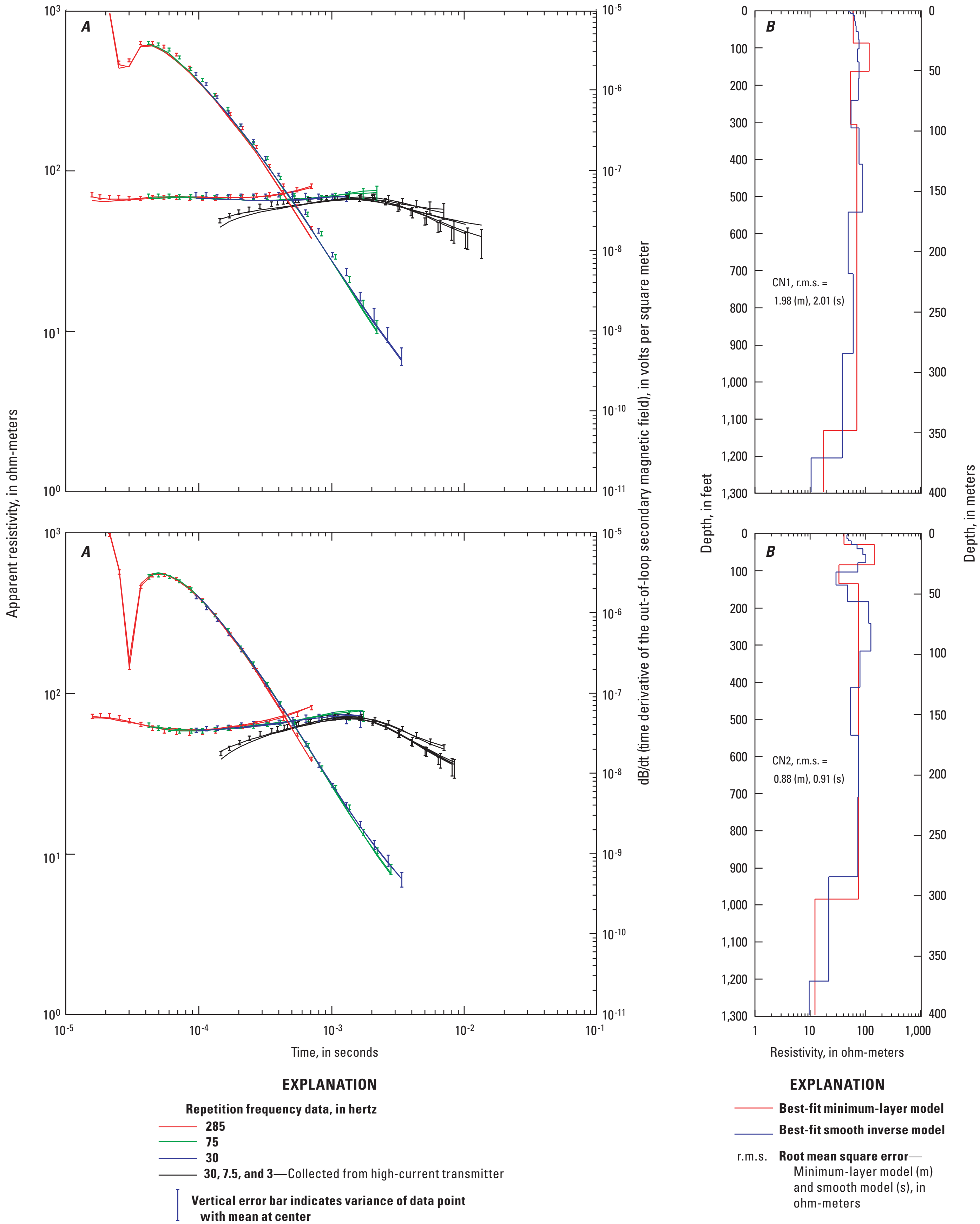

Figure 15. Relations between *A*, central-loop resistivity, out-of-loop vertical magnetic field (time-derivative, right axis), and time; *B*, depth below land surface and subsurface resistivity modeled from TDEM sounding for sites CN1 and CN2.

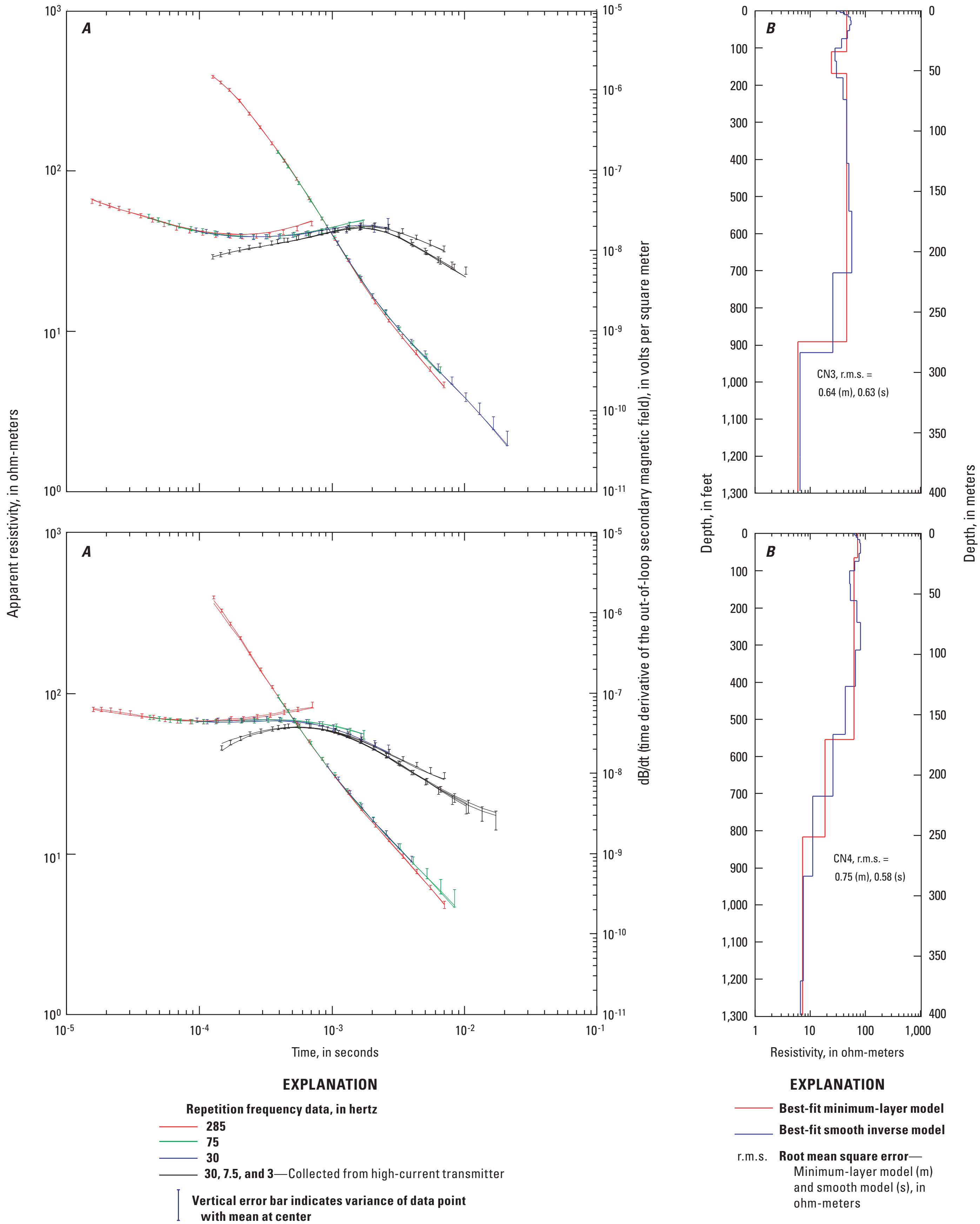

Figure 16. Relations between *A*, central-loop resistivity, out-of-loop vertical magnetic field (time-derivative, right axis), and time; *B*, depth below land surface and subsurface resistivity modeled from TDEM sounding for sites CN3 and CN4.

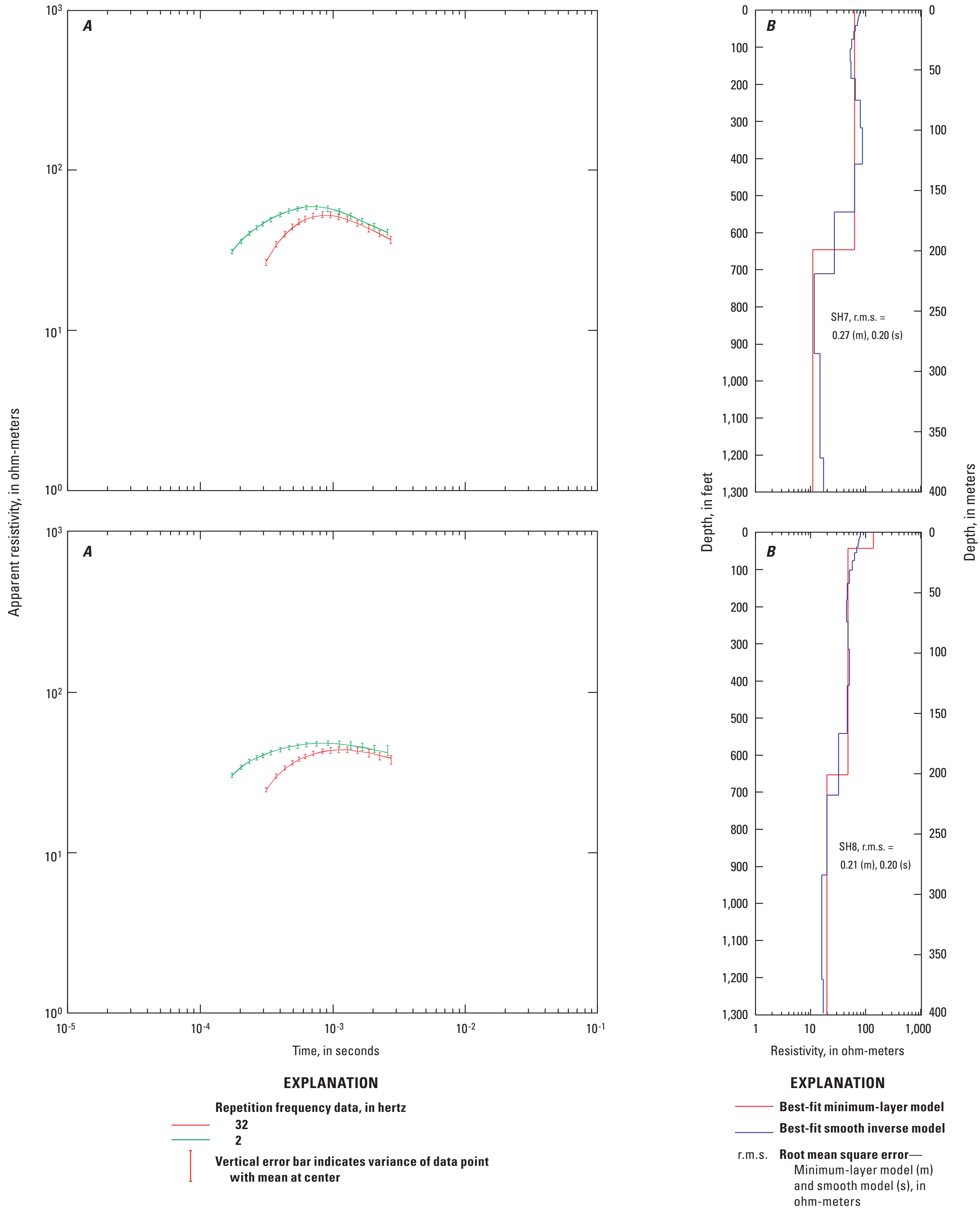

Figure 17. Relations between *A*, central-loop resistivity and time; *B*, depth below land surface and apparent resistivity modeled from TDEM sounding for sites SH7 and SH8.

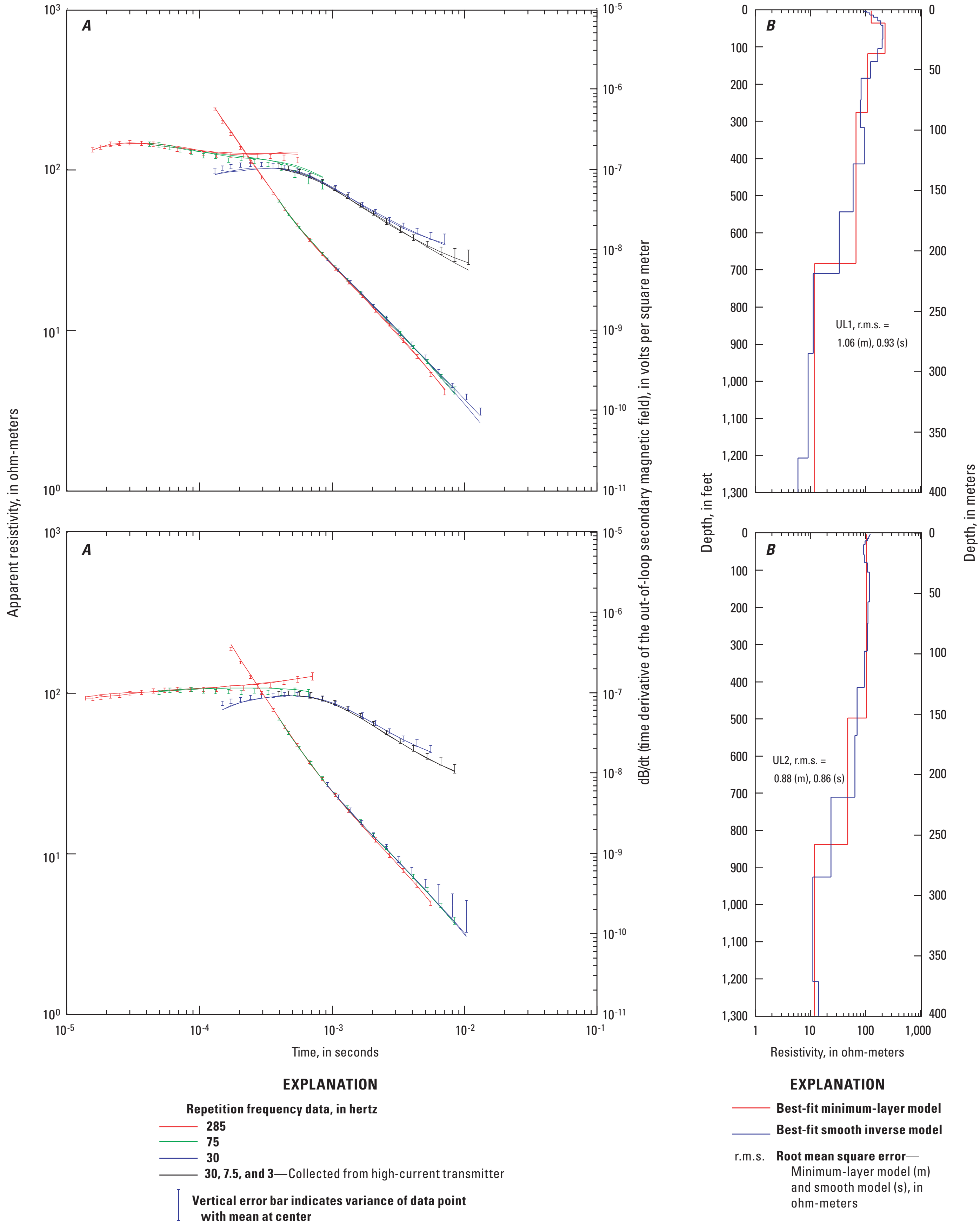

Figure 18. Relations between *A*, central-loop resistivity, out-of-loop vertical magnetic field (time-derivative, right axis), and time; *B*, depth below land surface and subsurface resistivity modeled from TDEM sounding for sites UL1 and UL2.

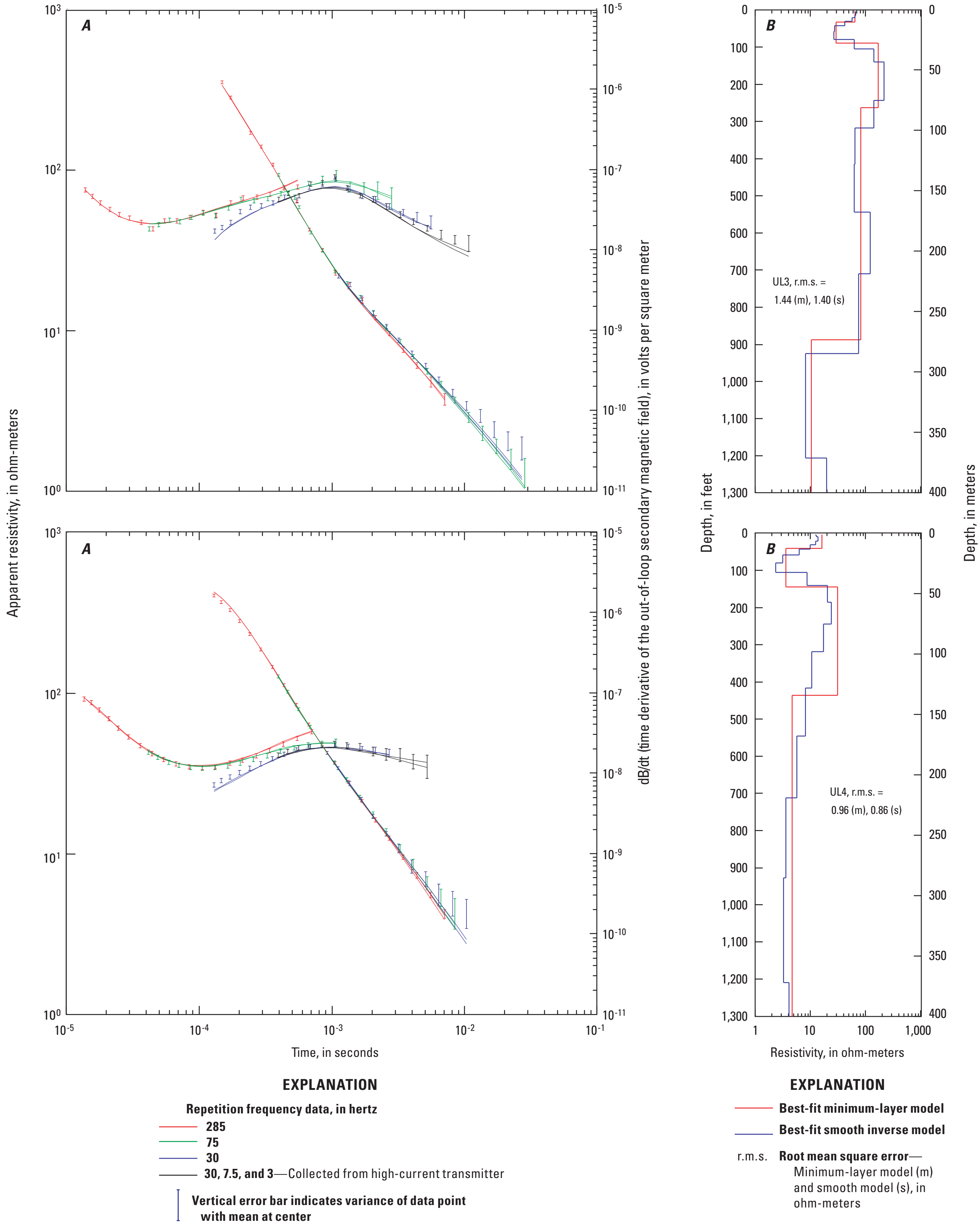

Figure 19. Relations between *A*, central-loop resistivity, out-of-loop vertical magnetic field (time-derivative, right axis), and time; *B*, depth below land surface and subsurface resistivity modeled from TDEM sounding for sites UL3 and UL4.

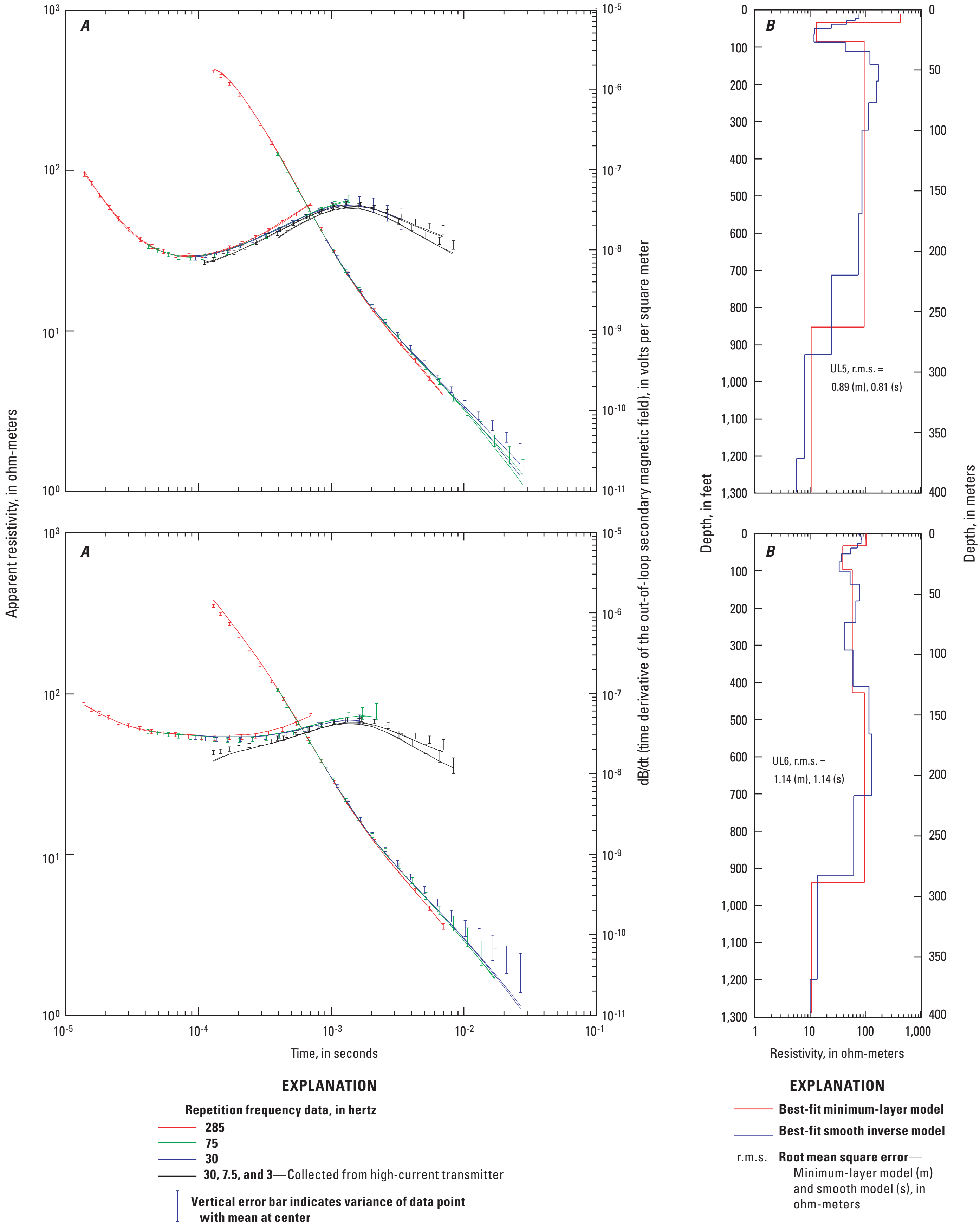

Figure 20. Relations between *A*, central-loop resistivity, out-of-loop vertical magnetic field (time-derivative, right axis), and time; *B*, depth below land surface and subsurface resistivity modeled from TDEM sounding for sites UL5 and UL6.

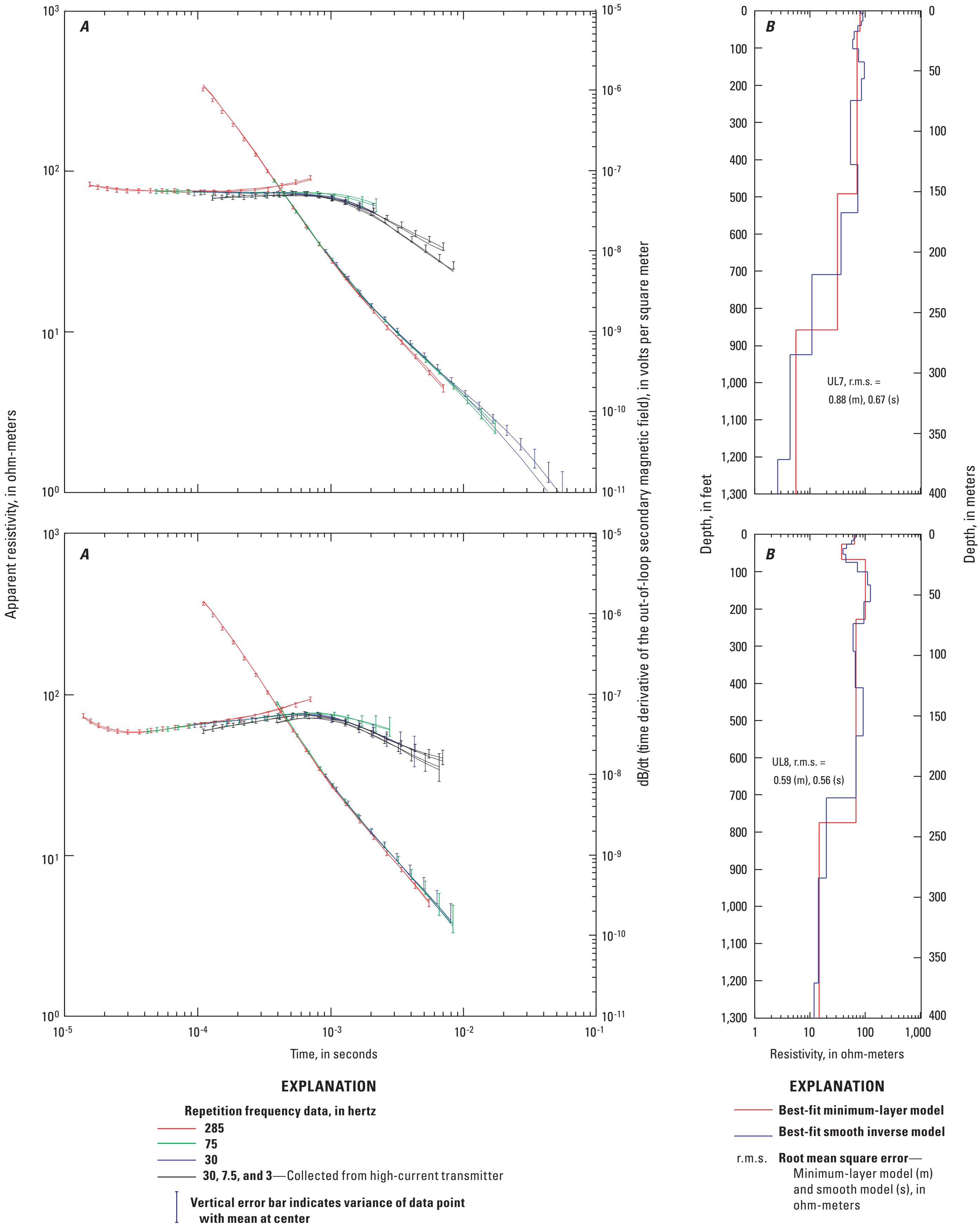

Figure 21. Relations between *A*, central-loop resistivity, out-of-loop vertical magnetic field (time-derivative, right axis), and time; *B*, depth below land surface and subsurface resistivity modeled from TDEM sounding for sites UL7 and UL8.

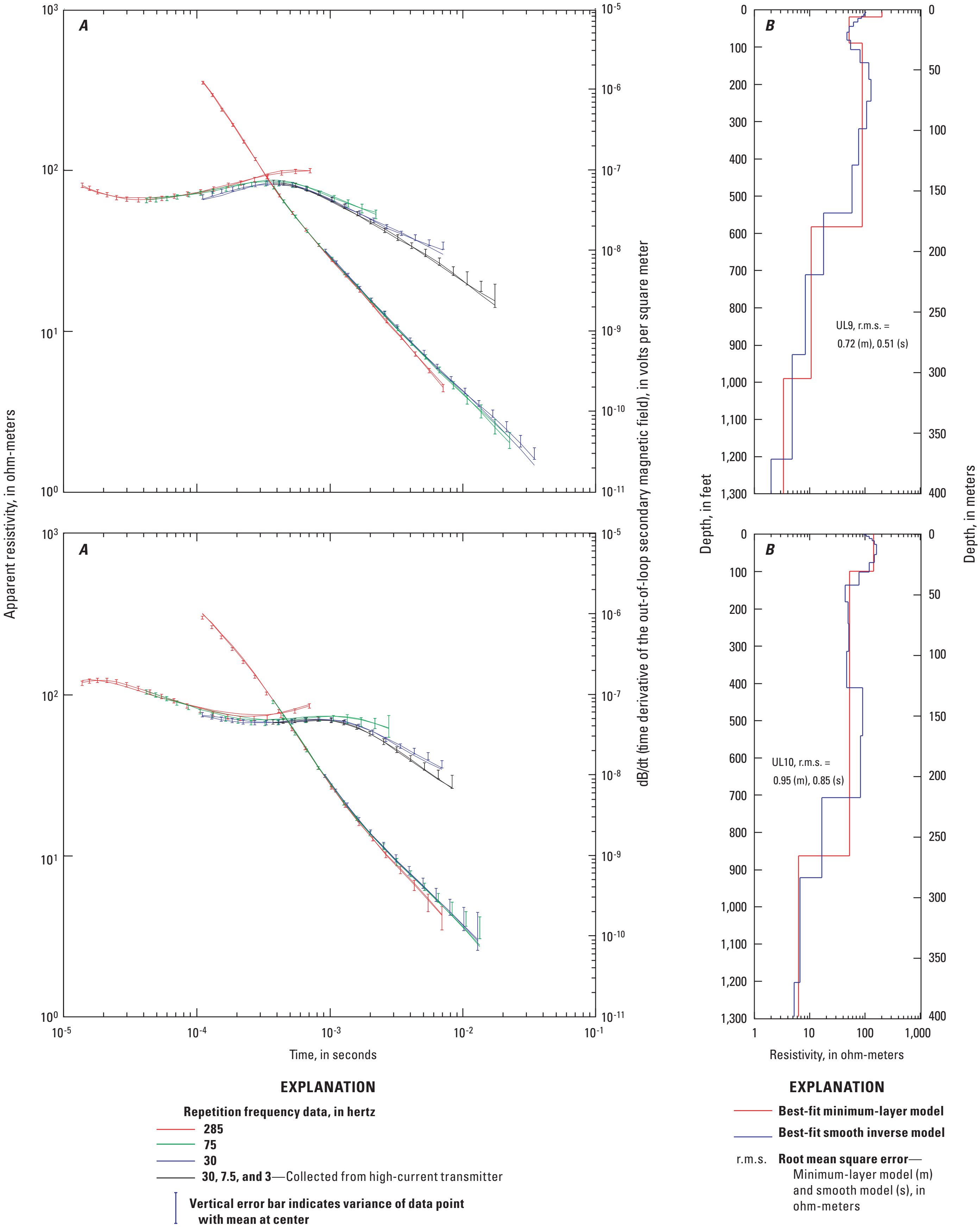

Figure 22. Relations between *A*, central-loop resistivity, out-of-loop vertical magnetic field (time-derivative, right axis), and time; *B*, depth below land surface and subsurface resistivity modeled from TDEM sounding for sites UL9 and UL10.

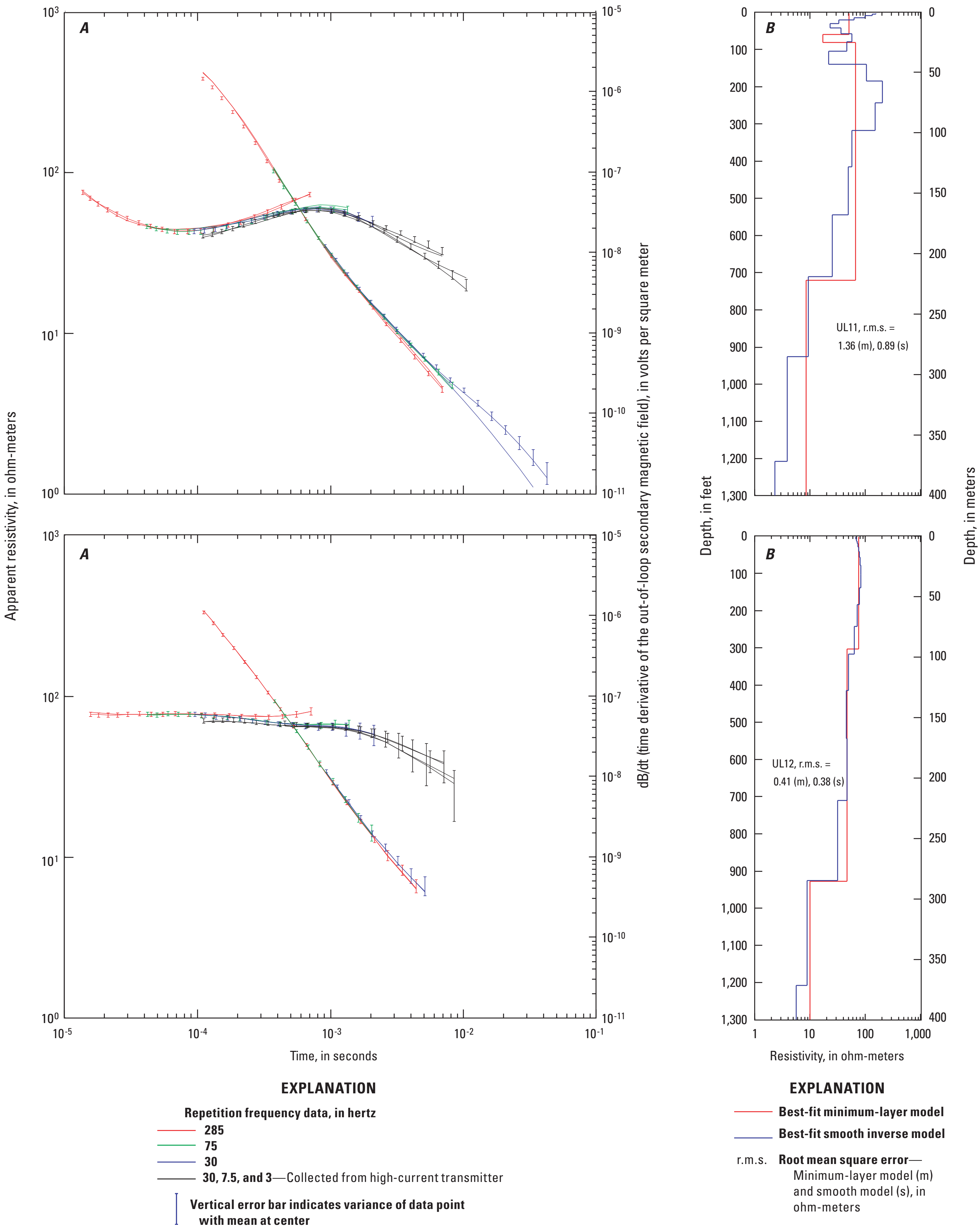

Figure 23. Relations between *A*, central-loop resistivity, out-of-loop vertical magnetic field (time-derivative, right axis), and time; *B*, depth below land surface and subsurface resistivity modeled from TDEM sounding for sites UL11 and UL12.

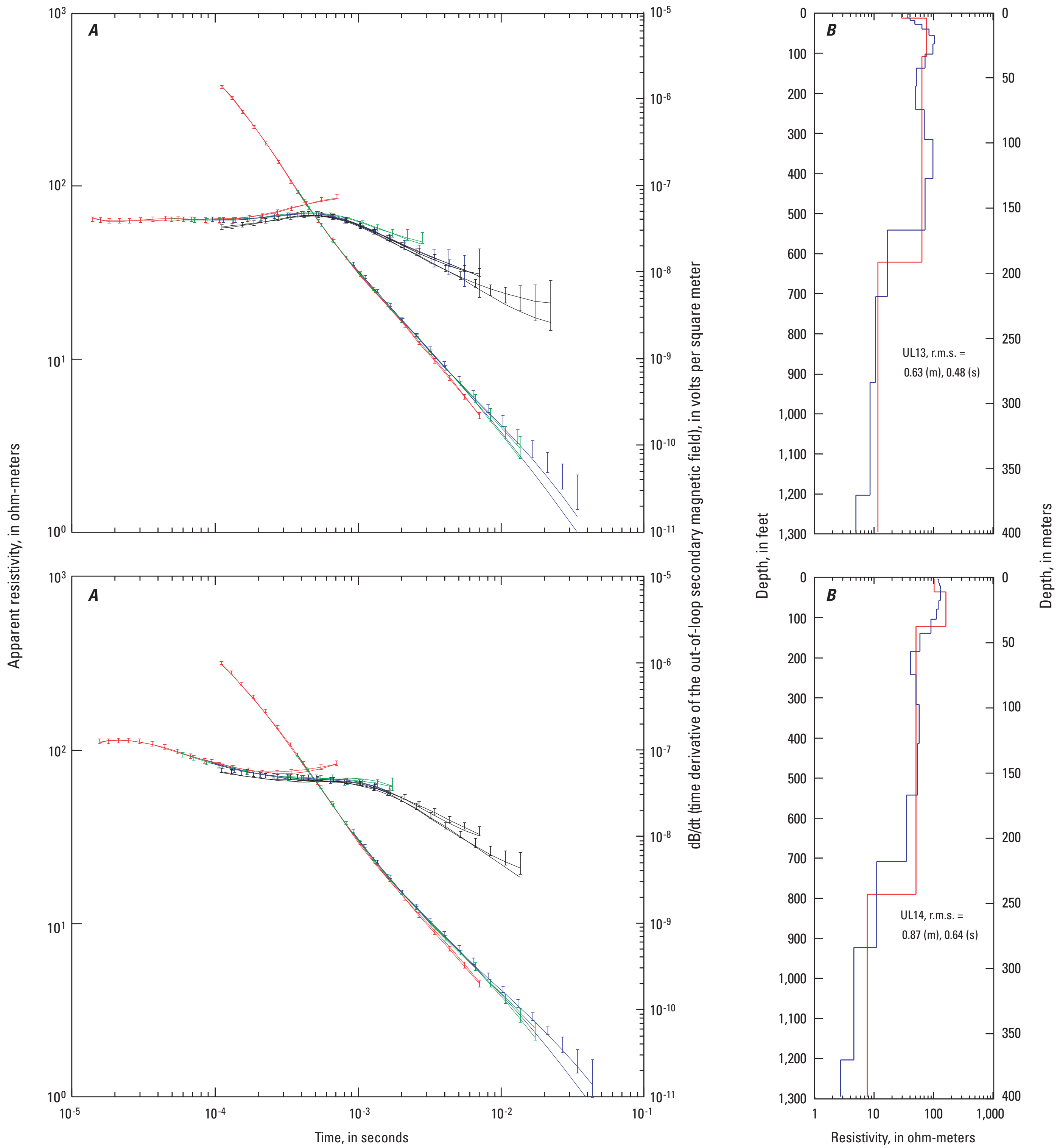

EXPLANATION

Repetition frequency data, in hertz

- **285**
- **75**
- **30**
- **30, 7.5, and 3**—Collected from high-current transmitter

Vertical error bar indicates variance of data point with mean at center

EXPLANATION

- **Best-fit minimum-layer model**
- **Best-fit smooth inverse model**

r.m.s. **Root mean square error**—Minimum-layer model (m) and smooth model (s), in ohm-meters

Figure 24. Relations between *A*, central-loop resistivity, out-of-loop vertical magnetic field (time-derivative, right axis), and time; *B*, depth below land surface and subsurface resistivity modeled from TDEM sounding for sites UL13 and UL14.

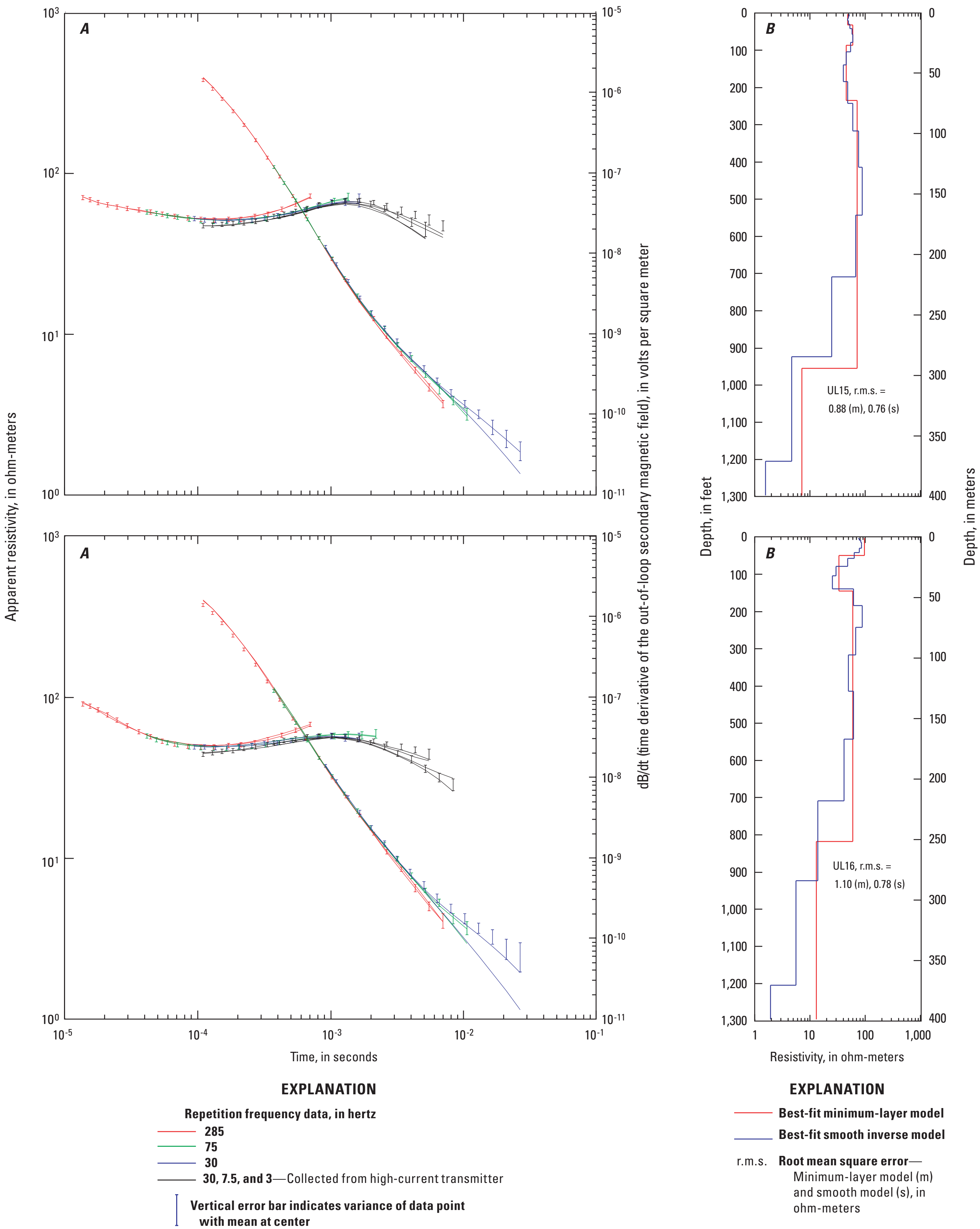

Figure 25. Relations between *A*, central-loop resistivity, out-of-loop vertical magnetic field (time-derivative, right axis), and time; *B*, depth below land surface and subsurface resistivity modeled from TDEM sounding for sites UL15 and UL16.

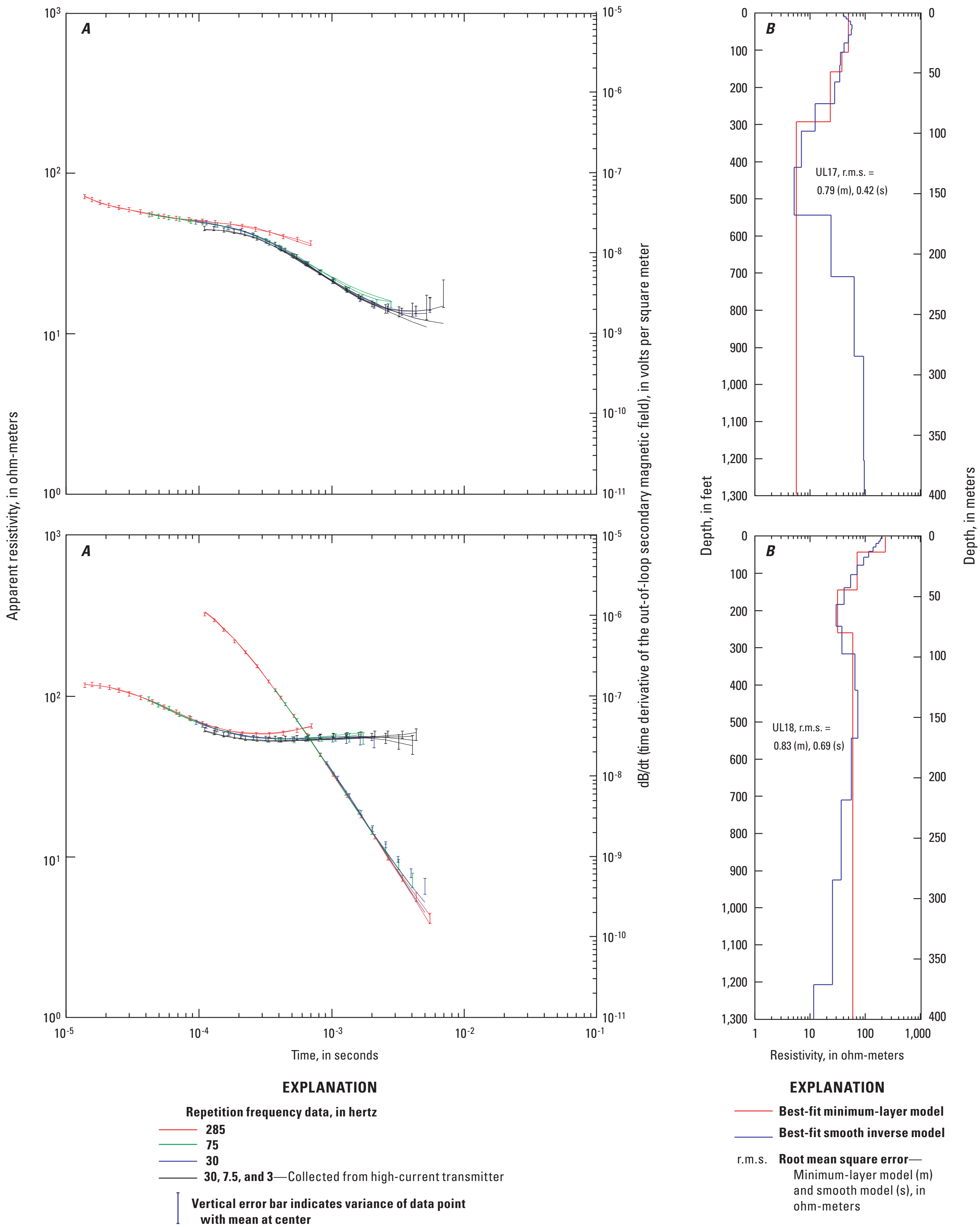

Figure 26. Relations between *A*, central-loop resistivity, out-of-loop vertical magnetic field (time-derivative, right axis), and time; *B*, depth below land surface and subsurface resistivity modeled from TDEM sounding for sites UL17 and UL18.

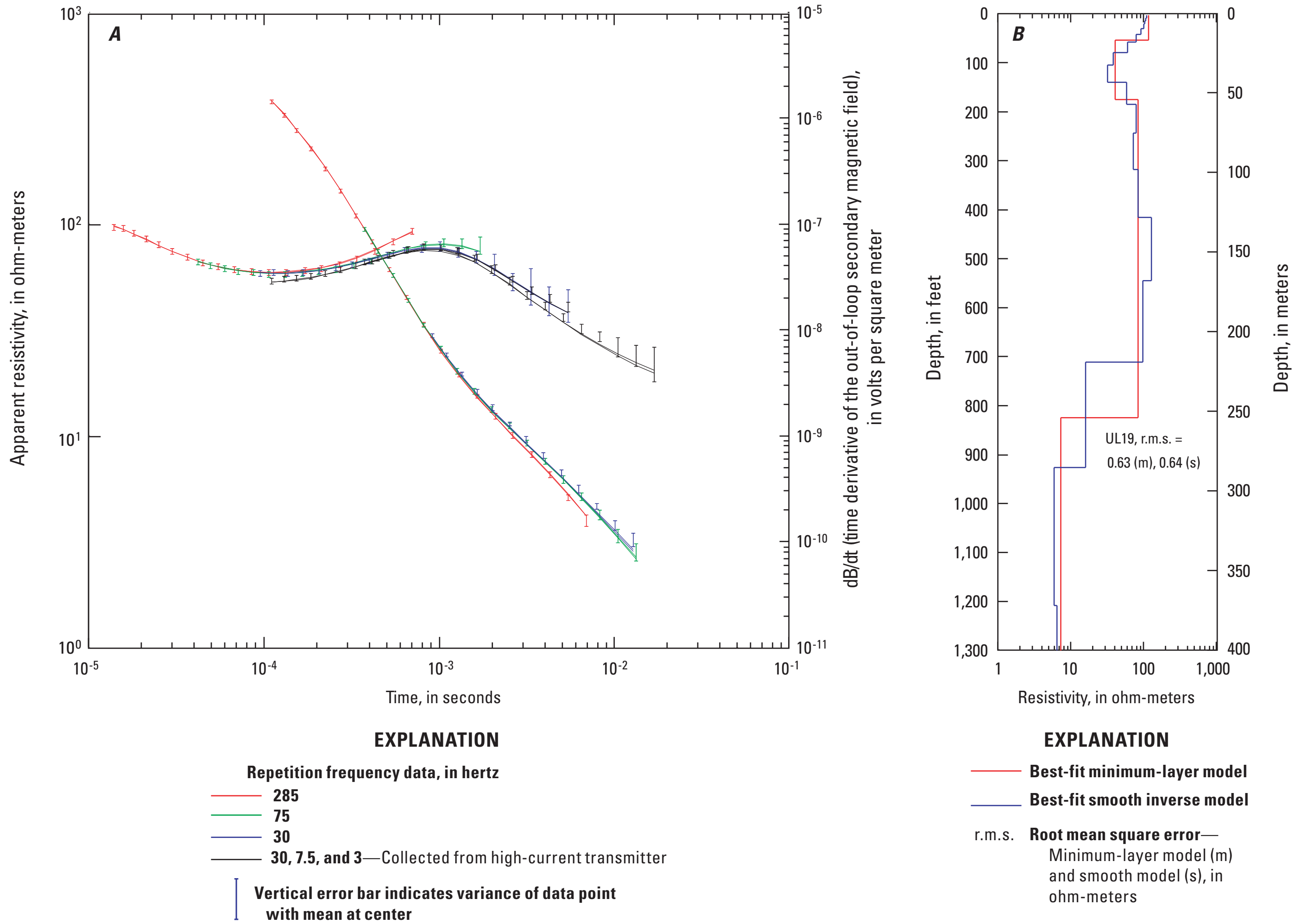

Figure 27. Relations between *A*, central-loop resistivity, out-of-loop vertical magnetic field (time-derivative, right axis), and time; *B*, depth below land surface and subsurface resistivity modeled from TDEM sounding for site UL19.

Publishing support provided by:
Rolla Publishing Service Center

For more information concerning this publication, contact:
Director, USGS Nebraska Water Science Center
5231 South 19 Street
Lincoln, Nebraska 68512
(402) 328–4100

Or visit the Nebraska Water Science Center Web site at:
http://ne.water.usgs.gov/

Hobza and others—**Hydrostratigraphic Interpretation of Test-Hole and Geophysical Data, Upper Loup River Basin, Nebraska, 2008–10**—Open-File Report 2011-1289